Solvable models of two-level systems coupled to itinerant electrons: Robust non-Fermi liquid and quantum critical pairing

Evyatar Tulipman,[1,*] Noga Bashan,[1,*] Jörg Schmalian,[2,3] and Erez Berg[1]
[1]*Department of Condensed Matter Physics, Weizmann Institute of Science, Rehovot 76100, Israel*
[2]*Karlsruher Institut für Technologie, Institut für Theorie der Kondensierten Materie, 76049 Karlsruhe, Germany*
[3]*Karlsruher Institut für Technologie, Institut für Quantenmaterialien und Technologien, 76021, Karlsruhe, Germany*

Strange metal behavior is traditionally associated with an underlying putative quantum critical point at zero temperature. However, in many correlated metals, e.g., high-T_c cuprate superconductors, strange metallicity persists at low temperatures over an extended range of microscopic parameters, suggesting the existence of an underlying *quantum critical phase*, whose possible physical origins remain poorly understood. Systematic investigations of physical scenarios giving rise to such a critical, non-Fermi liquid (NFL) phase are therefore crucial to better understand this puzzling behavior. In a previous study [Bashan *et al.*, Phys. Rev. Lett. **132**, 236501 (2024)], we considered a solvable large-N model consisting of itinerant electrons coupled to local two-level systems (TLSs) via spatially random interactions, inspired by the possibility of emergent metallic glassiness due to frustrated competing orders, and found that the system hosts an NFL phase with tunable exponents at intermediate couplings. In this paper, we expand our investigation to the following: (i) We study the extent to which this NFL phase is generic by considering various deformations of our theory, including coupling of electrons to multiple operators of the TLSs and arbitrarily directed TLS fields. We find that the physical picture obtained in Bashan *et al.* [Phys. Rev. Lett. **132**, 236501 (2024)] qualitatively persist in a wide region of parameter space, showcasing the robustness of the NFL phase. (ii) We analyze the superconducting instability caused by the coupling of TLSs to electrons, and find a rich structure, including quantum critical pairing associated with the NFL phase and conventional BCS-like pairing in the weak and strong coupling limits. (iii) We elaborate on the analysis of Bashan *et al.* [Phys. Rev. Lett. **132**, 236501 (2024)], including single-particle, transport, and thermodynamic properties.

I. INTRODUCTION

One of the central problems in condensed matter physics concerns the low-temperature anomalous normal-state transport properties of correlated metals such as high-T_c cuprate superconductors and others [1–5]. A hallmark of the anomalous behavior is the linear-in-temperature scaling of the dc resistivity, known as "strange metal" behavior. Such behavior stands at odds with conventional Fermi-liquid theory, where a T^2 scaling is predicted, and is believed to indicate that quantum fluctuations are so pronounced as to completely invalidate the Landau Fermi-liquid quasiparticle picture [6–9].

The traditional theoretical approach to describe strange metals and other non-Fermi liquids (NFLs) involves coupling a Fermi surface to bosonic collective fluctuations of an order parameter, sometimes leading to NFL behavior when tuning the system to a quantum critical point (QCP) [10–12]. In this case, the NFL behavior manifests in a critical fan, emanating from a single (critical) point at $T \to 0$. Interestingly, while consistent with some materials, e.g., heavy fermion systems [13], there are numerous examples, e.g., cuprates [14–17] as well as twisted bilayer graphene, organic superconductors, and other systems [5,18–25], where NFL behavior persists over an extended region of nonthermal parameters at $T \to 0$ and thus cannot be ascribed to a single QCP. Rather, the extended NFL behavior raises the possibility of a quantum critical *phase*. Since no general prescription exists for this scenario, capturing such behavior within a controlled, physically motivated theory is considerably challenging.

One potential route to realize an extended critical NFL phase requires an efficient source of scattering for itinerant electrons over an extended region of nonthermal parameters, e.g., by identifying a physical setting where "critical" low-energy excitations (i.e., with support at the lowest energies) exist. To this end, in a recent paper [26], we demonstrated that an NFL phase can arise when itinerant electrons are interacting with fluctuations of a metallic glass (e.g., charge or stripe glass), described as a collection of two-level systems (TLSs) that correspond to quasilocal collective excitations, analogously to the excitations in structural glasses [29]. Physically, our theory is motivated by the complex phase diagrams of such strongly correlated materials that often host multiple frustrated, competing orders, which can give rise to glassiness, even in the absence of impurity disorder [30]. The presence of disorder could further stabilize such extended NFL behavior, as was observed in Ref. [31].

In fact, it has been long recognized that inelastic scattering of electrons off of local TLSs can result in a T-linear resistivity in the weak coupling limit [32]. Nonetheless, going beyond

[*]These authors contributed equally to this work.

weak coupling, the interaction with electrons may dramatically alter the properties of the TLSs, e.g., by renormalization of the bare TLS parameters or inducing inter-TLS correlations analogously to the Ruderman–Kittel–Kasuya–Yosida (RKKY) mechanism [33–35]. Clearly these effects can further affect the electrons themselves.

To study the evolution of the physical picture beyond weak coupling, in Ref. [26], we considered a large-N theory consisting of itinerant electrons interacting with local TLSs via spatially random couplings. We found that the non-Gaussian saddle point of the theory hosts a robust NFL phase with tunable exponents, which is not associated with quantum criticality; see Sec. V for a summary of our findings. Roughly speaking, the electrons constitute an ohmic bath for the TLSs, which results in a renormalization of the TLS energy splitting towards lower energies. At sufficiently strong couplings, a significant portion of the TLSs are renormalized to low energies, which in turn provides an efficient source of scattering for the electrons, resulting in an NFL behavior over a finite range of coupling strengths.

In Ref. [26], we have considered the special case where electrons are coupled to a single operator of TLSs (i.e., σ_x of spin-1/2 Pauli operators), which allowed us to focus on the effects of inelastic electron-TLS scattering in a simple setting. Specifically, we considered the case where electrons are coupled to σ_x of the TLSs, which we shall refer to as the "x model" henceforth. Aiming for a broader understanding, it is natural to ask whether the behavior of the x model persist to the generic case, where electrons may couple to all three operators of the TLSs. Another important aspect of the physical picture concerns TLS-induced pairing, which is expected to take over at sufficiently low temperatures.

In this paper, we investigate a class of large-N models, generalizing our study of the x model of Ref. [26] to more generic settings. We begin by considering the effect of coupling of spinless electrons to all operators of the TLSs. Importantly, the low-energy behavior is qualitatively identical to that of the x model within a wide range of parameters, showcasing the robustness of the NFL phase found in Ref. [26]. Towards a more realistic scenario, we generalize our analysis to spinful electrons and find a transition to a superconducting ground state due to TLS-induced pairing. Remarkably, the rich phenomenology of the normal state in our model is also manifested in the form of the critical temperature T_c, exhibiting various crossovers, where in particular the transition from the NFL phase assumes a quantum critical form. In addition to these key finding, we further study various aspects of the model, including transport and thermodynamic properties and $1/N$ corrections.

The structure of the paper is as follows. In Sec. II we present the model and discuss physically motivated choices of parameters. In Sec. III we provide a brief summary of our main results. In Sec. IV we provide a mapping from our model to a set of decoupled spin-boson (SB) models. In Sec. V we provide an extensive review of the x model, previously studied in Ref. [26], which corresponds to the special case where the electrons interact only with the $\hat{x}$ component of the TLSs. In Sec. VI we analyze the general case where the electrons interact with all operators of the TLSs (dubbed the xyz model), and in Sec.VII, to the most general case where the field acting on the TLS is allowed to point in arbitrary directions. In Secs. VIII, IX, and X we use our results to study transport, thermodynamic, and superconducting properties of the model, respectively. In Sec. XI we consider several finite-N corrections. Section XII contains a summary of our paper and discuss possible implications and further directions.

II. MODEL

We consider the following Hamiltonian, defined on a d-dimensional hypercubic lattice:

$$H = \sum_{\boldsymbol{k};i=1}^{N} (\varepsilon_{\boldsymbol{k}} - \mu) c^{\dagger}_{i\boldsymbol{k}} c_{i\boldsymbol{k}} + \sum_{\boldsymbol{r};i,j=1}^{N} \frac{1}{N^{1/2}} V_{ij,\boldsymbol{r}} c^{\dagger}_{i\boldsymbol{r}} c_{j\boldsymbol{r}} - \sum_{\boldsymbol{r};l=1}^{M} \boldsymbol{h}_{l,\boldsymbol{r}} \cdot \boldsymbol{\sigma}_{l,\boldsymbol{r}} + H_{\text{int}}, \tag{1}$$

where

$$H_{\text{int}} = \frac{1}{N} \sum_{\boldsymbol{r};i,j=1;l=1}^{N;M} \boldsymbol{g}_{ijl,\boldsymbol{r}} \cdot \boldsymbol{\sigma}_{l,\boldsymbol{r}} c^{\dagger}_{i\boldsymbol{r}} c_{j\boldsymbol{r}}. \tag{2}$$

Each site contains N electronic "orbitals" $i = 1, \ldots, N$, and M species of TLSs $l = 1, \ldots, M$ where $\boldsymbol{\sigma}_{l,\boldsymbol{r}}$ is a vector of spin-1/2 Pauli operators at position $\boldsymbol{r}$. $\varepsilon_{\boldsymbol{k}}$ and μ denote the electronic dispersion and chemical potential, respectively, and are assumed to be diagonal and i independent in orbital space. We approximate the electronic density of states around the Fermi surface by a constant up to the bandwidth W, which we assume to be much larger than any other energy scale in the problem (relaxing this assumption does not alter our results qualitatively). For simplicity, we consider spinless fermions. We will reintroduce the spin index later when we discuss superconductivity. Thus, electrons create a dynamic local field that acts on the TLSs while, at the same time, they scatter off those local degrees of freedom.

Each TLS is subjected to a field $\boldsymbol{h}_{l,\boldsymbol{r}} = (h^x_l, 0, h^z_l)$, with h^z being the asymmetry and h^x the tunneling rate between the two states associated with each TLS, both taken to be independent random variables drawn from a probability distribution $\mathcal{P}_{\beta_a}(h^a)$ with $a = x, z$. Below, we refer to this as the physical basis for $\boldsymbol{h}$. Note that $h^y \equiv 0$ in order to respect time-reversal symmetry. We focus on power-law distributions, $\mathcal{P}_{\beta_a}(h^a) \propto (h^a)^{\beta_a}$, supported on the interval $0 < h^a < h^a_c$. It suffices to consider positive fields as the sign of h^a can be absorbed into the definition of σ_z. h^a_c denote the TLS bare bandwidth and $\beta_a > -1$ is a tunable parameter. The generalization to other distributions is straightforward. In some cases, it will be convenient to rotate to the eigenbasis where $\boldsymbol{h} = h\hat{z}$, with $h = \sqrt{(h^x)^2 + (h^z)^2}$ being the energy splitting of the TLS. We call this the diagonal basis of $\boldsymbol{h}$.

While we present throughout this paper general results for arbitrary β_x and β_z, there are two physically motivated choices for the splitting distributions. Working in the "physical" basis (i.e., the eigenbasis of σ_z), we assume that the distribution of the level asymmetry h^z has finite weight around $h^z = 0$ [36], which corresponds to a uniform distribution with $\beta_z = 0$. It is then natural to consider the cases where the width of the distribution of the tunneling rate h^x is either comparable or

negligible compared to the asymmetry, corresponding to $\beta_x = 0$, $h_c^x = h_c^z \equiv h_c$, or setting $h_c^x \equiv 0$, respectively. In the latter the diagonal basis coincides with the physical basis, while in the former, changing to the diagonal basis results in a linear distribution of the eigenvalues h, i.e., $\beta_z = 1$.

The couplings $\boldsymbol{g}_{ijl,\boldsymbol{r}} = (g^x_{ijl,\boldsymbol{r}}, g^y_{ijl,\boldsymbol{r}}, g^z_{ijl,\boldsymbol{r}})$ are taken to be uncorrelated Gaussian random variables with zero mean and variance g_a^2. For $a = x, z$, we consider real-valued couplings with

$$\overline{g^a_{ijl,\boldsymbol{r}} g^a_{i'j'l',\boldsymbol{r}'}} = g_a^2 \delta_{\boldsymbol{r},\boldsymbol{r}'} \delta_{ll'} (\delta_{ii'}\delta_{jj'} + \delta_{ij'}\delta_{ji'}), \tag{3}$$

and to ensure that H is time reversal symmetric, g^y must be purely imaginary with

$$\overline{g^y_{ijl,\boldsymbol{r}} g^y_{i'j'l',\boldsymbol{r}'}} = -g_y^2 \delta_{\boldsymbol{r},\boldsymbol{r}'} \delta_{ll'} (\delta_{ii'}\delta_{jj'} - \delta_{ij'}\delta_{ji'}). \tag{4}$$

The g_a are all real valued. The different components are uncorrelated, i.e., $\overline{g^a g^{a'}} = 0$ if $a \neq a'$. $\overline{(\cdot)}$ denotes averaging over realizations of the coupling constants. Similarly, the on-site potential disorder $V_{ij,\boldsymbol{r}}$ is normally distributed with zero mean and variance V^2. Note that setting the couplings g_x and g_z to be uncorrelated in the physical basis or in the eigenbasis is not equivalent in the cases where both $h^x, h^z > 0$. Here we first consider simple variants of the model where g_x and g_z are uncorrelated in the diagonal basis (i.e., setting $h^x \equiv 0$) and later show that the qualitative physical picture persists when they are uncorrelated in the physical basis (with $h^x \neq 0$).

The Fermi energy E_F sets the largest energy scale in theory, and also corresponds to the cutoff energy of the electronic bath, traditionally denoted by $\omega_c (= E_F)$ in the spin-boson literature [37–39].

The TLS bandwidth satisfies $h_c \ll E_F$, and we restrict the on-site disorder strength V^2, such that $\Gamma = 2\pi \rho_F V^2 \ll E_F$ (Γ being the elastic scattering rate), therefore considering "good metals". We do not restrict the interaction strengths g_a, namely, our study covers the range from weak to strong coupling. We focus on the low-energy limit of the model, defined by $\omega, T \ll h_{c,R}$, where $h_{c,R}$ is the renormalized cutoff of the TLSs, to be defined below.

The dimensionless coupling parameters that will be used in the following are related to the interaction strengths by ($a = x, y, z$),

$$\alpha_a = \frac{\rho_F^2 g_a^2}{2\pi^2}, \tag{5}$$

$$\lambda_a = \frac{M}{N} \frac{\rho_F g_a^2}{h_{c,R}}. \tag{6}$$

The parameters α_a (defined in accordance to the spin-boson literature conventions) represent the strength of the dissipation acting on the TLSs, while λ_a quantify the strength of the scattering of electrons by TLSs at low energies.

Throughout this paper we consider the limit $N, M \to \infty$ with a fixed ratio M/N. We will see below that the limit $M \to \infty$ enables us to (i) reduce the electron's self-energy to a summation over rainbow diagrams containing only two-point correlation functions of the TLSs, which is not clear a priori as Wick's theorem does not hold for the TLSs; and (ii) invoke self-averaging of the TLSs, such that sums over the TLS flavors can be replaced by averages over the splitting distribution, $\sum_{l=1}^{M} f(h_l) \to M \int f(h) \mathcal{P}_\beta(h) dh$. Importantly, since the splitting distribution is independent of position, the self-averaging assumption translates to statistical translation invariance of the model. Note further that the $N \to \infty$ limit is essential for the mapping of our model to the spin-boson (SB) model, where the bosonic bath coupled to the TLSs is composed of particle-hole pairs, see Sec. IV.

III. BRIEF SUMMARY OF RESULTS

In the following sections we expound on the properties of different variants of the model. However, for the benefit of the reader, we first briefly outline the key conclusions of our paper. We first describe the physical picture of the x model and then show that this picture qualitatively persists to generic variants of the model.

Normal state. Consider the normal state properties at low T, corresponding to regions (I) and (II) in Fig. 1. In region (I), as the dimensionless coupling $\alpha = \alpha_x$ is increased, the system crosses over from a FL, MFL, and NFL, up to a critical value $\alpha \approx 1$ where the TLS freeze at $T = 0$. These regimes are defined by the exponent of the single-particle scattering rate, $\Sigma''(\omega) - \Sigma''(0) \propto |\omega|^\gamma$, $\gamma(\alpha, \beta) = (1+\beta)(1-\alpha)$ (shown for $\beta = 1$ in Fig. 1). This is also manifested in the dc resistivity, $\rho - \rho_0 \propto T^\gamma$. In region (II), the TLSs are frozen at $T = 0$, such that scattering off of TLS is mainly elastic. At finite T for $\alpha \gtrsim 1$, however, residual quantum fluctuations of the TLSs provides a source for inelastic scattering, leading to an additional sequence of NFL-MFL-FL crossovers with an inelastic scattering exponent $2(\alpha - 1)$. This residual contribution corresponds to a weak T variation of the dc resistivity as shown in Fig. 1. The behavior in the critical region $\alpha \approx 1$ and $T \to 0$, separating regions (I) and (II), is more involved and show logarithmic T dependence of the single-particle scattering rate (and the dc resistivity) that smoothly interpolates between the two regions.

Superconductivity. Considering the model with spinful electrons, a superconducting transition occurs below a critical temperature T_c due to TLS-induced pairing; see Fig. 1. Interestingly, T_c is a nonmonotonic function of the coupling α_x, with remarkably rich pairing phenomenology. Specifically, at intermediate couplings [corresponding, e.g., to the NFL phase of region (I) in Fig. 1] T_c assumes an algebraic, quantum critical scaling form, and, as the coupling is further increased beyond a certain threshold (but still at intermediate values), crosses over to an Allen-Dynes-like, strong coupling form [40]. In addition, T_c assumes the standard BCS-like form at weak coupling, but also at very strong coupling (e.g., for $\alpha > 3/2$ in Fig. 1), which corresponds to pairing due to the residual quantum fluctuations of the nearly frozen spins. Here BCS-like superconductivity describes a state where the frequency dependence of the bosonic mode that causes superconductivity does not change the dependence of T_c relative to phonon-mediated BCS theory.

Robustness. To test the extent to which the physical picture of the x model is generic, we allow for interactions with other operators of the TLSs. In Fig. 2, we show how the normal state $T = 0$ phase diagram of the x model changes upon introducing coupling to the y (top row) and z (bottom row) operators of the TLSs for constant and linear TLS-splitting distributions (left and right columns, respectively). We shall refer to these variants as the xy and xz models.

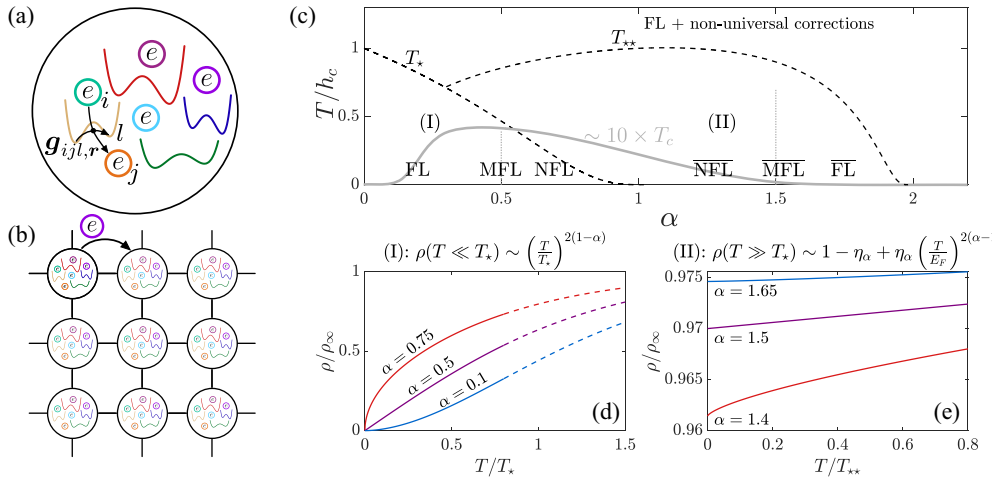

FIG. 1. (a), (b) Illustration of the lattice model Eqs. (1) and (2). (a) A unit cell containing a large number of electronic states and local two-level systems interacting via random couplings; (b) the electrons hop between unit cells. (c) Phase diagram of the x model in $\alpha - T$ plane ($\alpha = \alpha_x$ is the dimensionless coupling strength) for a linear splitting distribution ($\beta = 1$). Region (I), defined by $T \ll T_\star \sim h_{c,R}, h_{c,R}$ being the renormalized cutoff of the TLS-splitting, is characterized by the leading inelastic scattering exponent $2(1-\alpha)$ as manifested in the dc resistivity, see (d); the system crosses over from a Fermi liquid (FL) for $\alpha < 1/2$, to a marginal Fermi liquid (MFL) for $\alpha = 1/2$, and a non-Fermi liquid (NFL) for $1/2 < \alpha < 1$. At $\alpha \approx 1$, the TLSs undergo a freezing transition at $T = 0$. In Region (II), for $\alpha \gtrsim 1$ at finite T, scattering off of the TLSs is mainly elastic with small inelastic corrections that scale $\sim T^{2(\alpha-1)}$, namely, another set of crossovers from NFL ($1 < \alpha < 3/2$) to MFL ($\alpha = 3/2$) to FL ($\alpha > 2$); see (e). Region (II) is defined up to $T \sim T_{\star\star}$, where $T_{\star\star}$ is the scale at which standard FL behavior becomes dominant. The gray line denotes the transition temperature to the superconducting state, T_c, in the spinful version of the x model. (d)(e) Resistivity as a function of T for regions (I) and (II), respectively, where ρ_∞ is the resistivity due to saturated classical TLSs. Note that, in region (II), the α-dependent coefficient $\eta_\alpha \propto (h_c/E_F)^2 \ll 1$, corresponding to the weak T-variation of the dc resistivity.

In all cases, the qualitative behavior of the x model persists provided that the largest coupling is orthogonal to the direction of the TLS field (i.e., to $h_z\sigma_z$), namely, the characterizing exponent $\gamma(\boldsymbol{\alpha})$ varies from $1+\beta$ to 0 as the dominant coupling is increased, up to a critical value at which the TLSs freeze. This sequence of crossovers corresponds to region (I) in Fig. 1, while the residual crossovers of region (II) are expected to qualitatively change for sufficiently strong perturbations due to nonuniversal corrections. Note that when the dominant coupling is parallel to the TLS field (i.e., when $\alpha_z > \alpha_x$), the TLSs are essentially static and the system shows Fermi-liquid behavior with TLS-induced elastic scattering along with weak FL-like corrections.

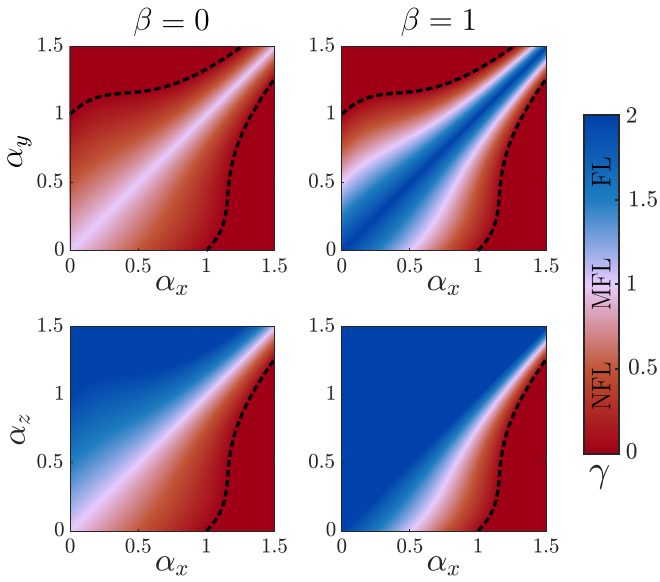

FIG. 2. $T = 0$ normal-state phase diagram of the xy model (top) and xz model (bottom), for constant ($\beta = 0$) and linear ($\beta = 1$) TLS splitting distributions. The color represents the exponent in the low-T behavior of the resistivity, $\rho - \rho_0 \propto T^\gamma$ [analogous to region (I) in Fig. 1]. The dashed line denotes the BKT transition over which the TLSs freeze, and beyond which there is a nonuniversal version of the $\overline{\text{NFL}}$ phase [similar to region (II) of Fig. 1 for $\alpha_x > 1$].

IV. MAPPING TO SPIN-BOSON MODEL

In this section, we use an effective action approach to map our theory to the SB model. We set $V^2 = 0$ for simplicity. An alternative diagrammatic derivation of the mapping is given in Appendix A.

We begin by considering the spin coherent-state path integral representation for the TLSs. The partition function is given by

$$Z[\boldsymbol{h}, \boldsymbol{g}] = \int \mathcal{D}[\boldsymbol{\sigma}, c, \bar{c}] e^{-S}, \tag{7}$$

with the action, $S = S_0 + S_{\text{int}}$,

$$S_0 = \sum_{\boldsymbol{r}} \sum_{l=1}^{M} S_{\text{Berry}}[\boldsymbol{\sigma}_{l,\boldsymbol{r}}] - \sum_{\boldsymbol{r}} \sum_{l=1}^{M} \int_\tau \boldsymbol{h}_{l,\boldsymbol{r}} \cdot \boldsymbol{\sigma}_{l,\boldsymbol{r}} + \sum_{i=1}^{N} \sum_{\boldsymbol{k}} \int_\tau \bar{c}_{i\boldsymbol{k}} (\partial_\tau + \varepsilon_{\boldsymbol{k}} - \mu) c_{i\boldsymbol{k}}, \tag{8}$$

$$S_{\text{int}} = \frac{1}{N} \sum_{\boldsymbol{r}} \sum_{i,j=1}^{N} \sum_{l=1}^{M} \int_\tau \boldsymbol{g}_{ijl,\boldsymbol{r}} \cdot \boldsymbol{\sigma}_{l,\boldsymbol{r}} \bar{c}_{i\boldsymbol{r}} c_{j\boldsymbol{r}}. \tag{9}$$

Here we kept the same symbols $\boldsymbol{\sigma}_{l,\boldsymbol{r}}$ for the unit vectors that result from the coherent state representation of the Pauli operators. S_{Berry} denotes the Berry's phase of the TLSs, see e.g., [41].

To proceed, we average over the random couplings using the replica method and introduce the bilocal fields

$$G_{\boldsymbol{r},\boldsymbol{r}'}(\tau,\tau') = \frac{1}{N}\sum_i \bar{c}_{i\boldsymbol{r}}(\tau)c_{i\boldsymbol{r}'}(\tau'), \tag{10}$$

$$\chi_{a,\boldsymbol{r}}(\tau,\tau') = \frac{1}{M}\sum_l \sigma^a_{l,\boldsymbol{r}}(\tau)\sigma^a_{l,\boldsymbol{r}}(\tau'). \tag{11}$$

The constraints (10) and (11) are enforced via conjugated fields, Σ and Π, respectively. Notice that, for now, we are considering spinless fermions. In this case, there is no pairing instability to leading order in $1/N$. Later on, we shall consider a model of spinful fermions, where the anomalous part of the Green's function must be considered, and an instability towards a superconducting state with an intraflavor, on-site order parameter occurs [42].

To proceed, we integrate over the fermions and substitute a replica-diagonal *Ansatz*, which allows us to express the partition function as $Z[\boldsymbol{h}] = \int \mathcal{D}[G,\boldsymbol{\chi},\Sigma,\boldsymbol{\Pi},\boldsymbol{\sigma}]e^{-S_{\text{eff}}}$, where the effective action is given by

$$\begin{aligned} S_{\text{eff}} = &-N\text{Tr}\ln\left(G_0^{-1}-\Sigma\right) - N\int_{\tau,\tau'}\sum_{\boldsymbol{r},\boldsymbol{r}'}\sum_\sigma G_{\boldsymbol{r},\boldsymbol{r}'}(\tau,\tau')\Sigma_{\boldsymbol{r},\boldsymbol{r}'}(\tau,\tau') + \frac{M}{2}\int_{\tau,\tau'}\sum_{\boldsymbol{r},a}\chi_{a,\boldsymbol{r}}(\tau,\tau')\Pi^a_{\boldsymbol{r}}(\tau',\tau) \\ &+ \frac{M}{2}\int_{\tau,\tau'}\sum_{\boldsymbol{r}}\sum_a g_a^2 G_{\boldsymbol{r}}(\tau,\tau')G_{\boldsymbol{r}}(\tau',\tau)\chi_{a,\boldsymbol{r}}(\tau,\tau') + \sum_{\boldsymbol{r}}\sum_{l=1}^M S_{\text{Berry}}[\boldsymbol{\sigma}_{l,\boldsymbol{r}}] - \int_\tau\sum_{\boldsymbol{r}}\sum_{l=1}^M \boldsymbol{h}_{l,\boldsymbol{r}}\cdot\boldsymbol{\sigma}_{l,\boldsymbol{r}} \\ &- \frac{1}{2}\int_{\tau,\tau'}\sum_{\boldsymbol{r},a}\Pi^a_{\boldsymbol{r}}(\tau',\tau)\sum_{l=1}^M \sigma^a_{l,\boldsymbol{r}}(\tau)\sigma^a_{l,\boldsymbol{r}}(\tau'). \end{aligned} \tag{12}$$

In the limit of large M and N, with fixed ratio M/N, we can analyze the problem in the saddle point limit [43]. Performing the variation with respect to G and Σ gives

$$\Sigma_{\boldsymbol{r},\boldsymbol{r}'}(\tau) = \delta_{\boldsymbol{r},\boldsymbol{r}'}\frac{M}{N}\sum_a g_a^2 G_{\boldsymbol{r},\boldsymbol{r}}(\tau)\chi_{a,\boldsymbol{r}}(\tau) \tag{13}$$

as well as

$$G_{\boldsymbol{r},\boldsymbol{r}'}(i\omega) = \left(G_0^{-1}(i\omega)-\Sigma(i\omega)\right)^{-1}\big|_{\boldsymbol{r},\boldsymbol{r}'}. \tag{14}$$

Here, we have used thermal equilibrium to write the saddle-point equations with time-translation-invariant correlation functions and their Fourier transforms. In addition, the stationary point that follows from the variation with respect to χ is

$$\Pi_{a,\boldsymbol{r}}(\tau) = -g_a^2 G_{\boldsymbol{r},\boldsymbol{r}}(\tau)G_{\boldsymbol{r},\boldsymbol{r}}(-\tau). \tag{15}$$

The Berry phase term S_{Berry} that reflects the fact that no Wick's theorem exists for Pauli operators, implies that the TLSs cannot be simply integrated over as a Gaussian integral. However, it allows us to recast the TLS problem to that of M decoupled TLSs per site $\boldsymbol{r}$, $\sum_{\boldsymbol{r},l=1}^M S_{\boldsymbol{r},l}[\boldsymbol{\sigma}_{\boldsymbol{r},l}]$, coupled to a bosonic bath of particle-hole excitations. Each TLS is governed by the spatially local effective action

$$\begin{aligned} S_{\boldsymbol{r},l}[\boldsymbol{\sigma}] = &S_{\text{Berry}}[\boldsymbol{\sigma}] - \int_\tau \boldsymbol{h}_{l,\boldsymbol{r}}\cdot\boldsymbol{\sigma}(\tau) \\ &- \int_{\tau,\tau'}\Pi_{\boldsymbol{r}}(\tau'-\tau)\sigma^a(\tau)\sigma^a(\tau'). \end{aligned} \tag{16}$$

This is indeed the action of the spin-boson model after the bosonic bath degrees of freedom have been integrated out [39]. The latter give rise to the nonlocal in time coupling $\Pi^a_{\boldsymbol{r}}(\tau',\tau)$ that is, in general, different for each site. Of course, in our problem the origin of the bath function are not bosons but the conduction electrons. For the solution of this local problem this makes, however, no difference. $S_{\boldsymbol{r},l}$ still depends on the random configuration $\boldsymbol{h}_{l,\boldsymbol{r}}$ of the fields.

For a given realization of the fields $\boldsymbol{h}_{l,\boldsymbol{r}}$ the problem is not translation invariant and correlation functions like $\langle\sigma^a_{l,\boldsymbol{r}}(\tau)\sigma^a_{l,\boldsymbol{r}}(0)\rangle$ fluctuate in space. However, to determine the self-energy in Eq. (13) we only need to know the average $\chi_{a,\boldsymbol{r}}(\tau)$ of this correlation function over the M flavors. To proceed we assume that the model is self-averaging in the $M\to\infty$ limit, such that sums over the TLS flavors can be replaced with averaging over the TLS splitting distribution ($\sum_{l=1}^M \to M\int\mathcal{P}(\boldsymbol{h}_{\boldsymbol{r}})d\boldsymbol{h}_{\boldsymbol{r}}$). Since the splitting distribution is independent of position, the self-averaging assumption translates to a statistical translation invariance of the model, at least for the average of interest. Hence, $\chi_{a,\boldsymbol{r}}(\tau)=\chi_a(\tau)$ is independent on $\boldsymbol{r}$. The same must then hold for the bath function $\Pi_{a,\boldsymbol{r}}(\tau)=\Pi_a(\tau)$. From the saddle point equations (15) it follows that the local fermionic Green's function and through Eq. (14) the self-energy are both space independent. Hence we can go to momentum space and find that the theory is governed by a momentum-independent self-energy and the Dyson equation for the electrons read

$$\Sigma(\tau) = \frac{M}{N}\sum_a g_a^2\chi_a(\tau)G(\tau), \tag{17}$$

$$G_{\boldsymbol{k}}(i\omega) = \frac{1}{i\omega-\varepsilon_{\boldsymbol{k}}-\Sigma(i\omega)}, \tag{18}$$

where $G(\tau)=\int_{\boldsymbol{k}}G_{\boldsymbol{k}}(\tau)$ is the local Green's function. For a momentum-independent fermionic self-energy we obtain in the limit of large electron bandwidth

$$G(i\omega) = \int_{\boldsymbol{k}} G_{\boldsymbol{k}}(i\omega) \approx -i\pi\rho_F\,\text{sgn}(\omega). \tag{19}$$

The particle-hole correlation function can now be evaluated. We find

$$\Pi_a(\omega) = \frac{\rho_F^2 g_a^2}{2\pi}|\omega|, \tag{20}$$

irrespective of the electronic self-energy. We thus conclude that each TLS is coupled to an ohmic bath of particle-hole excitations that is independent of the back reaction of the TLS on the electronic degrees of freedom. This is a consequence of the fact that the Π_a are independent of Σ. Thus, we have shown that the (spatially local) TLS-correlator

$$\chi_a(\tau - \tau') = \frac{1}{M}\sum_l \left\langle \sigma_l^a(\tau)\sigma_l^a(\tau')\right\rangle, \tag{21}$$

is determined by the behavior of M decoupled SB models.

The strategy of the solution of our model in the large-N limit is therefore: (i) Solve the spin-boson problem with ohmic bath for a given realization of the field $\boldsymbol{h}$, (ii) average over the TLS distribution function of the fields, and (iii) use the resulting propagator $\chi_a(\omega)$ of the TLSs to determine the fermionic self-energy from Eq. (18). The nonlinear character of the problem is rooted in the rich physics of the spin-boson problem, along with the averaging over the distribution functions of the fields $\boldsymbol{h}$. Given the importance of the spin-boson model for our analysis we will give a summary of this model in the next section.

V. THE x MODEL

We begin with a review of the solution of the model for the simplest case where the electrons interact only with σ_x of the TLSs' pseudospins, i.e., we are working in the diagonal basis and setting $g^z, g^y = 0$, as in Ref. [26]. This special case allows for a more transparent discussion of the key steps of our analysis. In addition, we will see that the more general problem reduces in many cases to this model in the limit of sufficiently low energies. In terms of the mapping provided in Sec. IV, the model is mapped into the SB model with one bath. Throughout this section, since $\alpha_y, \alpha_z = 0$ we will use the notation $\alpha = \alpha_x$ for simplicity.

A. A simple view of the physical picture for $\alpha < 1$

Consider first the weak coupling limit, $\alpha \to 0$, where the effect of interactions can be studied perturbatively. To leading order in g^2 the decay rate of an electron with energy ω is proportional to the amount of TLSs at accessible energies, namely,

$$\Sigma''(\omega) \propto \int_0^\omega \mathcal{P}_\beta(h)dh \propto |\omega|^{1+\beta}, \tag{22}$$

where Σ'' denotes the imaginary part of the electronic retarded self-energy (F'' will denote the imaginary part of the retarded function F throughout the paper). For $\beta = 0$ this weak coupling analysis yields marginal Fermi-liquid behavior. On the other hand, for any $\beta > 0$, i.e., for distribution functions that vanish for $h \to 0$ one only finds Fermi-liquid behavior. Increasing the strength of the interaction modifies the behavior of the TLSs in two main aspects: it renormalizes the energy splitting of each TLS, such that $h_\ell \to h_R(h_\ell)$; and broadens the TLS spectral function. The broadening has negligible effect on the frequency dependence of Σ'' (at sufficiently low energies). However, as we show in detail below, the renormalization of the energy splitting leads to a renormalization of the bare TLS-splitting distribution, decreasing its exponent from β to $\beta - (1+\beta)\alpha$. Thus, increasing the interaction strength transfers the spectral weight of the TLSs towards lower energies (at the limit $\alpha \to 1$, the spectral weight is pushed to zero energy, signaling a BKT transition of the TLSs to a localized phase). Consequently, the naive perturbative argument will hold for the renormalized splitting distribution, resulting in a tunable exponent as a function of α.

B. Summary of the single-bath spin-boson model

The single-bath spin-boson model (1bSB), or the Caldeira-Leggett model [39,45], is given by the Hamiltonian (note that the commonly used convention in the SB literature swaps $\sigma_x \leftrightarrow \sigma_z$ relative to our convention)

$$H_{\text{1bSB}} = -h\sigma_z + g\sigma_x\phi + H_\phi. \tag{23}$$

The bosonic field $\phi = \sum_i (a_i + a_i^\dagger)$ is to be interpreted in terms of a bath of oscillators whose spectral function, dictated by the Hamiltonian H_ϕ, is assumed to be of power law form below some high-energy cutoff ω_c, $\Pi(\omega \ll \omega_c) \propto |\omega|^s$. The cases where $s < 1, s = 1, s > 1$ are respectively called the subohmic, ohmic, and superohmic baths. Throughout our paper we will exclusively be interested in the ohmic case $\Pi(\omega) = \frac{\pi}{2}\alpha\omega$, using this as the definition of the dimensionless coupling constant α. For extensive reviews, see, e.g., Refs. [37,39].

Historically, this model was proposed as a toy model for the study of quantum dissipation and decoherence [46]. For an ohmic bath, it was found that the spin gradually loses its coherence as α is increased and becomes overdamped [in terms of the one-point function $\langle\sigma_x(t)\rangle$] beyond $\alpha = 1/2$ [37,38]. At $\alpha = 1$, the spin undergoes a Berezinskii-Kosterlitz-Thouless (BKT) phase transition after which it becomes localized in one of the two $\hat{x}$ states [37,39].

For our purposes, the most important corollary is that in the delocalized regime ($\alpha < 1$), the TLS splitting h is renormalized due to the high-frequency modes of the bath, which must adjust to different positions whenever the $h\sigma_z$ term attempts to flip the TLS between the two $\hat{x}$ states (similarly to the Frank-Condon effect of electron-phonon coupling). This renormalization process, along with the BKT transition, are governed by the beta functions of α and the rescaled splitting $\tilde{h} \equiv h/\omega_c$, which, to order $\tilde{h}^2$, are given by

$$\frac{d\alpha}{d\ell} = -\alpha\tilde{h}^2, \tag{24}$$

$$\frac{d\tilde{h}}{d\ell} = (1-\alpha)\tilde{h}, \tag{25}$$

where e^ℓ is the renormalization group rescaling factor. The flow dictated by Eqs. (24) and (25) on the $\alpha - \tilde{h}$ plane is shown in Fig. 3: For α near 1 there exists a constant of flow, $x \equiv (1-\alpha)^2 - \tilde{h}^2$, such that the BKT seperatrix corresponds to the rightmost of the two $x = 0$ lines, with the localized (strong coupling) phase to the right of it. The effective energy

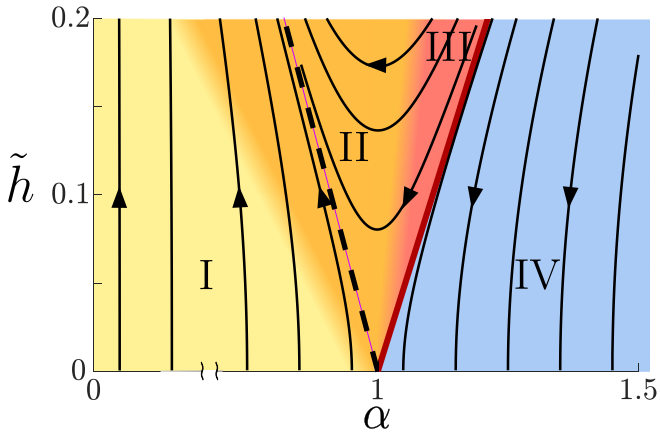

FIG. 3. Schematic flow diagram of the 1bSB model. We present the RG flow of Eqs. (24) and (25). The solid-red line is the BKT seperatrix between the dynamic phase (I − III) and the localized phase (IV), and the dashed-black line represents the set of points, which map into the isotropic Kondo model. For our purposes, we separate the dynamic phase into subregions according to the functional dependence of the renormalized scale h_R on the bare $\tilde{h}$. In region I, the flow is nearly vertical (the beta function of α is small), and the renormalization of h_R is power-law like. In region II, the flow behaves similarly to that of the isotropic Kondo model, and so the renormalized scale is exponential, with a weakly varying prefactor in the exponent. Finally, in region III the flow slows down significantly due to the vicinity to the BKT transition, and the renormalized scale is exponential and depends on the distance from the transition, vanishing exactly on the critical line.

scales, i.e., the renormalized splittings h_R in the different regions of the phase diagram are given by

$$h_R = c_\alpha \omega_c \times \begin{cases} \left(\frac{h}{\omega_c}\right)^{\frac{1}{1-\alpha}} & \text{I} & h/\omega_c \ll (1-\alpha) \\ e^{-b\frac{\omega_c}{h}} & \text{II} & h/\omega_c \approx (1-\alpha) \text{ or } h/\omega_c \gg |1-\alpha| \\ e^{-\frac{\pi}{\sqrt{|x|}}} & \text{III} & h/\omega_c \to \alpha - 1 \\ 0 & \text{IV} & \text{else} \end{cases} \tag{26}$$

where c_α is a numerical prefactor, which cannot be determined solely from the RG equations (but can be extracted using exact techniques such as bosonization or Bethe *Ansatz* [47–50]), and $b = b(\alpha, x)$ is a slowly varying function whose value is of order 1 away from the BKT transition (both are given explicitly in Appendix B). The localization of the TLSs in region IV is because of the fact that the effective tunneling h_R between the the two $\hat{x}$ states flows to zero in that region.

Using this information on the effective low-energy theory, we now turn to the study of correlation functions. As we apply the RG process, the operator σ_x remains supported at low energies, such that correlation functions of σ_x depend solely on parameters of the low-energy theory, α and h_R, and not explicitly on h or ω_c. That is, at zero temperature, the x susceptibility can be expressed in terms of a one-parameter scaling form [51],

$$\chi_x''(\omega) \equiv \frac{1}{\omega} f_\alpha\left(\frac{\omega}{h_R}\right), \tag{27}$$

with h_R given by (26), and $f_\alpha(x)$ being an α-dependent scaling function. This relation between the frequency and the h_R dependence of the susceptibility will be crucial for obtaining exact results in the rest of this section. Unlike σ_x, the correlation functions of the operators σ_z, σ_y contain substantial spectral weight at high energies (of order E_F), and hence cannot be reduced to a single-parameter scaling form as in Eq. (27), and will depend on ω_c explicitly [52]. This fact will be important when discussing the subleading contributions to the electronic self-energy in Sec. VI.

Another approach to the solution of the 1bSB model is via a mapping to the anisotropic Kondo model (AKM) or the resonant level model (RLM) [37,54–56]. Remarkably, at $\alpha = 1/2$, known as the "Toulouse point", the model maps to the noninteracting point of the RLM, and is thus exactly solvable. At this point the effective energy scale is $h_R = \pi h^2/4\omega_c$, and the temperature-dependent susceptibility is given by

$$\chi_x''(\omega, T) = \frac{4}{\pi^2} \frac{h_R}{\omega^2 + 4h_R^2} \left[\mathrm{Im}\Phi(\omega, T) - \frac{2h_R}{\omega} \mathrm{Re}\Phi(\omega, T) \right], \tag{28}$$

where

$$\Phi(\omega, T) = \psi\left(\frac{1}{2} + \frac{h_R}{2\pi T}\right) - \psi\left(\frac{1}{2} + \frac{h_R}{2\pi T} - i\frac{\omega}{2\pi T}\right) \tag{29}$$

[$\psi(z)$ being the Digamma function]. At zero temperature the scaling form takes the exact form

$$f_{1/2}(x) = \frac{4}{\pi^2} \frac{1}{x^2+4} [x \tan^{-1}(x) + \ln(1+x^2)]. \tag{30}$$

Having summarized the essential properties of the SB model, we shall now turn to evaluate the electronic properties of the x model using the fact that each TLS is equivalent to a spin with a randomly distributed splitting h. Note also that the scaling behavior at $T = 0$ can be extended to sufficiently small T (to be defined below), as can be verified explicitly in the Toulouse point and at weak coupling, which enables us to estimate the finite-T properties of the model in the following.

C. Averaged TLS susceptibility and electronic self-energy

Once we have determined the TLS susceptibility $\chi_i(\omega)$, we can determine the fermionic self-energy from Eq.(18). We compute the imaginary part of the retarded self-energy using

$$\Sigma''(\omega) = \frac{M}{N} \sum_{a=x,y,z} g_a^2 \int_{-\infty}^{\infty} \frac{d\nu}{2\pi} \chi_a''(\nu) G_R''(\omega+\nu) \times \left(\coth\left(\frac{\nu}{2T}\right) - \tanh\left(\frac{\nu+\omega}{2T}\right) \right). \tag{31}$$

If we use Eq. (19) for the fermion propagator we obtain that at $T = 0$ (here $g_y = g_z = 0$ and $g_x = g$),

$$\Sigma''(\omega) = -\frac{M}{N} \rho_F g^2 \int_0^\omega d\nu \left(\frac{1}{M} \sum_{i=1}^{M} \chi_{x,i}''(\nu) \right). \tag{32}$$

Since each of the M TLSs contributing to this sum has a randomly distributed splitting h_i, the self-energy of each electron will be a randomly distributed variable. However, since

$M \gg 1$ the central limit theorem guarantees that this random variable will be normally distributed, with width of order $M^{-1/2}$. We can thus replace this random variable by its expectation value (we will revisit this assumption, and consider when it breaks down for large but finite M, at the end of this section),

$$\frac{1}{M}\sum_{i=1}^{M}\chi''_{x,i}(\omega) \to \overline{\chi''_x}(\omega) = \int \mathcal{P}_\beta(h)\chi''_x(\omega,h)dh. \quad (33)$$

Our task thus reduces to the calculation of the TLS susceptibility averaged over the distribution of splittings $\mathcal{P}_\beta(h)$. We note, however, that the distribution, which is of interest to us is not that of the bare splittings, but of the renormalized splittings h_R. We can instead define the renormalized distribution

$$\mathcal{P}_r(h_R) = \left(\frac{dh_R}{dh}\right)^{-1}\mathcal{P}_\beta(h), \quad (34)$$

which is nonzero up to the renormalized bandwidth $h_{c,R} \equiv h_R(h_c)$. Combined with Eq. (27), we may write the averaged susceptibility as

$$\overline{\chi''_x}(\omega) = \mathrm{sgn}(\omega)\int_{|\omega|/h_{c,R}}^{\infty}\mathcal{P}_r\left(\frac{|\omega|}{x}\right)\frac{f_\alpha(x)}{x^2}dx. \quad (35)$$

We will now evaluate this integral for the different functional forms of $h_R(h)$ corresponding to the regions I–IV in Fig. 3 at zero temperature.

1. $\alpha < 1 - h_c/E_F$

In region I of Fig. 3, where the flow of α is weak, h_R is a power of h. Thus the effect of the renormalization would be to alter the exponent in the distribution,

$$\mathcal{P}_r(h_R) = \frac{\gamma h_R^{\gamma-1}}{h_{c,R}^{\gamma}}, \quad \gamma \equiv (1+\beta)(1-\alpha). \quad (36)$$

For energy scales far below the renormalized cutoff $\omega \ll h_{c,R}$, the result would not be sensitive to the exact form of the scaling function f_α, and we retrieve results similar to those presented in the perturbative argument in Sec. V A, albeit with a modified exponent,

$$\overline{\chi''_x}(\omega) = \mathrm{sgn}(\omega)A_\alpha\gamma\frac{|\omega|^{\gamma-1}}{h_{c,R}^{\gamma}}, \quad (37)$$

with $A_\alpha \equiv \int_{\omega/h_{c,R}}^{\infty}\frac{f_\alpha(x)}{x^{\gamma+1}}dx$. Since the scaling function $f_\alpha(x \to 0) \propto x^2$ (corresponding to the universal $1/t^2$ decay of the real-time correlation function at late times [37,39,53]), we may continue the lower limit of the integral to 0 (provided $\gamma < 2$), such that $A_\alpha = \int_0^{\infty}\frac{f_\alpha(x)}{x^{\gamma+1}}dx + \mathcal{O}((\frac{|\omega|}{h_{c,R}})^\gamma)$ [57].

Remarkably, observe that at low energies, the leading frequency dependence of the response of the whole collection of TLSs (which is the effective degree of freedom coupled to the electrons) is independent of broadening effects of the individual TLSs. Rather, it is governed solely by the renormalized distribution $\mathcal{P}_r$, while the functional form of the susceptibility of each individual TLS $f_\alpha(x)$ is absorbed into the prefactor A_α [58]. Hence, for $\omega \ll h_{c,R}$, we find that

$$\Sigma''(\omega) = -A_\alpha\frac{M}{N}\rho_F g^2\left|\frac{\omega}{h_{c,R}}\right|^\gamma \quad (38)$$

$$= -\lambda A_\alpha h_{c,R}\left|\frac{\omega}{h_{c,R}}\right|^\gamma. \quad (39)$$

We see that the self-energy depends on the parameters α and β only via γ. In particular, for any initial $\beta \geqslant 0$, the self-energy realizes a MFL form upon tuning the coupling to $\alpha = \frac{\beta}{1+\beta}$, and realizes any NFL exponent $\gamma < 1$ by increasing α towards 1. Note, however, that as we increase the coupling α, the effective TLS bandwidth $h_{c,R}$ decreases such that smaller NFL exponents are restricted to narrower low-energy intervals; see Fig. 1.

The temperature dependence of Σ'' at low T and zero frequency follows from similar considerations. The contribution of an individual TLS to the self-energy can be written as a scaling function,

$$\Sigma_1(\omega = 0, T, h) = -\rho_F g^2\frac{M}{N}f_\Sigma(T/h_R). \quad (40)$$

We can thus perform the averaging over h_R at this stage, and analogously to Eq. (35) we find that

$$\Sigma''(\omega = 0, T) = A'_\alpha\frac{M}{N}\rho_F g^2\left(\frac{T}{h_{c,R}}\right)^\gamma, \quad (41)$$

with $A'_\alpha = \gamma\int_0^{\infty}\frac{f_\Sigma(x)}{x^{1+\gamma}}dx$. Since $f_\Sigma(x \ll 1) \propto x^2$ and $f_\Sigma(x \to \infty) \to 1$, this is well defined for $0 < \gamma < 2$. This suggests an ω/T scaling of the form $\Sigma'' \propto \max(|\omega|, T)^\gamma$.

2. $\alpha > 1 + h_c/E_F$

For $\alpha > 1 + h_c/E_F$ all the TLSs have undergone the BKT transition and are in the localized phase, where the dominant TLS contribution at $T = 0$ is an elastic scattering term. However, residual quantum fluctuations of the TLSs at finite frequencies provide a weak inelastic scattering mechanism, which becomes the leading contribution to the temperature dependence of the dc resistivity. The finite frequency behavior follows from scaling considerations (Appendix D 4, [53]) and is given by

$$\overline{\chi''_x}(\omega) = (1-\eta_\alpha)\delta(\omega) + 2\eta_\alpha(\alpha-1)\frac{E_F^{2-2\alpha}}{|\omega|^{3-2\alpha}} \quad (42)$$

$$\eta_\alpha = \frac{2\alpha(1+\beta)}{(\alpha-1)(3+\beta)}\left(\frac{h_c}{E_F}\right)^2 \ll 1 \quad (43)$$

with $\eta_\alpha \propto (h_c/E_F)^2 \ll 1$. We thus find in this regime that the leading inelastic contribution to the self-energy is of the form

$$\Sigma''(\omega) = -\rho_F g^2\frac{M}{N}\left(1 - \eta_\alpha + \eta_\alpha\left(\frac{|\omega|}{E_F}\right)^{2\alpha-2}\right). \quad (44)$$

The low-energy excitations of the system are thus those of a NFL for $1 < \alpha < 3/2$, a MFL at $\alpha = 3/2$ and FL for $\alpha > 3/2$. However, note that unlike in the regime $\alpha < 1$, here the elastic contribution is much larger than the inelastic. Note that while this behavior persists up to a large energy scale (a fraction of E_F), it is expected to be the dominant contribution to the self-energy only below an energy scale of order

$1/\alpha^{4-2\alpha}(h_c/E_F)^{\frac{\alpha-1}{2-\alpha}}$, defined as the scale at which conventional FL-like corrections to resistivity become comparable (i.e., assuming ρ contains an additional T^2/E_F contribution).

3. $\alpha \approx 1$

In the "critical" region $|1-\alpha| < h_c/E_F$ the above descriptions are not valid, since the flow of h slows down and becomes comparable to the flow of α. This slowdown leads to a logarithmic behavior of the self-energy, which interpolates between the regimes described by Eqs. (39) and (42). As an example of the behavior in region II of Fig. 3, we consider specifically the case $\alpha = 1$. The renormalized scale is given by $h_R = c_1\omega_c \exp(-\frac{\pi\omega_c}{2h})$, and as a result the renormalized distribution becomes logarithmic,

$$\mathcal{P}_r(h_R) = \frac{(1+\beta)\log^{1+\beta}\left(\frac{\omega_c}{h_{c,R}}\right)}{h_R \log^{2+\beta}\left(\frac{\omega_c}{h_R}\right)}, \tag{45}$$

where we ignore subleading corrections [in $\log(\omega_c/h_{c,R})$], related to the prefactor c_1; see Appendix D 2. Inserting Eq. (45) into Eq. (35), we obtain that

$$\overline{\chi_x''}(\omega) = \frac{1}{\omega}(1+\beta)\log^{1+\beta}\left(\frac{\omega_c}{h_{c,R}}\right)\int_{\frac{|\omega|}{h_{c,R}}}^{\infty}\frac{f_1(x)}{x\log^{2+\beta}\left(\frac{\omega_c}{|\omega|}x\right)}dx. \tag{46}$$

Since the function $f_1(x)$ must decay faster than $1/x$ for $x \gg 1$ [due to the sum rule Eq. (C4)], and also since $|\omega|/\omega_c \ll |\omega|/h_{c,R}$, we may ignore the x inside the log in the denominator and then, as in the previous case, continue the lower limit of integration to 0. The resulting self-energy is given by

$$\Sigma''(\omega) = -\frac{M}{N}\frac{\rho_F g^2}{2}\left(\frac{\log\left(\frac{\omega_c}{h_{c,R}}\right)}{\log\left(\frac{\omega_c}{|\omega|}\right)}\right)^{1+\beta}. \tag{47}$$

Note that when α is not exactly 1, the only difference would be that the factor of $\pi/2$ in the exponent of h_R will vary slightly. Repeating the above calculations, this will only alter the value of $h_{c,R}$, but not the functional form of the self-energy.

For $1 < \alpha < 1 + h_c/E_F$, we must distinguish the TLSs into those, which are dynamical ($h/E_F > \alpha - 1$), and those that are localized/frozen ($h/E_F \leqslant \alpha - 1$). The contribution of the dynamical ones will be similar to that of the $\alpha = 1$ case [shown explicitly in Appendix D 3, the exact result is somewhat more involved, but maintains the logarithmic form of (47)], while the frozen ones will contribute an elastic scattering term to leading order (i.e., a delta function peak around $\omega = 0$), plus higher-order Fermi-liquid terms, which we ignore. Defining $m_\alpha \equiv \frac{\alpha-1}{h_c/\omega_c}$ as the fraction of frozen TLSs, the self-energy will include both a constant elastic contribution along with the NFL contribution attained earlier. For simplicity, setting $\beta = 1$ we find that the self-energy will be

$$\Sigma''(\omega) = -\frac{M}{N}\rho_F g^2\left(m_\alpha + (1-m_\alpha)B_\alpha\left(\frac{\log\left(\frac{\omega_c}{h_{c,R}}\right)}{\log\left(\frac{\omega_c}{|\omega|}\right)}\right)^2\right). \tag{48}$$

As α approaches $1 + h_c/\omega_c$ from below, both the relative weight $1 - m_\alpha$ of the inelastic contribution, as well as the energy scale $h_{c,R}$ vanishes.

VI. THE *xyz* MODEL

We consider a generalized variant of the model, where we allow electron-TLS coupling in arbitrary directions, i.e., $g_a^2 > 0$ for $a = x, y, z$ (keeping the field $\boldsymbol{h}$ parallel to the z direction), which we dub "xyz model". Remarkably, we will show that throughout much of the parameter space (of $g_x - g_y - g_z$), the behavior is qualitatively similar to that of the x model, namely, increasing the couplings will generically drive the model towards a BKT transition, leading to a tunable exponent in the electronic self-energy, which depends on the distance from the transition.

To proceed we recall that the electronic self-energy in the multichannel model is given by

$$\Sigma''(\omega) = -\frac{M}{N}\sum_{a=x,y,z}\rho_F g_a^2\int_0^\omega \overline{\chi_a''}(\nu)\frac{d\nu}{2\pi}. \tag{49}$$

As before, the TLSs are decoupled such that the dynamics of each TLS are determined by solving an independent SB model coupled to three ohmic baths. The corresponding multibath SB model (mbSB) for a single TLS is

$$H_{\text{mbSB}} = -h\sigma_z + \sum_{a=x,y,z} g_a\sigma_x^a\phi_a + \sum_{a=x,y,z} H_{\phi_a}, \tag{50}$$

where the bosonic field of Eq. (23) is generalized to three fields, ϕ_x, ϕ_y, ϕ_z, corresponding to three independent baths, which couple to the three spin directions. In our case, all three baths are ohmic and have the same cutoff (because $\omega_c = E_F$), such that the interaction strengths are measured via the three dimensionless couplings, $\alpha_a \equiv \rho_F^2 g_a^2/\pi^2$, $a = x, y, z$. Let us point out that the model (50) has two high-symmetry points: the $U(1)$ symmetric point, corresponding to $\alpha_x = \alpha_y$; and the $SU(2)$ symmetric point corresponding to $h = 0, \alpha_x = \alpha_y = \alpha_z$ (for relevant studies see, e.g., Refs. [59–61]). These points will not be of particular interest to us, as they are both unstable fixed points (see below) and require fine tuning.

Similar to the 1bSB model, the low-energy properties of the model can be obtained from an analysis of the RG flow. Here, the RG equations can be derived perturbatively in two out the of three couplings; while one of the couplings α_a is allowed to be arbitrarily large, the RG equations are valid to linear order in $\alpha_{b\neq a}$ [59–61]. Loosely speaking, the RG analysis is valid near the axes in the $(\alpha_x, \alpha_y, \alpha_z)$-coordinate system. The beta functions for the mbSB model are given by

$$\frac{d\tilde{h}}{d\ell} = (1 - \alpha_x - \alpha_y)\tilde{h}, \tag{51}$$

$$\frac{d\alpha_a}{d\ell} = -\left(2\sum_{b\neq a}\alpha_b + (1-\delta_{az})\tilde{h}^2\right)\alpha_a. \tag{52}$$

In order to simplify the analysis, we first discuss the cases where only two of the baths are active (by setting $\alpha_z = 0$ or $\alpha_y = 0$), treating one bath as dominant and the other as a perturbation. We then generalize the discussion to the case where all three baths are active, where, as we will show, the physical

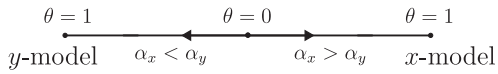

FIG. 4. Initial flow of the couplings in the xy model. $\theta = (\frac{\alpha_x-\alpha_y}{\alpha_x+\alpha_y})^2$ is the bath-anisotropy parameter.

pictures can be essentially reduced to the simplified cases (of the two active baths). Further, as the model does not contain any other stable fixed points, we expect that the RG analysis will qualitatively capture the physics for all couplings.

It is useful to think about the RG of the multibath cases as a two-step process: the first step describes the "fast" flow of the couplings, where the dominant bath assumes a weakly renormalized coupling while the other irrelevant baths flow to weak coupling; in the second step, the baths renormalize the TLS fields according to the renormalized couplings. We now proceed to analyze the different cases, where the usefulness of the two-step perspective becomes apparent.

A. The xy model

We start by setting $\alpha_z = 0$, i.e., the case where there are two active baths acting in the direction perpendicular to the field. The beta functions are given by

$$\frac{d\tilde{h}}{d\ell} = (1-\alpha_x-\alpha_y)\tilde{h}, \tag{53}$$

$$\frac{d\alpha_x}{d\ell} = -2\alpha_y\alpha_x - \tilde{h}^2\alpha_x, \tag{54}$$

$$\frac{d\alpha_y}{d\ell} = -2\alpha_x\alpha_y - \tilde{h}^2\alpha_y. \tag{55}$$

It is insightful to define the bath anisotropy parameter,

$$\theta \equiv \left(\frac{\alpha_x-\alpha_y}{\alpha_x+\alpha_y}\right)^2, \tag{56}$$

whose beta function is

$$\frac{d\theta}{d\ell} = (\alpha_x+\alpha_y)\theta(1-\theta). \tag{57}$$

The anisotropy is thus relevant whenever the couplings are not finely tuned to the $U(1)$ symmetric point $\theta = 0$, and flows towards the maximally anisotropic case $\theta = 1$, i.e., where the larger of the two couplings dominates and the other one becomes irrelevant, as depicted in Fig. 4. As we will now see, since the subdominant bath is irrelevant it can be integrated out easily, leading to a low-energy description similar to that of the x model with renormalized coupling.

Consider the case $\alpha_x \gg \alpha_y$. We focus on the regime $1-\alpha_x \gg \tilde{h}^2$ (i.e., far enough from the BKT transition), where simple analytical estimations can be made as the effect of $\tilde{h}$ on the flow of the couplings is negligible. Indeed, the equations can be solved by utilizing the fact that $\delta\alpha = \alpha_x - \alpha_y$ is an approximate constant along the flow. The resulting low-energy theory is described by the renormalized splitting h_R, and couplings, $\alpha_{x,R} = \delta\alpha \gg \alpha_{y,R} = (h_R/\omega_c)^{\delta\alpha}\alpha_y$. The BKT transition is determined by the renormalized value of the dominant coupling, $\alpha_{x,R}$, such that the system becomes localized when $\alpha_{x,R} > 1 + \mathcal{O}(h/\omega_c)$, and below this value the effective energy scale assumes the familiar form $h_R = \omega_c(h/\omega_c)^{1/(1-\alpha_{x,R})}$ (note that the exponent depends on $\alpha_{x,R}$ and not on the bare value). More details on the RG flow are shown in Appendix E.

To proceed, we note that the low-energy theory we have arrived at is nearly identical to that in the 1bSB, the one difference being a remaining weak coupling to the y bath ($\alpha_{y,R} \ll 1$), which we may now treat perturbatively. The operator σ_x is only weakly dressed (it is renormalized only in the short first section of the flow when α_y is of order 1), and thus we can once again conclude that its correlation functions will assume a one parameter scaling form, as in Eq. (27),

$$\chi_x''(\omega) = \frac{1}{\omega} f_{\alpha_{x,R}}\left(\frac{\omega}{h_R}\right) + \delta\chi_x''(\omega), \tag{58}$$

where $f_{\alpha_{x,R}}$ is a scaling function and the perturbative correction due to the coupling to the losing bath is of the form $\delta\chi_x''(\omega) = \alpha_{y,R}\frac{1}{\omega}\tilde{f}_{\alpha_{x,R}}(\frac{\omega}{h_R})$, with a different scaling function $\tilde{f}_{\alpha_{x,R}}$. When averaging over the second term, the strong renormalization of the losing bath, $\alpha_{y,R} = (h_R/\omega_c)^{\delta\alpha}\alpha_y$, effectively enhances the exponent in the renormalized distribution, which results in a subleading frequency dependence of the averaged $\delta\chi_x''$; see Appendix F.

In contrast, the y susceptibility does not assume a one parameter scaling form. Rather, it is suppressed by additional factors of h_R/ω_c, such that in the IR limit all spectral weight is shifted to frequencies of order ω_c; see Appendix F.

The electronic self-energy can be evaluated following the analysis of Sec. V C. Remarkably, the leading term in (58) assumes the same form as in the x model,

$$\Sigma''(\omega) = -A_{\alpha_{x,R}}\rho_F g_x^2 \left|\frac{\omega}{h_{c,R}}\right|^\gamma, \tag{59}$$

where $\gamma = (1+\beta)(1-\alpha_{x,R})$, and $A_{\delta\alpha_{x,R}} = \int_0^\infty \frac{f_{\alpha_{x,R}}(x)}{x^{1+\gamma}}dx$. The subleading correction owing to $\delta\chi_x''$ is of the form $\delta\Sigma''(\omega) = -B\alpha_y\frac{\gamma}{\gamma+\delta\alpha}\rho_F g_x^2|\frac{\omega}{h_{c,R}}|^\gamma|\frac{\omega}{\omega_c}|^{\delta\alpha}$ with $B = \int_0^\infty \frac{\tilde{f}_{\delta\alpha}(x)}{x^{1+\gamma+\delta\alpha}}dx$. An additional subleading contribution to Σ'' is related to the coupling to the y susceptibility, which we denote by $\delta\Sigma_y''$. While an explicit evaluation of $\delta\Sigma_y''$ is more challenging, the fact that $\delta\Sigma_y''$ is also subleading follows from the additional "nonuniversal" factors of h_R/ω_c, which it contains, similar to the case of $\delta\chi_x''$.

As mentioned before, this RG-based analysis is perturbative in the strength of the weaker coupling α_y. However, at strong coupling (when $\alpha_x \gtrsim \alpha_y$) the value of $\alpha_{x,R}$ is no longer equal to $\delta\alpha$, and the BKT line $\alpha_{x,R} = 1$ changes accordingly. The problem has been solved numerically for varying coupling strengths by [62], who found that at strong coupling the BKT line approaches the line $\alpha_x = \alpha_y$ asymptotically. This behavior is depicted schematically in Fig. 2.

Note that for $U(1)$-symmetric points, $\alpha_x = \alpha_y = \alpha$, the coupling to the two baths is frustrated and the system flows to weak coupling [60,61,63]. This case will be discussed in an upcoming paper [64].

B. The xz model

Consider now the case where $\alpha_x, \alpha_z > 0$ and $\alpha_y = 0$, dubbed xz model. The major difference in this case compared to the xy model is the fact that the z bath is aligned with the "field" h_z, making the two baths inequivalent. The flow

equations in this case are

$$\frac{d\tilde{h}}{d\ell} = (1-\alpha_x)\tilde{h}, \tag{60}$$

$$\frac{d\alpha_x}{d\ell} = -2\alpha_z\alpha_x - \tilde{h}^2\alpha_x, \tag{61}$$

$$\frac{d\alpha_z}{d\ell} = -2\alpha_x\alpha_z. \tag{62}$$

As before, we neglect the effect of $\tilde{h}$ on the initial flow of the couplings, assuming that it is sufficiently small.

Let us start with the case $\alpha_x \gg \alpha_z$. Then, as the x bath dominates, the flow is essentially identical to the xy model with z replacing y. The main difference is that σ_z, albeit being strongly dressed in the low-energy theory, has a nonzero equilibrium expectation value, i.e., $\langle\sigma_z\rangle \neq 0$. The z susceptibility therefore contains a term proportional to $\langle\sigma_z\rangle^2\delta(\omega)$. Fortunately, $\langle\sigma_z\rangle$ may be evaluated using the sum rule Eq. (C5), yielding

$$\langle\sigma_z\rangle_\infty = \left(\frac{h_R}{\omega_c}\right)^{\delta\alpha}\left(a + b\frac{1-\left(\frac{h_R}{\omega_c}\right)^{1-2\delta\alpha}}{1-2\delta\alpha}\right), \tag{63}$$

with a and b being numerical constants, which depend on α_x, α_z. Interestingly, this static piece contributes an elastic scattering term to the electronic self-energy,

$$\Sigma''_{\rm el}(\omega) \propto -\rho_F g_z^2 \begin{cases} \left(\frac{h_{c,R}}{\omega_c}\right)^{2\delta\alpha} & \delta\alpha < 1/2, \\ \frac{h_{c,R}}{\omega_c}\log^2\left(\frac{\omega_c}{h_{c,R}}\right) & \delta\alpha = 1/2, \\ \left(\frac{h_{c,R}}{\omega_c}\right)^{2-2\delta\alpha} & 1/2 < \delta\alpha < 1, \end{cases} \tag{64}$$

where $\mathcal{O}(1)$ numerical coefficients have been suppressed for clarity. The leading "inelastic" part of Σ'' due to the x bath is identical to Eq. (59), with appropriate renormalized value $\alpha_{x,R}$. It is worth recalling that the interaction-induced elastic term of Eq. (64) adds to the elastic scattering term due to on-site potential in the general model. We comment on this matter further in the discussion on the dc resistivity in Sec. VIII.

We move on to the second scenario, where $\alpha_z \gg \alpha_x$. In this case, the z bath dominates such that the coupling flows to a finite value, $\alpha_{z,R} = \delta\alpha = \alpha_z - \alpha_x$. Unlike the previous case, h_z is only marginally renormalized, such that the low-energy parameters are given by

$$h_R = \frac{\delta\alpha}{\alpha_z}h_z, \tag{65}$$

$$\alpha_{x,R} = \alpha_x\left(\frac{h_R}{\omega_c}\right)^{\delta\alpha}. \tag{66}$$

Note that when $\delta\alpha \to 0$, h_R assumes the form shown in the xy isotropic case, although the system is not $U(1)$ symmetric because of h_z. For $\alpha_x = 0$ the TLS is static, and the scattering is solely elastic. The effect of α_x is an addition of a weak inelastic term to χ''_z, as well as a coupling of the electrons to χ''_x. This will result in an inelastic contribution in the self-energy such that $\Sigma'' = \Sigma''_{\rm el} + \Sigma''_{\rm inel}$ with

$$\Sigma''_{\rm el} \approx -\frac{\rho_F g_z^2}{2\pi}, \tag{67}$$

$$\Sigma''_{\rm inel}(\omega) \propto -\frac{|\omega|^{\gamma+2\delta\alpha}}{h_{c,R}^{\gamma}\omega_c^{2\delta\alpha}}, \tag{68}$$

where $\gamma = (1+\beta)$. While this is the leading inelastic contribution, it does not give rise to any MFL/NFL behavior for the considered splitting distributions with $\beta \geqslant 0$. For more details, see Appendix F.

C. The *xyz* model

Understanding the physical picture in the more general case where the electrons are coupled to all operators of the TLSs (i.e., $\alpha_a > 0$ for $a = x, y, z$ and $h_x \equiv 0$), dubbed xyz model, rests upon the fact that the anisotropy remains relevant such that one bath dominates over the others at low energies. The qualitative behavior is thus reduced to one of the two previous cases. In the case where the coupling to the x or y baths is the largest, the behavior is qualitatively similar to the x model, albeit with a renormalized coupling, $\alpha_R(\boldsymbol{\alpha})$ (of the dominating bath), which depends on the initial values of the couplings. Specifically, the leading inelastic contribution to the self-energy satisfies

$$\Sigma''(\omega) - \Sigma''(0) \sim -|\omega|^\gamma, \quad \gamma = (1+\beta_z)(1-\alpha_R), \tag{69}$$

as we have demonstrated above. In addition, above a critical value, $\alpha_R(\boldsymbol{\alpha}) \geqslant 1$, the TLSs undergo a BKT transition to the localized phase, where most of the scattering is elastic. If, on the other hand, the z bath dominates, the TLSs act essentially as static impurities, with an additional weak, FL-like inelastic contribution to the self-energy (as in the xz model with dominant z bath).

VII. "BIASED" MODEL

All of our above analyses relied on the assumption that the field $\boldsymbol{h}$ is parallel to the $\hat{z}$ direction. Note that this cannot always be made the case by rotating a generic field $\boldsymbol{h} = (h_x, 0, h_z)$ to point in this direction, since this would induce correlations between the couplings g_x, g_z, and in turn will lead to a mbSB model with correlated baths. We thus keep the couplings uncorrelated and treat the case were $h_x, h_z \neq 0$.

A. Biased *x* model

We start by considering the x model with finite parallel fields $h_x > 0$. We thus allow $\boldsymbol{h}$ to be randomly distributed in the x–z plane with a joint distribution $\mathcal{P}_{\beta_x,\beta_z}(h_x, h_z) \propto h_x^{\beta_x}h_z^{\beta_z}$ for $h_x, h_z < h_c$. This variant maps into the "biased" 1bSB, where a field parallel to the bath coupling $h_x\sigma_x$ is added to the Hamiltonian [37,39]. The main difference in this case is that h_x is unaffected by the bath (it commutes with the interaction), while h_z is renormalized as before. In addition, the presence of a nonzero h_x implies that $\langle\sigma_x(t\to\infty)\rangle \neq 0$, which leads to an "elastic" delta function term in $\chi''_x(\omega)$, namely, the x susceptibility can be written as $\chi''_x \equiv \chi''_{\rm el} + \chi''_{\rm inel}$, with

$$\chi''_{x,\rm el}(\omega) = \left(\frac{2}{\pi}\tan^{-1}\left(\frac{h_x}{h_R}\right)\right)^2\delta(\omega), \tag{70}$$

$$\chi''_{x,\rm inel}(\omega) = \frac{1}{\omega}f\left(\frac{\omega}{h_R}, \frac{\omega}{h_x}\right). \tag{71}$$

To leading order in $h_{c,R}/h_c$, we find that the low-energy self-energy is given by $\Sigma'' \equiv \Sigma''_{\rm el} + \Sigma''_{\rm inel}$, with

$$\Sigma''_{\rm el}(\omega) = -\frac{M}{N}\rho_F g^2, \tag{72}$$

$$\Sigma''_{\rm inel}(\omega) \propto -\frac{M}{N}\rho_F g^2 \left|\frac{\omega}{h_c}\right|^{1+\beta_x} \left|\frac{\omega}{h_{c,R}}\right|^{(1+\beta_z)(1-\alpha)}. \tag{73}$$

Note that since $h_c/h_{c,R} \propto (\omega_c/h_c)^{\alpha/(1-\alpha)} \gg 1$, the elastic term contributes most of the spectral weight to χ_x, and correspondingly, $\Sigma''_{\rm el} \gg \Sigma''_{\rm inel}$ at low energies. We provide an explicit calculation using the two parameter scaling form along with exact evaluation at the TP in Appendix D 5. Notice that for the reasonable case of $\beta_x \geqslant 0$ this results in a FL for $\alpha < 1$ and approaches a MFL behavior near $\alpha = 1$.

B. Biased *xyz* model

We now treat the most general variant of our model, where the couplings and fields are all allowed to point in generic directions. The behavior of the biased *xyz* model can be similarly understood from the RG analysis, where Eqs. (52) are modified as [65]

$$\frac{d\tilde{h}_z}{d\ell} = (1-\alpha_x-\alpha_y)\tilde{h}_z, \tag{74}$$

$$\frac{d\tilde{h}_x}{d\ell} = (1-\alpha_z-\alpha_y)\tilde{h}_x, \tag{75}$$

$$\frac{d\alpha_a}{d\ell} = -\left(\sum_{b\neq a}\alpha_b + (1-\delta_{az})\tilde{h}_z^2 + (1-\delta_{ax})\tilde{h}_x^2\right)\alpha_a, \tag{76}$$

where $\tilde{h}_x \equiv h_x/\omega_c$. Importantly, there are no cross terms between the fields h_x, h_z such that the qualitative behavior can be understood in terms of the approximately independent flow of the individual fields. Furthermore, since a bias along $\hat{y}$ is forbidden in order to respect time-reversal symmetry, the physical picture in the biased *xyz* model is determined by whether or not the y bath dominates. In the case where the y bath dominates, both the "field" h_z and the "bias" h_x will be renormalized according to Eq. (26) with $\alpha \to \alpha_{y,R}$. Consequently, the leading inelastic contribution to the self-energy will take the form

$$\Sigma''(\omega) \ - \Sigma''(0) \sim -|\omega|^\gamma, \tag{77}$$

$$\gamma = (2+\beta_x+\beta_z)(1-\alpha_{y,R}), \tag{78}$$

along with elastic scattering terms as in Eq. (64). In contrast, if the x or z baths dominate, the behavior will be analogous the biased x model with the appropriate renormalized couplings of the dominant bath; see Eq. (73).

VIII. TRANSPORT

Let us begin by considering the electronic contribution to the electrical conductivity, and later incorporate the effect of the TLSs on the optical conductivity. Using the Kubo formula, the real part of the conductivity (associated with the electrons) is given by

$$\sigma_{\rm el}(\Omega) = \frac{{\rm Im}\Pi^R_{J_x}(\Omega)}{\Omega}, \tag{79}$$

where $\Pi^R_{J_x}$ is the retarded current correlator (along the x direction). The current operator is given by $\boldsymbol{J} = \sum_a \int_{\boldsymbol{k}} \boldsymbol{v}_{\boldsymbol{k}} c^\dagger_{a\boldsymbol{k}} c_{a\boldsymbol{k}}$ and $\boldsymbol{v}_{\boldsymbol{k}} = \nabla_{\boldsymbol{k}}\varepsilon_{\boldsymbol{k}}$. The evaluation of $\Pi^R_{J_x}$ is greatly simplified since all vertex corrections vanish due to the spatial randomness of the couplings to the local TLSs (similarly to Refs. [66,67]). The electronic optical conductivity is thus given by

$$\sigma_{\rm el}(\Omega) = \frac{1}{\Omega}\int_\omega \int_{\boldsymbol{k}} v_{\boldsymbol{k}}^2 \mathcal{A}_{\boldsymbol{k}}(\omega)\mathcal{A}_{\boldsymbol{k}}(\Omega+\omega)[f(\omega)-f(\Omega+\omega)]. \tag{80}$$

Here $\mathcal{A}_{\boldsymbol{k}}(\omega) \equiv -\frac{1}{\pi}{\rm Im}G^R_{\boldsymbol{k}}(\omega)$ is the electronic spectral function and $f(\omega)$ denotes the Fermi distribution function.

In the dc limit, the conductivity is given by

$$\sigma_{\rm el}(\Omega\to 0) = \frac{v_F^2\rho_F}{16T}\int \frac{d\omega}{2\pi}\frac{1}{|\Sigma''(\omega)|}{\rm sech}^2\left(\frac{\omega}{2T}\right). \tag{81}$$

Hence, the T scaling of the dc resistivity follows the single-particle lifetime. It is instructive to first consider $\rho(T)$ in the x model. For $\alpha < 1$, the low-T behavior, $T \ll h_{c,R}$, is of the form

$$\rho(T) = \rho_0 + AT^\gamma, \tag{82}$$

where here we have restored the on-site disorder by setting $V^2 > 0$, corresponding to the residual resistivity term ρ_0, and $\gamma = (1+\beta)(1-\alpha)$. Similarly, for $\alpha = 1$, we have that $\rho(T) - \rho_0 \propto 1/|\log(T)|^{1+\beta}$; and for $\alpha > 1 + h_c/\omega_c$, the TLSs are frozen at $T = 0$, and thus contribute to the residual resistivity, with FL-like finite-T corrections [$\rho(T) - \rho_0 \propto T^2$]. In the intermediate regime, $1 < \alpha < 1 + h_c/\omega_c$, the resistivity interpolates smoothly between these two behaviors. In the more general *xyz* model, the resistivity follows the behavior of the x model whenever the transverse couplings α_x or α_y dominate (as discussed extensively in the Sec. VI). Whereas, if the parallel coupling α_z dominates, the scattering is mainly elastic with weak FL-like temperature scaling. Similarly, the biased *xyz* model follows analogous behavior to that of the x model provided that the y bath dominates, and to the biased x model if the x or z bath dominates.

We proceed to consider the optical conductivity. In addition to the contribution due to the itinerant electrons, we also assume that each TLS carries a randomly distributed dipole moment (recall the TLS are phenomenologically related to charged collective degrees of freedom), which depends on the state of the TLS,

$$H_{\rm dipole} = \sum_{r,l} \boldsymbol{E}_r \cdot \left(\boldsymbol{d}^z_{r,l}\sigma^z_{r,l} + \boldsymbol{d}^x_{r,l}\sigma^x_{r,l}\right). \tag{83}$$

Here $\boldsymbol{E}_r$ is the local electric field and $\boldsymbol{d}^{x,z}_{r,l}$ denote uncorrelated Gaussian random dipole moments of the TLS flavors, with variances $d^2_{x,z}$. In total, the (longitudinal) optical conductivity takes the two-component form

$$\sigma(\Omega) = \sigma_{\rm el}(\Omega) + \sigma_{\rm TLS}(\Omega). \tag{84}$$

The electronic contribution is standard and follows straightforwardly from the form of the self-energy. In particular, at

low energies, where $-\Sigma''(\omega) = \frac{\Gamma}{2} + c|\omega|^\gamma$ (i.e., we restore the elastic scattering term that does not affect any of the previous results), if the scattering is mainly inelastic ($\Gamma \ll c|\Omega|^\gamma$),

$$\sigma_{\rm el}(\Omega) \sim \begin{cases} \frac{1}{\Omega^\gamma} & \gamma < 1, \\ \frac{1}{\Omega \log^2(1/\Omega)} & \gamma = 1, \\ \frac{1}{\Omega^{2-\gamma}} & \gamma > 1. \end{cases} \tag{85}$$

while if the scattering is mainly elastic ($\Gamma \gg c|\Omega|^\gamma$),

$$\sigma_{\rm el}(\Omega) \sim \frac{1}{\Gamma} - \frac{2^{\gamma+1}c}{(\gamma+1)\Gamma^2}|\Omega|^\gamma. \tag{86}$$

At higher energies, $\Omega \gtrsim h_{c,R}$, the TLS contribution to Σ'' saturates to a constant such that $\sigma_{\rm el}(\Omega \gtrsim h_{c,R}) \sim 1/\Omega$.

The TLS contribution is given by

$$\sigma_{\rm TLS}(\Omega) = \Omega\big(d_x^2\overline{\chi_x''}(\Omega) + d_z^2\overline{\chi_z''}(\Omega)\big). \tag{87}$$

Interestingly, the TLS contribution follows the frequency dependence of the inelastic part of Σ'' (provided that the y bath is not dominant). In particular, if the dipole moments are not negligibly small, $\sigma_{\rm TLS}$ might constitute the leading frequency dependence, leading to a positive slope and nonmonotonic behavior of the optical conductivity. Defining the energy scale $\Omega_* = \sqrt{\rho_F} v_F/d_a$, we find that if the scattering is dominantly elastic and $\Gamma \gg \Omega_*$ then there will be an increasing optical conductivity around zero frequency. If inelastic scattering dominates, $\Gamma \ll \Omega_*$, the optical conductivity will always be decreasing around zero frequency, but will begin increasing for frequencies of order $\Omega_{\rm mIR} \sim Z\Omega_*$ if the system is a FL (with Z the quasiparticle weight), or $\Omega_{\rm mIR} \sim (\Omega_*/c)^{1/\gamma}$ if the system is a NFL (i.e., if $\gamma \leqslant 1$), leading to a so-called mid-IR peak around energies of order $h_{c,R}$ (assuming that $\Omega_{\rm mIR} < h_{c,R}$) [26].

The assumption that led to Eq. (87) was that there are sufficiently many TLSs that carry a dipole moment and can therefore be optically excited. At the same time one expects that there are TLSs that locally come with a quadrupole moment. For example, they could locally distort a state of fourfold rotation symmetry to a lower symmetry. In this case one can excite the TLS via inelastic light scattering and the Raman response function [68,69] will measure directly the TLS susceptibilities

$$R_{\alpha,\beta}(\Omega) = \big(q^x_{\alpha,\beta}\big)^2\overline{\chi_x''}(\Omega) + \big(q^x_{\alpha,\beta}\big)^2\overline{\chi_z''}(\Omega). \tag{88}$$

Here $q^\kappa_{\alpha,\beta}$ is the quadrupole moment due to the κ component of the TLS pseudospin. The individual tensor elements can be detected by an appropriate combination of the polarization of the incoming and scattered light. Hence, the presence of TLS can, at least partially account for the broad Raman continuum that has been observed in many correlated electron materials [68].

It is intriguing to examine the MFL/NFL transport properties of our model through the viewpoint of Planckian dissipation and the putative bound on transport times [7]. Since there is no unique definition for the transport time, we consider two different approaches. Following Ref. [7], we can associate the transport time to the single-particle lifetime as the two are proportional in our model. In that case, the inverse transport time is Planckian in the sense that $1/\tau_{\rm tr} \sim T$ with an $\mathcal{O}(1)$ coefficient for the NFL phase while at the MFL point the coefficient is $\mathcal{O}(1/\ln(1/T))$. In particular, our model trivially satisfies a "Planckian bound" because of the Kramers-Kroning relations between the real and imaginary parts of Σ [70]. Alternatively the inverse transport time can be defined in terms of the energy scale for which the dc and ac conductivities become comparable [66]: $\sigma(\tau_{\rm tr}^{-1}(T), T = 0) \sim \sigma(\Omega = 0, T)$. This procedure agrees with the single-particle lifetime result for NFLs while for the MFL case the transport time contains an additional log correction: $\tau_{\rm tr}^{-1} \sim T/\log^2(T)$.

Lastly, relying on the analysis of the weakly disordered MFL (or NFL) model in Ref. [71], we note that the Wiedemann-Franz law is obeyed as $T \to 0$, regardless of the existence of well-defined Landau quasiparticles (in the absence of vertex correction, as we have here, the analysis is essentially identical).

IX. THERMODYNAMICS

In this section, we study thermodynamic properties of the model. We mainly consider the x model and further discuss the expected behavior in the xyz model. It is worth noting that a direct evaluation of the free energy from the saddle point of the large-N effective action is challenging due to its non-Gaussian nature. Instead, we obtain the specific heat from the internal energy, and corroborate our results with an alternative derivation of the specific heat from the entropy, where in particular we confirm the absence of $T = 0$ residual entropy in our model.

Consider the internal energy density

$$U \equiv \frac{1}{N\mathcal{V}}\langle H_{\rm el} + H_{\rm TLS} + H_{\rm int}\rangle, \tag{89}$$

where $H_{\rm el}$ and $H_{\rm TLS}$ correspond to the first two terms in (1), respectively, and $\mathcal{V}$ is the volume of the system. Let us henceforth suppress the factor $1/(N\mathcal{V})$ and assume $r = N/M = 1$ for simplicity. By employing the equation of motion for the retarded and advanced electronic Green's functions (see Appendix G), we may write

$$\langle H_{\rm el} + H_{\rm int}\rangle = \int_{\boldsymbol{k}}\int_\omega \omega n_F(\omega)\mathcal{A}_{\boldsymbol{k}}(\omega) \equiv U_{\rm el,0}, \tag{90}$$

where $n_F(\omega)$ is the Fermi function. Note that because of the locality of the self-energy, $U_{\rm el,0}$ corresponds to the internal energy of noninteracting electrons. To see this, we use the fact that $\int_{\boldsymbol{k}} \mathcal{A}(\omega, \boldsymbol{k}) = \rho_F$, hence $U_{\rm el,0} = \rho_F \int_\omega \omega n_F(\omega)$. The specific heat related to $U_{\rm el,0}$ is given by

$$c_{\rm el,0} = \rho_F \int_\omega \omega \frac{\partial n_F(\omega)}{\partial T} = \frac{\pi^2}{3}\rho_F T, \tag{91}$$

i.e., the specific heat of noninteracting electrons. Interestingly, all interaction effects are encoded in the renormalized TLS part of the internal energy, $U_{\rm TLS} = \langle H_{\rm TLS}\rangle$, which we will now evaluate. Using the sum rule Eq. (C5), we may express the

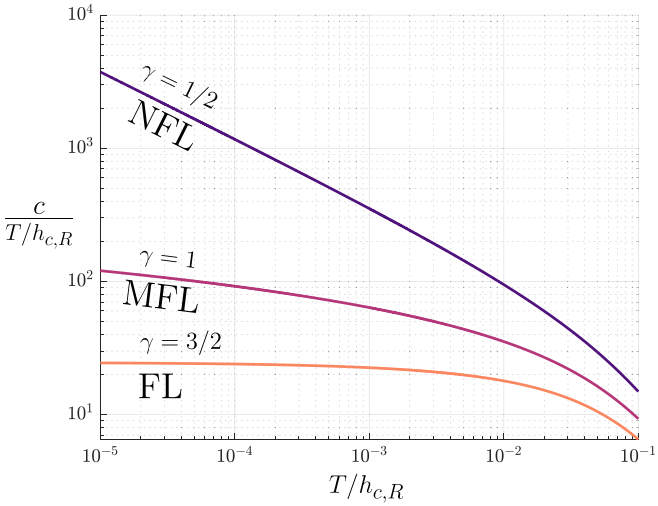

FIG. 5. Specific heat, as extracted from the internal energy at the Toulouse point, for values of γ for FL, MFL, and NFL behavior (corresponding to $\beta = 2, 1, 0$). As expected from the above scaling arguments (99), at low temperatures the ratio c/T approaches a constant for the FL, has logarithmic divergence for the MFL, and polynomial divergence with exponent $1-\gamma$ for the NFL.

TLS specific heat as

$$c_{\rm TLS} = \frac{1}{2}\int_\omega \omega \frac{\partial \overline{\chi_x''}(\omega, T)}{\partial T}. \tag{92}$$

As $h_{c,R}$ is the only energy scale, for $\omega, T \ll h_{c,R}$ one can write the TLS susceptibility as a two-component scaling form, i.e., $\overline{\chi''}(\omega, T) = \frac{1}{\omega}F(\frac{\omega}{h_{c,R}}, \frac{\omega}{T})$. For concreteness, we assume the following scaling form:

$$\overline{\chi_x''}(\omega, T) = \overline{\chi_x''}(\omega, T=0) \times \left(\frac{|\omega|}{\sqrt{\omega^2 + (aT)^2}}\right)^\varphi \tag{93}$$

with $a \sim \mathcal{O}(1)$ some numerical coefficient and scaling exponent $\varphi > 0$ [72], which both affect the result only by a numerical prefactor and not the T dependence.

Using Eq. (92), we obtain that

$$c_{\rm TLS} \sim \begin{cases} \frac{T}{h_{c,R}} & \gamma > 1, \\ \frac{T}{h_{c,R}} \log \frac{h_{c,R}}{T} & \gamma = 1, \\ \left(\frac{T}{h_{c,R}}\right)^\gamma & \gamma < 1. \end{cases} \tag{94}$$

In addition, Eq. (92) can be evaluated numerically at the Toulouse point where the exact temperature dependence of $\chi''(\omega, T)$ is known analytically. The results, confirming the T dependence found in Eq. (94), are shown in Fig. 5 for h distributions corresponding at the Toulouse point to a FL, MFL and NFL.

We corroborate the above discussion with an alternative derivation of the specific heat from the entropy. To do so, we consider the addition of a single TLS per site to the theory with $M = 0$. In the language of the SB model, the excess entropy added to the system, defined by $\delta S \equiv S(M = 1) - S(M = 0)$, is known as the "impurity contribution" [38]. Importantly, δS is determined by the spectral function of the bath, the renormalized splitting and the temperature. Hence, since the TLSs are decoupled for any M provided that $N \gg 1$ (as $\overline{g_{ijl}g_{ijl'}} = 0$ for $l' \neq l$), and the particle-hole bath is ohmic, we may write the entropy of M TLSs by adding the impurity contributions of the individual TLSs.

Considering the x model, the impurity contribution of a single TLS for $\alpha < 1$ is given by [38,53,73,74]

$$\delta S(x) = \begin{cases} \frac{\alpha\pi}{3}x + \mathcal{O}(x^3) & x \ll 1, \\ \log 2 & x \gg 1, \end{cases} \tag{95}$$

where $x = T/h_R$. The entropy of the full system (i.e., in the large-M, N limit) can therefore be written as

$$S(T) = S_0(T) + \Delta S(T), \tag{96}$$

where $S_0 = S(M = 0)$ denotes the contribution of the noninteracting electrons and

$$\Delta S(T) = M\mathcal{V}\int_0^{h_{c,R}} \mathcal{P}_r(h_R)\delta S\left(\frac{T}{h_R}\right)dh_R. \tag{97}$$

To evaluate ΔS, we divide the integral over h_R to $h_R < T$ and $h_R > T$, denoted by $S_<$ and $S_>$, respectively, and, substituting (36) in (97), we obtain

$$S_<(T) \approx \frac{\pi\alpha\gamma}{3h_{c,R}^\gamma}\frac{T}{h_{c,R}}\frac{h_{c,R}^{\gamma-1} - T^{\gamma-1}}{\gamma - 1}, \tag{98}$$

$$S_>(T) \approx \frac{\pi\alpha}{3}a_\gamma\left(\frac{T}{h_{c,R}}\right)^\gamma, \tag{99}$$

where $a_\gamma \equiv \int_0^1 \delta S(\frac{1}{x})x^{\gamma-1}dx \approx 1/\gamma$. Hence, for $T \ll h_{c,R}$,

$$\Delta S(T) \sim \begin{cases} \frac{T}{h_{c,R}} & \gamma > 1, \\ \frac{T}{h_{c,R}} \log \frac{h_{c,R}}{T} & \gamma = 1, \\ \left(\frac{T}{h_{c,R}}\right)^\gamma & \gamma < 1. \end{cases} \tag{100}$$

Since $S_0 \sim T$, the total entropy S obeys the same scaling as ΔS, which also holds for the specific heat, in agreement with Eq. (94).

It is also worth noting that there is no residual extensive entropy at $T = 0$, in contrast to theories of MFLs constructed from variants of the Sachdev-Ye-Kitaev model [6].

Physically, the T scaling of the impurity contribution in Eq. (96) stems from scattering of the low-energy modes of the bath by the TLS. Hence in the cases where α_x or α_y dominate, the impurity contribution is expected to follow Eq. (96) since the low-energy theory is identical to that of the x model (up to weak perturbations). It therefore follows that $S(T)$ satisfies Eq. (100). Moreover, when α_z dominates, the system realizes a FL (with additional static impurities) and weak renormalization of the splittings, such that $S(T) \propto T$.

X. SUPERCONDUCTIVITY

In order to study the superconducting instability, we introduce spinful electrons to the Hamiltonian, Eqs. (1) and (2), namely, we let $c_{i,\boldsymbol{r}}^\dagger \to c_{i,s,\boldsymbol{r}}^\dagger$ with $s = \{\uparrow, \downarrow\}$. Note that since the TLSs have no spin structure (assuming that the underlying glass is nonmagnetic), the couplings $\boldsymbol{g}$ do not depend on spin

index s, and the interaction term is diagonal in spin space. The mapping of the spinful variant of the Hamiltonian onto a spin-boson problem is similar to the spinless case, but one must also consider the anomalous bilocal field, analogously to Eqs. (10) and (11), defined as

$$F_{r,r'}(\tau,\tau') = \frac{1}{N}\sum_i c_{i,\downarrow,r}(\tau)c_{i,\uparrow,r'}(\tau'), \tag{101}$$

and enforced via the anomalous self-energy $\Phi_{r,r'}(\tau,\tau')$ [42,75]; see Appendix H.

We study the critical temperature T_c as a function of the couplings $\boldsymbol{\alpha}$. Approaching the SC state from the normal state, where $\Phi = 0$, we obtain T_c as the solution for the linearized Eliashberg equation (in imaginary frequency) for the local anomalous self-energy $\Phi(i\omega)$,

$$\Phi(i\omega) = T\sum_{\omega'}\frac{D_\Phi(i\omega - i\omega')}{|\omega' + i\Sigma(i\omega')|}\Phi(i\omega'), \tag{102}$$

where the bosonic propagator is

$$D_\Phi(i\omega) = \sum_{a=x,y,z}\lambda_a h_{c,R}\chi_a(i\omega)\times(-1)^{\delta_{a,y}}. \tag{103}$$

Notice that while the interactions via g_x and g_z mediate pairing, g_y is pair breaking, as it couples to a current in fermion-flavor space (i.e., to an antisymmetric fermionic bilinear). By rewriting Eq. (102) as $\Phi(i\omega) = \sum_{\omega'} K(i\omega, i\omega')\Phi(i\omega')$, we see that T_c is determined as the minimal temperature for which the largest eigenvalue of the kernel K is equal to 1.

In the following we first obtain T_c in the spinful variant of the x model as a representative example and later comment on the behavior of T_c in other variants. Specifically, we estimate T_c analytically by focusing on the "weak" ($\lambda \equiv \lambda_x \ll 1$) and "strong" ($\lambda \gg 1$) coupling regimes, where T_c is much smaller or larger than the characteristic energy scale $h_{c,R}$, respectively. Note that "weak" and "strong" coupling regimes do not necessarily correspond to small or large values of α. For simplicity we further assume that $h_c/E_F \ll |1-\alpha|$ (to avoid the complications resulting from the slowdown of the RG flow of h around $\alpha = 1$) and mainly focus on the parametric dependence of T_c, ignoring various $\mathcal{O}(1)$ coefficients.

1. *Weak coupling* ($\lambda \ll 1$)

In the weak-coupling regime, we rely on the $\alpha < 1$ and $T = 0$ form of the susceptibility given in Eq. (37), and assume an ω/T scaling with exponent $\varphi > 0$ [similar to Eq. (93)],

$$\overline{\chi_x''}(\omega,T) = \mathrm{sgn}(\omega)\gamma A_\alpha\frac{|\omega|^{\gamma-1}}{h_{c,R}^{\gamma}}\times\min\left(1,\frac{|\omega|}{T}\right)^{\varphi}. \tag{104}$$

We perform analytical continuation to imaginary frequencies (see Appendix H) and obtain

$$D_\Phi(i\omega_n) \propto \frac{\gamma\lambda}{\gamma-1}\left(1-\left|\frac{\omega_n}{h_{c,R}}\right|^{\gamma-1}\right). \tag{105}$$

In the FL phase $\gamma > 1$, the leading piece of D_Φ at low T is constant, resulting in the conventional BCS-like form of T_c. However, in the MFL point or NFL phase, where $\gamma \leqslant 1$, $D_\Phi(i\omega)$ diverges logarithmically or with exponent $\gamma - 1$, respectively. Consequently, T_c crosses over from a BCS-like form to an algebraic, quantum critical form. Explicitly, by solving the Eliashberg equation in this regime, we obtain

$$T_c \propto h_{c,R}\begin{cases}\exp\left(-\frac{\gamma-1}{\gamma\lambda}\right), & \gamma > 1+\mathcal{O}(\sqrt{\lambda})\\ \exp\left(-\frac{1}{\sqrt{\lambda}}\right), & \gamma = 1\\ \left(\frac{\gamma\lambda}{1-\gamma}\right)^{\frac{1}{1-\gamma}}, & \gamma < 1-\mathcal{O}(\sqrt{\lambda}).\end{cases} \tag{106}$$

The results for $\gamma \leqslant 1$ are similar to those found by [76–78] for other cases of quantum critical pairing. For consistency, we must require that $T_c \ll h_{c,R}$, which translates into $\lambda \ll 1$. Because of the vanishing of $h_{c,R}$ as $\alpha \to 1$, the problem will eventually cross over to the strong coupling regime, where $T_c \gg h_{c,R}$, beyond some intermediate value $\alpha < 1$.

2. *Strong coupling* ($\lambda \gg 1$)

We now consider the transition to superconductivity at temperatures $T \gg h_{c,R}$. In this regime, we obtain the finite-T TLS susceptibility via a combination of scaling arguments with known results. For details, see Appendix H. We find that

$$\overline{\chi_x''}(\omega,T) \propto \frac{h_c^2}{E_F^{2\alpha}}\frac{(\max(|\omega|, a_\alpha T))^{2-2\alpha}}{\omega} \tag{107}$$

where $a_\alpha = \mathcal{O}(1)$. Similarly to the weak coupling limit, we obtain the parametric form of T_c by performing the analytical continuation and solving the linearized Eliashberg equation; see Appendix H. Remarkably, in an analogous fashion to the "weak coupling" regime, we find that T_c exhibits a series of crossovers from a quantum critical, to a "marginal BCS" [76], to a conventional BCS-like form as the coupling is *increased* (rather than decreased, as in the "weak coupling" case). Explicitly, we have that

$$T_c \propto E_F\begin{cases}\left(\frac{\alpha^2}{3-2\alpha}\epsilon\right)^{\frac{1}{3-2\alpha}}, & \alpha < 3/2-\mathcal{O}(\sqrt{\epsilon})\\ \exp\left(-\frac{1}{\alpha\sqrt{\epsilon}}\right), & \alpha = 3/2\\ \exp\left(-\frac{2\alpha-3}{\alpha^2\epsilon}\right), & \alpha > 3/2+\mathcal{O}(\sqrt{\epsilon})\end{cases} \tag{108}$$

where we defined the small parameter $\epsilon \equiv \frac{M}{N}(\frac{h_c}{E_F})^2 \ll 1$. Interestingly, T_c decreases up to $\alpha = 3$, where it has a local minimum. For larger values of α, it increases and approaches the limiting form $T_c \propto E_F\exp(-1/\alpha\epsilon)$. We expect our results to hold as long as $\alpha \ll E_F/h_c$ (such that $\alpha\epsilon \ll 1$). For consistency of the strong coupling analysis we must require that $T_c \gg h_{c,R}$. While this is trivially fulfilled when $\alpha > 1$, for $\alpha < 1$ this results in the requirement $\lambda \gg 1$, which is, as expected, complimentary to the weak coupling condition.

Intuitively, the reduction of T_c for larger values of the coupling corresponds to the fact that at finite T, while the TLSs are nearly frozen (i.e., resemble classical impurities), they preserve their quantum mechanical nature and can thus mediate pairing. The accessible low-energy spectral weight for pairing diminishes with the coupling strength and therefore suppresses superconductivity (this trend is reversed beyond $\alpha = 3$, where the increase in the coupling strength is more

significant than the shift of the remaining spectral weight to high frequencies).

3. Superconductivity in other model variants

Following from the discussion of the x model, we comment on the expected behavior of T_c in generic variants of the model. Let us first consider cases with $g_y = 0$ (i.e., without pair-breaking interactions). In the "weak coupling" regime, in the sense defined above, T_c is determined by the behavior of the dominant bath, such that it qualitatively follows that of the x model if α_x is dominant, or otherwise assumes a conventional BCS-like form (see Fig. 2). In the "strong coupling" limit, however, the behavior of T_c is nonuniversal, namely, it is determined by the susceptibility of the least irrelevant operator. Mapping out the quantitative form of $T_c(\boldsymbol{\alpha})$ necessitate the exact renormalized exponents of the TLS susceptibilities and is beyond the scope of our paper (given the leading exponents, the analysis is identical to that of the x model). However, recalling that in both cases where α_x or α_z dominates, the strong coupling behavior approaches a BCS-like form, we expect that at intermediate couplings, T_c will smoothly interpolate from a quantum critical to a BCS-like form as α_z is increased for fixed α_x. Lastly, introducing pair-breaking interactions, i.e., a nonzero α_y, suppresses T_c [75].

XI. 1/N CORRECTIONS

In this section, we discuss two perturbative corrections that arise at leading order in $1/N$: the validity of the self-averaging assumption and the effect of electron-mediated TLS-TLS interactions, i.e., RKKY-like interactions.

A. Validity of self-averaging

An important assumption of our above analysis lies in the self-averaging of the model, which allows us to replace the sum over many TLS susceptibilities by its mean value [with respect to $\mathcal{P}_r(h)$], because of the fact that its variance is suppressed by a factor of $1/M$. While this assumption is clearly valid in the limit $M \to \infty$, for any finite (but still large) M the standard deviation may dominate over the mean at sufficiently low energies because of its different frequency dependence. Indeed, consider the variance of the average TLS autocorrelation function in imaginary time,

$$\mathrm{Var}\left(\frac{1}{M}\sum_{i=1}^{M}\left\langle\sigma_x^i(\tau)\sigma_x^i(0)\right\rangle\right) = \frac{1}{M}\int \mathcal{P}_r(h_R)S(\tau)^2 dh_R. \quad (109)$$

For simplicity let us focus on the regime of interest $\alpha < 1$ in the x model. By dimensional considerations, at long times the dimensionless integral must be proportional to $(h_{c,R}\tau)^{-\gamma}$ (assuming that there is no obstruction to taking the upper integration limit to ∞, which is the case for $\gamma < 4$). As a result, by taking the square root and transforming to the frequency domain, we obtain the root-mean square of the TLS susceptibility,

$$\sqrt{\overline{(\chi_x'')^2}}(\omega) \sim \frac{1}{\sqrt{M}}\frac{|\omega|^{\gamma/2-1}}{h_{c,R}^{\gamma/2}}. \quad (110)$$

Comparing Eq. (110) to the mean in Eq. (37), we conclude that statistical fluctuations can be neglected above a parametrically small energy scale, $\omega \sim M^{-1/\gamma}h_{c,R}$. For energies below this scale, the self-averaging assumption is no longer valid and a more systematic treatment of the $1/M$ (and $1/N$) fluctuations is needed to determine the behavior of the model.

B. RKKY interactions

Another effect arising when N is taken to be large but finite, is the emergence of RKKY-like interactions between the different TLSs, mediated by the itinerant electrons. We analyze this perturbative effect in the spirit of Ref. [79]. We shall consider the x model for simplicity, the generalization to other variants is straightforward.

Including the RKKY-like term,

$$H_{\mathrm{RKKY}} = \sum_{jk}\frac{g_{ijk,\boldsymbol{r}}g_{i'j'k',\boldsymbol{r}'}}{N^2g^2} \times \Pi_{jk}(\boldsymbol{r}-\boldsymbol{r}',\tau-\tau')\sigma^x_{i,\boldsymbol{r}}(\tau)\sigma^x_{i',\boldsymbol{r}'}(\tau'), \quad (111)$$

each TLS will now feel the effect of a subohmic bath arising from the RKKY coupling to other TLSs, in addition to the ohmic particle-hole bath. Following the analysis of Ref. [79], this contribution to the bath will be proportional to $\overline{\chi_x(i\omega)}$, and thus the full bath will be of the form

$$\Pi(i\omega) = \alpha|\omega| + \frac{\lambda^2}{N}h_{c,R}^{2-\gamma}|\omega|^{\gamma-1} \quad (112)$$

with subohmic exponent $2-\gamma$.

In the limit of large yet finite M, N, the subohmic contribution to the bath may be neglected above the small energy scale $\omega \sim (\frac{\lambda^2}{\alpha N})^{1/(2-\gamma)}h_{c,R}$. However, even for very large N this energy scale will eventually approach $h_{c,R}$ near $\alpha \to 1$ since λ diverges as $h_{c,R} \to 0$. Below this scale, the self-consistent approximation of a TLS-induced subohmic bath acting on itself breaks down, and a more systematic analysis is needed to determine the behavior at very low energies. The low-energy behavior in similar cases [80] suggests that this state remains nontrivial in the sense that γ is expected to remain less than 2.

Lastly, note that the subohmic nature of the TLS-induced bath considered above is a result of perturbing around the $N, M \to \infty$ saddle point. In a more realistic finite-but-large-M setting, we expect the subohmic behavior to crossover to ohmic below a small energy scale, corresponding to the lowest renormalized splitting of the nearby TLSs. In this case, a qualitative change in the behavior of the TLSs is less obvious, and the system might remain stable to the weak RKKY-like interactions even at low energies.

XII. DISCUSSION AND OUTLOOK

In this paper, we have studied a class of large-N models of itinerant electrons interacting with local two-level systems via spatially random couplings. These models, inspired by the possibility of metallic glassiness in strongly correlated materials, exhibit a remarkably rich phenomenology at low energies. Most strikingly our theory hosts a robust extended NFL phase in a considerable part of parameter space. At the crossover from FL to NFL our theory realizes a MFL that

shows strange metallic behavior with T-linear resistivity and $T\log(1/T)$ specific heat. Note that the MFL/NFL behavior does not necessitate the existence of a quantum critical point. Physically, the departure from FL behavior is rooted in the fact that the characteristic energy of each TLS is algebraically suppressed by the interaction, thus providing significant spectral weight of low-energy excitations, which constitute an efficient scattering mechanism for the electronic degrees of freedom. These abundant low-energy excitations further manifest in a rich phenomenology of the critical transition temperature to the superconducting ground state of the system.

The physical picture of the simplest variant of our theory (the x model), studied in Ref. [26], qualitatively persists upon relaxing several simplifying assumptions, such as allowing for interactions with different operators of the TLSs and introducing arbitrary TLS fields. Aiming at more realistic models, we further considered the effects of relaxing additional simplifications, such as $1/N$ corrections, spatial correlations in $\boldsymbol{g}_{ijl,\boldsymbol{r}}$ and the self-averaging assumption. While these tend to suppress the NFL behavior found in this paper below some energy scale suppressed by powers of N, there are physical reasons to think that this scale remains small in a realistic setting. Specifically, recalling that TLSs in physical systems are extended objects, the interaction would retain a high degree of connectivity (i.e., each TLS would interact with many electrons and vice versa), which in turn could preserve the self-averaging property, and frustrate effects of RKKY-like interactions.

It is interesting to ask what is the relation between the interaction strengths ($\alpha_{x,y,z}$) and the actual physical knobs in realistic systems. This is a complicated question as the microscopic origin of such TLSs is not well understood. However, there have been many studies attempting to provide a microscopic theoretical framework for understanding these objects [27,76,81–85]. It is possible that as the system approaches a glassy charge or spin ordering transition, the shape, size, and other properties of these TLSs change, affecting the magnitude of their coupling to electrons, or the relative sizes of the couplings to the x, y, z operators. Thus, tuning a physical knob of the system could be parameterized as a nontrivial path in the space of couplings, leading to a nontrivial variation of the exponent in the electronic self-energy.

To this end, another issue concerns the density of states of TLSs, which is parametrically larger than that of the electrons (i.e., $h_{c,R}^{-1} \gg \rho_F$). A direct consequence is the seemingly enhanced coupling $\lambda \equiv \frac{M}{N}\frac{\rho_F}{h_{c,R}}\alpha$ that appears in the electronic self-energy. It appears, however, natural to expect that $\alpha \sim \lambda$ at least up to some intermediate coupling strength. This is the case if $M/N \sim h_{c,R}^{-1}/\rho_F \ll 1$, i.e., if the TLSs are sparse compared to the electrons. Physically, this seems plausible based on the mesoscopic considerations mentioned above.

Non-Fermi-liquid behavior is ultimately tied to an anomalous spectrum of gapless excitations. Such a spectrum is usually believed to emerge from collective modes with soft long wavelength fluctuations. As we showed in this paper, it can also be the result of quantum fluctuations of modes that are localized in a region of size l, where each mode has an excitation gap $E_{\min} \sim h_R$ but is governed by a singular distribution function $\mathcal{P}(h_R) \propto h_R^{\gamma-1}$ with $\gamma > 0$. Even if the correlation function for a given h_R decays rapidly in time, $\chi_{h_R}(\tau) \sim \exp(-h_R\tau)$, the average $\chi_{\rm av}(\tau) = \int dh_R \mathcal{P}(h_R)\chi_{h_R}(\tau)$ then decays like a power law $\propto \tau^{-\gamma}$ and the system becomes critical. For the static susceptibility, $\chi_{\rm av}(T) = \int^{1/T} d\tau\, \chi_{\rm av}(\tau)$, it follows that $\chi_{\rm av}(T) \propto T^{\gamma-1}$ and $C \propto T^{\gamma}$ for the heat capacity. Non-Fermi-liquid behavior occurs for $\gamma < 1$.

Such a singular distribution function was also obtained from quantum Griffiths behavior [86]. Let us therefore compare and contrast our results with the ones that follow from quantum Griffiths physics, where rare, large droplets of size l occur with probability $p_l \propto e^{-cl^d}$ and possess an exponentially small gap $h_l \propto e^{-bl^d}$ [86]. This yields a power law form

$$\mathcal{P}(h_R) = \int dl^d p_l \delta(h_R - h_l) \propto h_R^{\gamma-1}, \tag{113}$$

with nonuniversal exponent $\gamma = b/c$. Exponentially small gaps occur for the random transverse-field Ising model [86]. However, as soon as one includes the coupling to conduction electrons, large droplets will freeze by the Caldeira-Leggett mechanism, and one rather finds superparamagnetic behavior of classical droplets [87,88]. On the other hand, for systems with a continuous order parameter symmetry power-law quantum Griffiths behavior becomes possible even in the presence of particle-hole excitations [89]. This behavior was also seen in recent numerical simulations [31]. In contrast to this quantum Griffiths behavior, in our approach we consider the coupling of TLSs of characteristic size of several lattice spacings to conduction electrons. While isolated TLSs are governed by $\mathcal{P}(h) \propto h^{\beta}$, that is, on its own, not sufficiently singular ($\beta > 0$), strong local quantum fluctuations due to the coupling to conduction-electrons renormalize the excitation gap $h \to h_R \sim h^{1/(1-\alpha)}$, which reduces the exponent $\beta + 1 \to \beta_R + 1 = (\beta + 1)(1 - \alpha)$.

While our theory does not aim to realistically describe any specific material, the existence of a tunable non-Fermi-liquid phase in a controlled microscopic theory could shed light on some aspects of strange metallicity. It provides a viewpoint on the widely observed extended strange metal regime [14–16,90,91] that does not rely on a putative quantum critical point. Further, while our theory does not describe any specific material, the results that we obtained could be more general than the model used to derive them and might give a hint that one should interpret a $AT + BT^2\,T$ dependence of the resistivity [4,14,15,90,92–95] in terms of an intermediate exponent [96]. Interestingly, this interpretation (also known as power-law liquid) has been shown to be consistent with experimental data of strange metals [25,97–100].

Several natural questions remain open. Aiming to better understand more realistic scenarios, a systematic study of our model for finite-N is called for, either by analytical or numerical methods. In addition, the behavior deep inside the superconducting state might exhibit interesting new physics, as the electrons constituting the ohmic bath in the normal state are becoming gapped, which has nontrivial effects on the TLSs and vice versa. More broadly, one may consider various other physical systems containing a coexistence of electrons

and two-level systems, where the framework developed in this paper can be applied.

ACKNOWLEDGMENTS

We thank G. Grissonnanche, S. A. Kivelson, C. Murthy, A. Pandey, B. Ramshaw, and B. Spivak for numerous discussions and for a collaboration on prior unpublished work. We are grateful to Natan Andrei, Girsh Blumberg, Andrey Chubukov, Rafael Fernandes, Tobias Holder, Yuval Oreg, and Alexander Shnirman for helpful discussions. J.S. was supported by the German Research Foundation (DFG) through CRC TRR 288 "ElastoQMat," Project B01 and a Weston Visiting Professorship at the Weizmann Institute of Science. E.B. was supported by the European Research Council (ERC) under grant HQMAT (Grant Agreement No. 817799) and by the Israel-US Binational Science Foundation (BSF). Some of this work was performed at KITP, supported in part by the National Science Foundation under Grant No. PHY-1748958.

APPENDIX A: DIAGRAMMATIC APPROACH TO MAPPING

We now present an alternative approach for the mapping to the spin-boson model, where we demonstrate, by a perturbative expansion of the interaction, that the electrons constitute an ohmic bath to the TLSs. Importantly, because of the spatial randomness of the couplings, the bath is that of noninteracting particle-hole pairs, i.e., it is independent of the electronic self-energy. Consider the correlation function for a single TLS of flavor s, $S_s^x(\tau) \equiv \langle T_\tau\{\sigma_s^x(\tau)\sigma_s^x(0)\}\rangle$. The expansion in interaction vertices reads (we suppress the spatial index $\boldsymbol{r}$ since all operators act on the same site)

$$S_s^x(\tau) = \left\langle T_\tau\left\{\sigma_s^x(\tau)\sigma_s^x(0)\sum_{n=0}^{\infty}\frac{(-1)^n}{n!}\left[\prod_{i=1\ldots n}\left(\int d\tau_i \sum_{abc}\frac{g_{abc}}{N}\sigma_a^x(\tau_i)c_b^\dagger(\tau_i)c_c(\tau_i)\right)\right]\right\}\right\rangle, \tag{A1}$$

which decouples into a sum of terms of the form

$$I_n = \int_{\tau_1,\tau_2\ldots\tau_n}\sum_{a_1b_1c_1a_2b_2c_2\ldots}\left(\frac{g_{a_1b_1c_1}}{N}\frac{g_{a_2b_2c_2}}{N}\ldots\right)\langle T_\tau\{\sigma_s^x(\tau)\sigma_s^x(0)(\sigma_{a_1}^x(\tau_i)\ldots\sigma_{a_n}^x(\tau_n))\}\rangle\langle T_\tau\{c_{b_1}^\dagger(\tau_{i_1})c_{c_1}(\tau_{i_1})c_{b_2}^\dagger(\tau_{i_2})c_{c_2}(\tau_{i_2})\cdots\}\rangle. \tag{A2}$$

By integrating over the realizations of g_{abc}, we note that (i) terms where all interaction TLS indices $a_1,\ldots,a_n \neq s$ are "disconnected" and cancel with the vacuum diagrams; and (ii) if only some (but not all) $a_i = s$, the contribution is either subleading in $1/N$ or corresponds to a self-energy insertion for the electrons (see Fig. 6). Thus if we treat the electrons self-consistently as being fully dressed, the only relevant insertions of the interaction are those in which $a_i = s$.

Hence I_n can be written as (all TLS indices $= s$)

$$I_n = \int_{\tau_1,\tau_2\ldots}\sum_{b_1c_1b_2c_2\ldots}\left(\frac{g_{sb_1c_1}}{N}\frac{g_{sb_2c_2}}{N}\ldots\right)\langle T_\tau\{\sigma_s^x(\tau)\sigma_s^x(0)(\sigma_s^x(\tau_i)\ldots\sigma_s^x(\tau_n))\}\rangle\langle T_\tau\{c_{b_1}^\dagger(\tau_{i_1})c_{c_1}(\tau_{i_1})c_{b_2}^\dagger(\tau_{i_2})c_{c_2}(\tau_{i_2})\cdots\}\rangle \tag{A3}$$

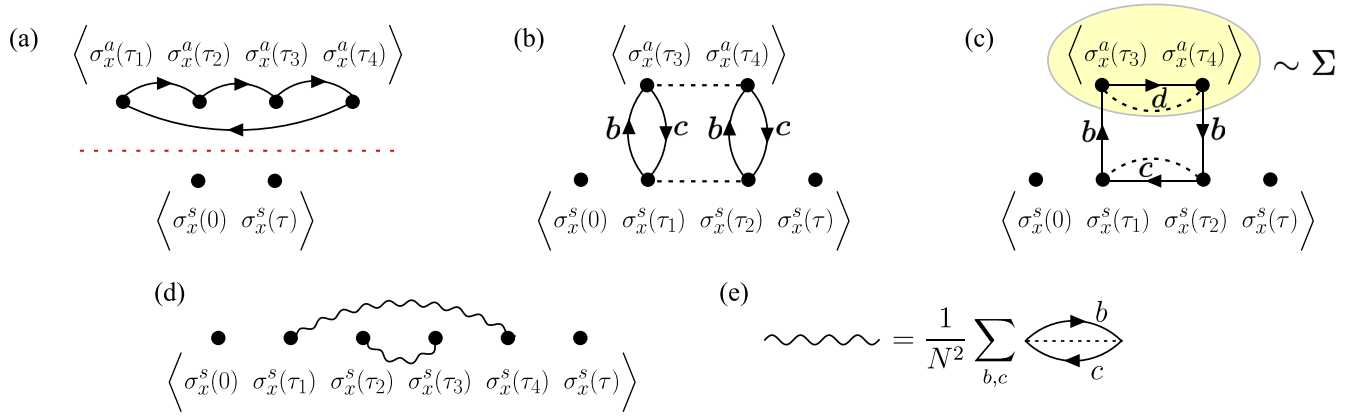

FIG. 6. Examples of diagrams considered in the mapping. (a) If all insertions are of other TLSs, the bubble disconnects from the "external vertices" and cancels with the vacuum diagrams. (b) Other insertions of different TLSs become subleading in N. (c) The contribution of insertions of a different TLS $a \neq s$ can be absorbed into the full electron green function. (d) Example of a contributing diagram, with the wavy lines representing particle hole pairs [as defined in (e)]. Here electrons are denoted by solid line, contractions over realizations of g_{abc} by dashed lines and TLS operators, which do not admit a direct diagrammatic expansion, by full circles.

Considering the electronic part (including the couplings $g_{sb_ic_i}$), we see that the leading order contribution in $1/N$ corresponds to terms with $b_1 \neq c_1 \neq b_2 \ldots$ (all indices are distinct), namely,

$$C_n \equiv \sum_{b_1 c_1 b_2 c_2 \ldots} \frac{1}{N^n} \left(g^2_{sb_1c_1} g^2_{sb_2c_2} \ldots\right) \left\langle T_\tau \left\{ c^\dagger_{b_1}(\tau_{i_1}) c_{c_1}(\tau_{i_1}) c^\dagger_{c_1}(\tau_{i_2}) c_{b_1}(\tau_{i_2}) \right\} \right\rangle \tag{A4}$$

$$\times \left\langle T_\tau \left\{ c^\dagger_{b_2}(\tau_{i_1}) c_{c_2}(\tau_{i_3}) c^\dagger_{c_2}(\tau_{i_4}) c_{b_2}(\tau_{i_4}) \right\} \right\rangle \ldots + \text{permutations} + \mathcal{O}\left(\frac{1}{N}\right). \tag{A5}$$

The particle-hole pairs obey the bosonic Wick's theorem since the couplings g_{abc} obey it. Therefore,

$$C_n = \tilde{J}(\tau_{i_1} - \tau_{i_2}) \tilde{J}(\tau_{i_3} - \tau_{i_4}) \cdots + \text{permutations} \tag{A6}$$

where we have denoted

$$\tilde{J}(\tau_{i_1} - \tau_{i_2}) \equiv g^2 G(\tau_{i_1} - \tau_{i_2}) G(\tau_{i_2} - \tau_{i_1}). \tag{A7}$$

As mentioned earlier, the fact that the bath is ohmic follows from spatial randomness of the couplings, which translates to the TLS being coupled to the local particle-hole correlators, with $G(\tau) = \int_{\boldsymbol{k}} G(\tau, \boldsymbol{k})$. Upon analytical continuation, the spectral function of the bath is given by

$$\tilde{J}(\omega) = \frac{g^2 \rho_F^2}{2\pi} \omega \equiv \eta \omega, \tag{A8}$$

such that the dimensionless coupling strength (using the conventions of Ref. [39]) is given by

$$\alpha \equiv \frac{2}{\pi} \eta = \frac{g^2 \rho_F^2}{\pi^2}. \tag{A9}$$

Generalizing the derivation to the xyz model is straightforward.

APPENDIX B: DETAILS OF RG FLOW OF 1bSB

We present here the calculation of the renormalized scale h_R in the different regimes I − III in the 1bSB. As a reminder, the flow equations are, to order $\tilde{h}^2$,

$$\frac{d\alpha}{d\ell} = -\tilde{h}^2 \alpha, \tag{B1}$$

$$\frac{d\tilde{h}}{d\ell} = (1-\alpha)\tilde{h}. \tag{B2}$$

We allow the couplings to flow until there is only one energy scale in the problem, i.e., until the cutoff $\Lambda = \omega_c * \exp(-\ell)$ and TLS energy $h_R = \tilde{h}\Lambda'$ become equal, which is given by $\tilde{h}(\ell^*) = 1$.

We start with the regime where $(1-\alpha) \gg \tilde{h}^2$ so that the flow of α is much slower than the flow of $\tilde{h}$. We can thus solve the flow of $\tilde{h}$ while treating α as a constant, and the weak change in α at the end of the flow (when $\tilde{h}$ approaches 1) will only change the result by a multiplicative factor, which is absorbed into the definition of the prefactor c_α in Eq. (B4). Therefore, allowing $\tilde{h}$ to flow until it reaches the value 1 we find that

$$(1-\alpha)\ell^* = \log \frac{\omega_c}{h}. \tag{B3}$$

Inserting Eq. (B3) into the definition of h_R, we find that

$$h_R = c_\alpha \omega_c \left(\frac{h}{\omega_c}\right)^{\frac{1}{1-\alpha}}. \tag{B4}$$

As mentioned in the main text, this prefactor c_α cannot be determined merely from the RG flow. However, it can be extracted using exact techniques such as bosonization or Bethe ansatz [47–50], and is given by

$$c_\alpha = \left(\Gamma(1-\alpha) \exp\left(\alpha \log \alpha + (1-\alpha)\log(1-\alpha)\right)\right)^{\frac{1}{1-\alpha}}, \tag{B5}$$

which satisfies the two known limits $c_0 = 1, c_{1/2} = \pi/4$. We now study the regime near the BKT transition, $\alpha \approx 1$. In this regime, we define $J = 1 - \alpha$ such that $|J| \ll 1$. The RG equations then approximately become

$$\frac{dJ}{d\ell} = \tilde{h}^2, \tag{B6}$$

$$\frac{d\tilde{h}}{d\ell} = \tilde{h} J. \tag{B7}$$

Note that the combination $x_0 \equiv \tilde{h}^2 - J^2$ obeys

$$\frac{1}{2}\frac{dx_0}{d\ell} = \tilde{h}\frac{d\tilde{h}}{d\ell} - J\frac{dJ}{d\ell} = 0 \tag{B8}$$

so x_0 is constant along flow lines. Using this relation the equations can thus be solved easily

$$\frac{d\tilde{h}}{d\ell} = \tilde{h}\sqrt{\tilde{h}^2 - x_0}, \tag{B9}$$

$$\ell^* = \int_{\tilde{h}_0}^{1} \frac{d\tilde{h}}{\tilde{h}\sqrt{\tilde{h}^2 - x_0}}, \tag{B10}$$

where $\tilde{h}_0 = h/\omega_c$. We now separate to the cases where $x_0 > 0$ and $x_0 < 0$. If $x_0 < 0$, we have that

$$\ell^* = \frac{\operatorname{asinh}\left(\frac{\sqrt{-x_0}}{\tilde{h}_0}\right) - \operatorname{asinh}(\sqrt{-x_0})}{\sqrt{-x_0}}, \tag{B11}$$

$$h_R = \omega_c \left(\frac{\frac{\sqrt{-x_0}}{\tilde{h}_0} + \sqrt{1 - \frac{x_0}{\tilde{h}_0^2}}}{\sqrt{-x_0} + \sqrt{1 - x_0}} \right)^{-\frac{1}{\sqrt{-x_0}}}. \tag{B12}$$

If $\tilde{h}_0^2 \ll J$ this expression simplifies to the power law given earlier. On the other hand, for $x_0 \to 0$ this expression becomes the familiar Kondo scale of the isotropic Kondo model $h_R \propto \omega_c \exp(-1/\tilde{h}_0)$. For $x_0 > 0$, we obtain that

$$\ell^* = \frac{\operatorname{atan}\left(\sqrt{\frac{1-x_0}{x_0}}\right) - \operatorname{sgn}(J)\operatorname{atan}\left(\sqrt{\frac{\tilde{h}_0^2 - x_0}{x_0}}\right)}{\sqrt{x_0}}. \tag{B13}$$

Taking $x_0 \to 0$ also gives the isotropic Kondo result $\ell = 1/\tilde{h}_0$. Setting $J = 0$ we find that $\ell = \pi/2\tilde{h}_0$. Therefore, in this regime we can approximately think of the renormalized scale as taking the form $h_R \propto \omega_c \exp(-b(J,\tilde{h}_0)/\tilde{h}_0)$ with b being a slowly varying function of order 1. However, when the flow approaches the BKT line $J = -\tilde{h}$ this approximation does not hold, and instead the renormalized scale is set by the distance from the transition

$$h_R \propto \omega_c \exp\left(-\frac{\pi}{\sqrt{x_0}}\right). \tag{B14}$$

APPENDIX C: SUM RULES FOR THE 1bSB

This is based on a short analysis first derived in [53]. We define the correlation function

$$\langle \sigma_x(t)\sigma_x(0)\rangle = \int_\omega e^{i\omega t} A_x(\omega). \tag{C1}$$

This is related to the dynamical susceptibility by the fluctuation dissipation theorem [41],

$$A_x(\omega) = \left(1 + \coth\left(\frac{\beta\omega}{2}\right)\right)\chi_x''(\omega). \tag{C2}$$

Additionally, the following equation of motion derives from the Hamiltonian (23):

$$i\frac{d\sigma_x}{dt} = -2h\sigma_y. \tag{C3}$$

Thus, by Fourier transforming $\langle\sigma_x(t)\sigma_x(0)\rangle$, $\langle\frac{d\sigma_x}{dt}(t)\sigma_x(0)\rangle$ and $\langle\frac{d\sigma_x}{dt}(t)\frac{d\sigma_x}{dt}(0)\rangle$, setting $t = 0$ and using the antisymmetry of $\chi_x''(\omega)$ we obtain the three sum rules

$$1 = \int_\omega \chi_x''(\omega)\coth\left(\frac{\beta\omega}{2}\right), \tag{C4}$$

$$2h\langle\sigma_z\rangle = \int_\omega \omega\chi_x''(\omega), \tag{C5}$$

$$4h^2 = \int_\omega \omega^2\chi_x''(\omega)\coth\left(\frac{\beta\omega}{2}\right). \tag{C6}$$

APPENDIX D: EXPLICIT CALCULATION OF $\overline{\chi_x''}$ FOR THE x MODEL

The average (imaginary part of the) susceptibility is given by

$$\overline{\chi_x''} = \int_0^{h_c} \chi_x''(\omega,h)\mathcal{P}_\beta(h)dh \tag{D1}$$

$$= \int_0^{h_{c,R}} \frac{1}{\omega} f_\alpha\left(\frac{\omega}{h_R}\right)\mathcal{P}_r(h_R)dh_R \tag{D2}$$

$$= \mathrm{sgn}(\omega)\int_{|\omega|/h_{c,R}}^{\infty} \frac{f_\alpha(x)}{x^2}\mathcal{P}_r(|\omega|/x)dx. \tag{D3}$$

The result of this integral thus depends on the renormalized distribution $\mathcal{P}_r$.

1. $\alpha < 1$

Starting with $h_R = c_\alpha\omega_c(h/\omega_c)^{1/(1-\alpha)} \Rightarrow h = (h_R/c_\alpha)^{1-\alpha}\omega_c^{-\alpha}$,

$$\mathcal{P}(h_R) = \mathcal{P}(h)\left(\frac{dh}{dh_R}\right) \tag{D4}$$

$$= \mathcal{N}h_R^{\beta(1-\alpha)-\alpha}. \tag{D5}$$

Since the distribution is cut off at $h_{c,R} = h_R(h_c)$, the normalization constant must be $\mathcal{N} = \gamma/h_{c,R}^{\gamma}$, with $\gamma = \beta(1-\alpha) - \alpha + 1 = (1+\beta)(1-\alpha)$. Inserting this into the averaged susceptibility gives

$$\overline{\chi_x''} = \mathrm{sgn}(\omega)\int_{|\omega|/h_{c,R}}^{\infty} \frac{f_\alpha(x)}{x^2}\frac{\gamma|\omega|^{\gamma-1}}{h_{c,R}^{\gamma}x^{\gamma-1}}dx \tag{D6}$$

$$= \frac{1}{\omega}\left|\frac{\omega}{h_{c,R}}\right|^{\gamma} \times \gamma\int_{|\omega|/h_{c,R}}^{\infty}\frac{f_\alpha(x)}{x^{\gamma-1}}dx. \tag{D7}$$

Using that fact that at long times $\chi(t) \propto 1/t^2$, we see that $\chi_x''(\omega/h_R) \propto \omega \Rightarrow f_\alpha(x \ll 1) \propto x^2$. Near the lower integration limit the integrand is $\propto 1/x^{\gamma-3}$. If $\gamma < 2$ then the integral converges when taking $\omega/h_{c,R} \to 0$, and can thus be considered as a constant. (If $\gamma > 2$ then the integral diverges and the resulting frequency dependence is $\overline{\chi_x''} \propto \omega$. This is because the averaged susceptibility cannot decay faster than the susceptibility of the TLSs with highest h.)

2. $\alpha \approx 1$

In this case we use $h_R = c_\alpha\omega_c\exp(-b\omega_c/h) \Rightarrow h = \frac{b\omega_c}{2\log(\frac{c_\alpha\omega_c}{h_R})}$, which gives the renormalized distribution

$$\mathcal{P}(h_R) = \frac{\mathcal{N}}{h_R\log^{2+\beta}\left(\frac{c_\alpha\omega_c}{h_R}\right)}, \tag{D8}$$

and the normalization can be found to be $\mathcal{N} = (1+\beta)\log^{1+\beta}(\omega_c/h_{c,R})$. We neglect for simplicity the factor of $c_\alpha \sim \mathcal{O}(1)$ inside the logarithm. The averaged susceptibility is then given by

$$\overline{\chi_x''} = \mathrm{sgn}(\omega)(1+\beta)\log^{1+\beta}(\omega_c/h_{c,R}) \times \int_{|\omega|/h_{c,R}}^{\infty}\frac{f_\alpha(x)}{x\log^{2+\beta}(x\omega_c/|\omega|)}dx. \tag{D9}$$

In order to simplify the integral, we rely on the fact that $f_\alpha(x \gg 1) \propto 1/x^{4-2\alpha}$ [53] and $f(x \ll 1) \propto x^2$, such that most of the weight of the integral is around $x \sim \mathcal{O}(1)$, for which $|\log(x)| \ll \log(\omega_c/|\omega|)$. Thus we may neglect the x dependence inside the log, giving the form of the susceptibility presented in the main text [using the sum rule Eq. (C4) for $\int_0^\infty f(x)/xdx = 1/2$].

3. Through the BKT transition ($1 < \alpha < 1 + h_c/E_F$)

The behavior around the BKT transition is slightly more convoluted, since when $x_0 \to 0^-$ the dependence of h_R on $\tilde{h}$ is slightly different. However, if we work close enough to the transition, we can just change variables to $y_0(\tilde{h}) = \sqrt{-x_0}$, and use the form (B14), which explicitly depends only on y_0. Changing variables we thus find that

$$\mathcal{P}(y_0) = \frac{1+\beta}{h_c^{1+\beta}}y_0\left(y_0^2 + J^2\right)^{\frac{-1+\beta}{2}} \tag{D10}$$

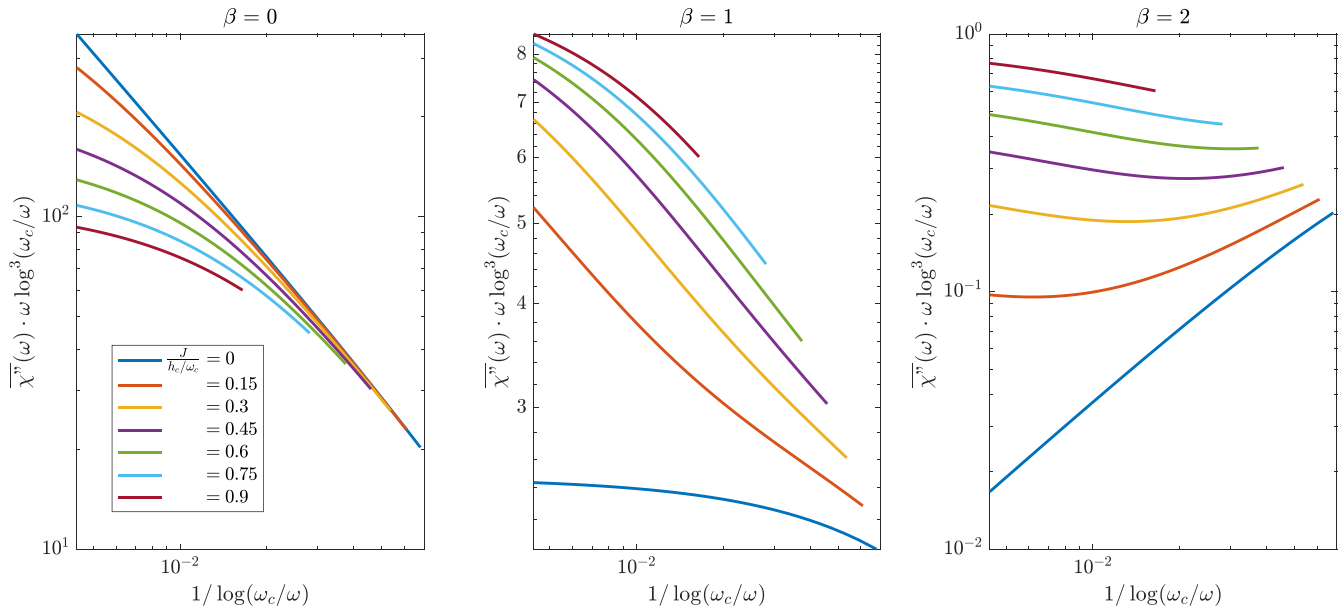

FIG. 7. Averaged susceptibility of TLSs around the BKT transition, for $\beta = 0, 1, 2$ and varying values of $1 < \alpha < 1 + h_c/\omega_c$. As expected, for $\alpha = 1$ ($J = 0$) the susceptibility is $\propto 1/\omega \log^{\beta+2}(\omega_c/\omega)$, while as $\alpha \to 1 + h_c/\omega_c$ ($J \to h_c/\omega_c$) this changes smoothly into $\propto 1/\omega \log^3(\omega_c/\omega)$. Note that the change in the cutoff of the values in the x axis with increasing J is due to the lowering of $h_{c,R}$.

with the cutoff $y_c = \sqrt{(h_c/w_c)^2 - J^2}$, and note that the range $y \in (0, y_c)$ covers only the range $h \in (|J|, h_c)$, since the TLSs with $h < |J|$ are in the localized phase. Thus, if $y_c \ll J$ we can approximate $\mathcal{P}(y_0) \propto y_0$ for any β, and we will therefore find that the distribution of $\mathcal{P}(h_R)$ will be identical to (D8) with $\beta = 1$. Thus, while for $\alpha = 1$ the exponent of the log will be $1 + \beta$, it will change smoothly to 2 near the end of the transition. We evaluate this numerically for any value of $1 < \alpha < 1 + h_c/\omega_c$ using the form given in (B13), and for the sake of the computation using the simplification $\chi''(\omega) = \delta(|\omega| - 2h_R)$ (since the results should not depend on the actual function $f(x)$ but rather on the form of the distribution $\mathcal{P}_r$). The results, confirming the analysis presented in this subsection and the previous one, are shown in Fig. 7.

4. Localized phase ($\alpha > 1 + h_c/E_F$)

In the localized phase, where $h_R = 0$, most of the weight of $\chi_x''(\omega)$ lies in a delta function at zero frequency. However, there are still weak residual quantum fluctuations. The form of these fluctuations can be found using a simple scaling analysis: We write the susceptibility at finite frequency as some function $\chi_x''(\omega) = \frac{1}{\omega} F(h/E_F, |\omega|/E_F)$. Reducing the cutoff to $E_F \to E_F/b$, the field rescales to $h/E_F \to h/E_F/b^(1-a)$. Since the result must be independent of b, we can set $b = |\omega|/E_F$ and find that

$$\chi_x'' = \frac{1}{\omega} F\left(\frac{h}{E_F}\left(\frac{E_F}{|\omega|}\right)^{1-\alpha}, 1\right) = \frac{1}{\omega} F\left(\frac{h(\omega)}{|\omega|}, 1\right) \tag{D11}$$

with $h(\omega) = h(|\omega|/E_F)^\alpha$ the frequency-dependent energy scale. Since $h(\omega) \ll \omega$, we may expand to second order using Fermi's golden rule, and find

$$\chi_x''(\omega) \propto \frac{1}{\omega}\left(\frac{h(\omega)}{\omega}\right)^2 \propto \mathrm{sign}(\omega)\frac{h^2}{E_F^{2\alpha}|\omega|^{3-2\alpha}}. \tag{D12}$$

The constant of proportionality may be set using the sum rule Eq. (C6), and then averaging over h we obtain Eq. (42) of the main text.

5. Biased case

For the biased case, the $\langle\sigma_x\rangle$ has an equilibrium value, so that $\langle\sigma_x(t \to \infty)\sigma_x(0)\rangle \to \langle\sigma_x\rangle^2$. We therefore decompose

$$\chi_x''(\omega) = \langle\sigma_x\rangle^2\delta(\omega) + \chi_{\mathrm{inel}}''(\omega). \tag{D13}$$

The equilibrium value, which contributes to the elastic scattering rate, is given by [56]

$$\langle\sigma_x\rangle = \frac{2}{\pi}\mathrm{atan}\left(\frac{h_x}{h_R}\right). \tag{D14}$$

Since $h_c/h_{c,R} \propto (\omega_c/h_c)^{\alpha/(1-\alpha)} \gg 1$, when averaging over h_x, h_R will not have much effect, and thus

$$\overline{\langle\sigma_x\rangle^2} = 1 - \mathcal{O}\left(\frac{h_{c,R}}{h_c}\right). \tag{D15}$$

The inelastic contribution χ_{inel}'' will now have a two-parameter scaling form

$$\chi_{\mathrm{inel}}''(\omega) = \frac{1}{\omega} f_\alpha\left(\frac{\omega}{h_R}, \frac{h_x}{h_R}\right). \tag{D16}$$

For $\alpha < 1$, the distributions are $\mathcal{P}(h_R) = \frac{\gamma}{h_{c,R}^\gamma} h_R^{\gamma-1}$, $\mathcal{P}(\epsilon) = \frac{1+\beta_x}{h_c^{1+\beta_x}} h_x^{\beta_x}$. Thus

$$\overline{\chi_{\mathrm{inel}}''}(\omega) = \int \mathcal{P}(h_R, h_x)\frac{1}{\omega} f_\alpha\left(\frac{\omega}{h_R}, \frac{h_x}{h_R}\right) dh_R dh_x$$

$$= (1+\beta_x)\gamma \frac{1}{h_{c,R}^{\gamma} h_c^{\beta_x+1}} \times \int h_R^{\gamma+\beta_x} y^{\beta_x} f_\alpha\left(\frac{\omega}{h_R}, y\right) \frac{dh_R}{\omega} dy$$
$$= (1+\beta_x)\gamma \frac{\omega^{\gamma+\beta_x}}{h_{c,R}^{\gamma} h_c^{\beta_x+1}} \int_{\omega/h_{c,R}}^{\infty} \frac{dx}{x^{\gamma+\beta_x+2}} \times \int_0^{h_c x/\omega} dy f(x,y).$$

Since $h_c/h_{c,R} \gg 1$, the upper limit of the y integral is large for any value of $x > \omega/h_{c,R}$. Therefore defining $\tilde{f}_\alpha(x) = \int_0^\infty f_\alpha(x,y)dy$, we can rewrite the susceptibility in a form similar to earlier,

$$\overline{\chi''_{\text{inel}}}(\omega) \approx (1+\beta_x)\gamma \frac{\omega^{\gamma+\beta_x}}{h_{c,R}^{\gamma} h_c^{1+\beta_x}} A_\alpha,$$
$$A_\alpha = \int_0^\infty \frac{\tilde{f}_\alpha(x)}{x^{\gamma+\beta_x+2}} dx.$$

Here we have assumed that the upper limit of the y integral and the lower limit of the x integral can be continued to ∞ safely. In this case, the validity of this assumption is not as clear as it was in the unbiased case. We verify this by an explicit calculation at the TP. There, the scaling function is given exactly by [56]

$$f(x,y) = \frac{4}{\pi}\frac{1}{x^2+4}\left(x\text{atan}(x+y) + x\text{atan}(x-y) + \ln\left(\frac{(1+(x+y)^2)(1+(x-y)^2)}{(1+y^2)^2}\right)\right). \quad \text{(D17)}$$

For large y, $f(x,y) \propto \frac{1}{y^2}$, so the integral over y indeed converges (this should generically be the case since the single-TLS susceptibility is an analytic symmetric function of y, which vanishes for $y \to \infty$). In this case the integral can be evaluated exactly, and we find that

$$\tilde{f}(x) = \frac{4x^2}{x^2+4}. \quad \text{(D18)}$$

We confirm that $\tilde{f}(x \ll 1) \propto x^2$, just as in the 1bSB, and our approximation is justified as long as $\gamma + \beta_x \leqslant 1$.

Near the critical point $\alpha \to 1$, the splitting distribution takes the form $\mathcal{P}(h_R) \propto \frac{1}{h_R(\log \omega_c/h_R)^{2+\beta_z}}$. When integrating over y, the effective distribution will change to $\mathcal{P}(h_R) \propto \frac{h_R^{\beta_x}}{(\log \omega_c/h_R)^{2+\beta_z}}$. Therefore the self-energy will be of the form

$$\Sigma''_{\text{inel}}(\omega) \propto \frac{\omega^{1+\beta_x}}{(\log \omega_c/h_R)^{2+\beta_z}}. \quad \text{(D19)}$$

Note that for the physical case $\beta_x = \beta_z = 0$ this will result in MFL-like behavior around $\alpha \approx 1$.

APPENDIX E: RG FLOW OF 2bSB

We now discuss the details of the RG flow of the two-bath SB model. We will mainly consider the region of interest, which is analogous to the $\alpha < 1$ region in the 1bSB, where the effect of h on the flow of the couplings is negligible and the renormalization of h_R is a power law. Therefore, we begin by examining the effect of the two couplings on each other. For example, for the xy model the RG equations will be [as in Eq. (55)]

$$\frac{d\alpha_x}{d\ell} = \frac{d\alpha_y}{d\ell} = -2\alpha_x\alpha_y + \mathcal{O}(\tilde{h}^2). \quad \text{(E1)}$$

We can simplify these equations by using the constant of flow $\delta\alpha = \alpha_x - \alpha_y$, which is approximately conserved along flow. We assume $\delta\alpha > 0$ without loss of generality. We can then simply integrate the equations,

$$2\ell = \int_{\alpha_x(\ell)}^{\alpha_x^0} \frac{d\alpha_x}{\alpha_x(\alpha_x - \delta\alpha)} = \frac{\log\left(\frac{r}{1-\delta\alpha/\alpha_x}\right)}{\delta\alpha} \quad \text{(E2)}$$

where $r = \alpha_y^0/\alpha_x^0$, and α_a^0 are the bare couplings. We thus find that

$$\alpha_x(\ell) = \frac{\delta\alpha}{1 - re^{-2\delta\alpha\ell}}, \quad \text{(E3)}$$
$$\alpha_y(\ell) = \frac{r\delta\alpha}{e^{2\delta\alpha\ell} - r}. \quad \text{(E4)}$$

Assuming that the initial $h/\omega_c \ll 1$ is small enough, the flow will reach $\delta\alpha\ell \ll 1$, at which point the dominant coupling, which in this case is α_x, saturates at the value $\alpha_{x,R} = \delta\alpha$, while the subleading coupling continues to decrease, $\alpha_{y,R} = r\delta\alpha(\Lambda'/\omega_c)^{\delta\alpha}$. Since the flow stops when $h_R = \Lambda'$ then in the low-energy theory $\alpha_{y,R} = r\delta\alpha(h_R/\omega_c)^{\delta\alpha}$. Once this point has been reached, we can examine the beta function of $\tilde{h}$,

$$\frac{d\tilde{h}}{d\ell} = (1 - \alpha_x - \alpha_y)\tilde{h}. \quad \text{(E5)}$$

As mentioned above, after some "time" $\ell \sim \delta\alpha^{-1}$ (which importantly does not depend on the initial value of h/ω_c), α_x will saturate, while α_y becomes negligible. Thus at this point the flow is identical to the flow of the 1bSB, with $\alpha = \delta\alpha$. We therefore find that if $\delta\alpha > 1$ the tunneling flows to zero and the TLS becomes localized, while for $\delta\alpha < 1$ the renormalized tunneling assumes the familiar form $h_R \propto \omega_c(h/\omega_c)^{1/(1-\delta\alpha)}$. Note that in this case the proportionality constant will depend on the time it took α_x to saturate, which is a quantity which depends on α_x^0, α_y^0 and not on h, ω_c. This can be found exactly by inserting $\alpha_{x,y}(\ell)$ into (E5) and integrating,

$$\log\frac{\omega_c}{h} = \int_0^{\ell^*}\left(1 + \delta\alpha\frac{1+re^{-2\delta\alpha\ell}}{1-re^{-2\delta\alpha\ell}}\right)d\ell = (1-\delta\alpha)\ell^* - \log\left(\frac{1-re^{-2\delta\alpha\ell^*}}{1-r}\right) \quad \text{(E6)}$$

$$\Rightarrow h_R \propto (1-r)^{\frac{2}{1-\delta\alpha}}\omega_c\left(\frac{h}{\omega_c}\right)^{\frac{1}{1-\delta\alpha}}. \quad \text{(E7)}$$

The flow of the couplings in the xz model is identical. However, if the dominant coupling is α_z then after $\ell \gtrsim \delta\alpha^{-1}$ the flow of h will slow down, and thus h will only by renormalized by a multiplicative factor. We find in this case [analogous to only inserting $\alpha_y(\ell)$ into (E5)]

$$\log\frac{\omega_c}{h} = \int_0^{\ell^*}\left(1+\delta\alpha\frac{re^{-2\delta\alpha\ell}}{1-re^{-2\delta\alpha\ell}}\right)d\ell$$
$$= \ell^* - \log\left(\frac{1-re^{-2\delta\alpha\ell^*}}{1-r}\right) \tag{E8}$$
$$\Rightarrow h_R = \frac{\delta\alpha}{\alpha_z}h. \tag{E9}$$

APPENDIX F: SUBLEADING CORRECTIONS IN *xyz* MODEL

Following the methods of Ref. [53], we characterize the magnitude of the different subleading corrections in the multi-bath case. There are two types of subleading corrections: the susceptibilities of the subdominant baths, which appear in the self-energy, and perturbative corrections to the susceptibility of the dominant bath because of the weak coupling to the losing baths. We will study these in the xy model and in the xz model, and the generalization to the xyz model is straightforward since the couplings to the subleading baths are perturbative in the low-energy theory.

1. *xy* model

As usual we will assume without loss of generality that $\alpha_x > \alpha_y$. As mentioned above, there are two types of corrections to the self-energy. We start with that due to perturbative corrections to χ_x. As presented in [53], if only the x bath was present after integrating out the high-energy modes, we could expand the ground and excited states as (performing perturbation theory in the low-energy modes)

$$|g\rangle_0 = |\tilde{\downarrow}\rangle + \frac{\phi_x}{h_R}|\tilde{\uparrow}\rangle + \frac{1}{2}\left(\frac{\phi_x}{h_R}\right)^2|\tilde{\downarrow}\rangle + \cdots \tag{F1}$$
$$|\omega_i, x\rangle_0 = b^\dagger_{x,i}|g\rangle + \cdots \tag{F2}$$

where $\phi_\alpha = \sum_i \frac{\sqrt{\Pi^a(\omega_i)}}{h_R}(b^\dagger_{a,i} + b_{a,i})$, $\Pi^a(\omega) \propto \alpha^r_a$, and $b^\dagger_{a,i}, b_{a,i}$ are respectively the bath operator, bath spectral function, and boson creation and annihilation operators of the a bath. Importantly, the states $|\tilde{\uparrow}, \tilde{\downarrow}\rangle = 1/\sqrt{2}(|\tilde{+}\rangle \pm |\tilde{-}\rangle)$ are superpositions of the *high-frequency-model dressed x* states $|\tilde{\pm}\rangle$. This gives the expected $\chi_x(\omega \ll h_R) \propto \alpha_{x,R}\omega/h_R^2$ at low frequencies, but for general frequencies should be treated in a nonperturbative manner in $\alpha_{x,R}$. However, since $\alpha_{y,R}$ is small, we can add it perturbatively only to first order,

$$|g\rangle \approx |g\rangle_0 - i\frac{\phi_y}{h_R}\left(1+\left(\frac{\phi_x}{h_R}\right)^2+\cdots\right)|\tilde{\uparrow}\rangle \tag{F3}$$

and the relevant excited states will involve insertions of one y boson with multiple x bosons. Using the spectral decomposition for χ_x,

$$\chi_x(\omega) = \sum_n |\langle n|\sigma_x|g\rangle|^2\delta(E_n-\omega), \tag{F4}$$

we find that the leading correction will come from matrix elements of the form $\langle\omega_1,\cdots\omega_{2k}, x; \omega_j, y|\sigma_x|g\rangle$. While the summation over the many orders of ϕ_x is nontrivial, we know that it must produce a scaling function that only depends on ω/h_R, and we may thus write

$$\chi_x''(\omega,\alpha_{y,R}) = \chi_x''(\omega,0) + \alpha_{y,R}\frac{1}{\omega}\tilde{f}_{\alpha_{x,R}}\left(\frac{\omega}{h_R}\right) \tag{F5}$$
$$= \frac{1}{\omega}f_{\alpha_{x,R}}\left(\frac{\omega}{h_R}\right) + \alpha_y\left(\frac{h_R}{\omega_c}\right)^{\alpha_{x,R}}\frac{1}{\omega}\tilde{f}_{\alpha_{x,R}}\left(\frac{\omega}{h_R}\right) \tag{F6}$$

where in the second line we inserted the expression for α_y. While averaging over the first term will give the usual contribution, in the second term we can treat the distribution as effectively having an increased exponent $\tilde{\mathcal{P}}_r \sim h_R^{\gamma-1+\alpha_{x,R}}$, which will in turn produce a term with a subleading frequency dependence in the averaged susceptibility $\propto \omega^{\gamma-1+\alpha_{x,R}}$.

We now consider the susceptibility χ_y, whose spectral decomposition is

$$\chi_y(\omega) = \sum_n |\langle n|\sigma_y|g\rangle|^2\delta(E_n-\omega). \tag{F7}$$

Using the fact that the bare σ_y flips the TLS without properly adjusting the high-energy bosons, we have that

$$\langle\tilde{\uparrow}|\sigma_y|\tilde{\downarrow}\rangle \propto \frac{h_R}{h} \propto \left(\frac{h_R}{\omega_c}\right)^{\alpha_{x,R}}. \tag{F8}$$

For small frequencies we may use the perturbative form ($F2$) and find that $\chi_y'' \propto (\frac{h_R}{\omega_c})^{2\alpha_{x,R}}\chi_x''$, which will naively translate into a frequency dependence $\omega^{\gamma-1+2\alpha_{x,R}}$ in the averaged susceptibility. However, the averaged susceptibility depends on the full χ_y'', and since for intermediate and high frequencies this perturbation theory is not applicable, we cannot fully determine the nonuniversal prefactor, and can only argue that $\overline{\chi_y''} \propto \omega^{\gamma-1+\epsilon}$ with $\epsilon > 0$.

2. *xz* model

We begin by studying the similar case where $\alpha_x > \alpha_z$. The susceptibility χ_x'' will now acquire similar corrections due to α_z. However, the matrix elements with single insertions of $\sigma_z\phi_z$ vanish, and we must instead go to second order in $\sigma_z\phi_z$. This means that the corresponding correction to the averaged susceptibility will be $\propto \omega^{\gamma-1+2\alpha_{x,R}}$. The susceptibility χ_z'' will be nonuniversal due to considerations identical to (F8), and will thus be suppressed by a prefactor $(\frac{h_R}{\omega_c})^{2\alpha_{x,R}}$ at low frequencies, although we do not know the generalization of it to higher frequencies. However, in addition this susceptibility includes a static delta function peak due to the equilibrium value of $\langle\sigma_z\rangle_\infty$. For small $\alpha_z \ll 1$ this can be calculated using the sum rule Eq. (C5),

$$\langle\sigma_z\rangle = \frac{1}{h}\int_0^{\omega_c} f(\omega/h_R)d\omega = \left(\frac{h_R}{\omega_c}\right)^{\alpha_x}\times\left(\int_0^{\omega_c/h_R} f(x)dx\right). \tag{F9}$$

We must therefore find if this integral converges or diverges when the upper limit is taken to $\omega_c/h_R \to \infty$. Reference [53]

shows that $f(x \gg 1) \propto 1/x^{2-2\alpha}$, so that for $\alpha < 1/2$ this integral converges to some constant $= A_\alpha$ while for $\alpha > 1/2$ this integral diverges as a power law $= A_\alpha(\omega_c/h_R)^{2\alpha-1}$ [for $\alpha = 1/2$ it diverges logarithmically $\propto \log(\omega_c/h_R)$]. Thus we can write

$$\chi_z'' \approx \delta(\omega) \times A_{\alpha_x}\left(\frac{h_{c,R}}{\omega_c}\right)^{\min(\alpha_x, 1-\alpha_x)} + \cdots \tag{F10}$$

with the dots referring to the subleading frequency-dependent terms.

We now turn to the case where $\alpha_z > \alpha_x$. Here, with no α_x the ground state is exactly a coherent state of all the bosons centered around the location corresponding to $|\downarrow\rangle$. Acting with the high-frequency mode dressed $\tilde{\sigma}_x$ will only agitate the low-energy modes, and thus we can write $\langle\tilde{\uparrow}|\tilde{\sigma}_x|\tilde{\downarrow}\rangle = s_x \sim \mathcal{O}(1)$. Therefore incorporating the effects of $\alpha_{x,R}$ perturbatively will modify the ground state as

$$|g\rangle = \left(1 + \frac{1}{2}s_x^2\left(\frac{\phi_x}{h_R}\right)^2\right)|\tilde{\uparrow}\rangle + s_x\frac{\phi_x}{h_R}|\tilde{\downarrow}\rangle + \cdots. \tag{F11}$$

In terms of the resulting modification to χ_z'', we can easily see that the elastic peak will decrease by a small amount proportional to $\alpha_{x,R}$, and the inelastic part will be modified by a term proportional to $(\alpha_{x,R})^2\omega/h_R^2$ (assuming that $\omega/h_R \ll 1/\alpha_{x,R}$), which in turn will give a correction to $\overline{\chi_z''}$ proportional to $\omega^{\gamma-1+2\alpha_{z,R}}$. The susceptibility χ_x'' is simply a delta function time the factor corresponding to (F8),

$$\chi_x''(\omega) = \left(\frac{h_R}{\omega_c}\right)^{2\alpha_{z,R}}\delta(\omega \pm 2h_R), \tag{F12}$$

$$\overline{\chi_x''}(\omega) \propto \omega^{\gamma-1+2\alpha_z^z}. \tag{F13}$$

And we can thus conclude that the frequency dependence of the self-energy in this case will be

$$\Sigma''(\omega) - \Sigma''(0) \propto \frac{|\omega|^{\gamma+2\alpha_{z,R}}}{h_{c,R}^{\gamma}\omega_c^{2\alpha_{z,R}}}. \tag{F14}$$

Note that when averaging over h_R we neglect the contribution from TLS whose splitting obeys $\omega/h_R \gg (\omega_c/h_R)^{\alpha_{z,R}} \to h_R \ll \omega(\omega/\omega_c)^{\alpha_{z,R}/(1-\alpha_{z,R})}$, for which the perturbation theory breaks down.

APPENDIX G: DERIVATION OF SPECIFIC HEAT FROM INTERNAL ENERGY

Here we derive Eq. (90) that enables us to obtain the specific heat of the model following Ref. [101]. Considering the Hamiltonian (1)

$$H = \sum_\alpha \varepsilon_\alpha c_\alpha^\dagger c_\alpha + \sum_{\alpha\beta\gamma,l} g^l_{\alpha\beta\gamma} c_\alpha^\dagger c_\beta \sigma_\gamma^l + \sum_\gamma h_\gamma \sigma_\gamma^z. \tag{G1}$$

The single-particle quantum numbers stand for combinations of momenta and flavor indices and we also suppress factors of M and N for brevity. It is useful to introduce an arbitrary retarded fermionic Green's function

$$\langle\langle A, B\rangle\rangle_t^r \equiv -i\theta(t)\langle[A(t), B]_+\rangle \tag{G2}$$

and its Fourier transform $\langle\langle A, B\rangle\rangle_\omega^r$. Here $[A, B]_+$ is the anticommutator. The advanced Green's function is given by $\langle\langle A, B\rangle\rangle_\omega^a = (\langle\langle A, B\rangle\rangle_\omega^r)^*$where $(\cdot)^*$ denotes complex conjugation. We use the fact that the retarded and advanced Green's functions both obey the equation of motion,

$$\omega\langle\langle A, B\rangle\rangle_\omega = \langle[A, B]_+\rangle_\omega + \langle\langle[A, H]_-, B\rangle\rangle_\omega. \tag{G3}$$

We use Eq. (G3) to obtain the equation for motion of the retarded/advanced fermionic Green's function,

$$(\omega - \varepsilon_\alpha)\langle\langle c_\alpha, c_\alpha^\dagger\rangle\rangle_\omega = 1 + \sum_{\alpha\beta\gamma,l} g^l_{\alpha\beta\gamma}\left\langle\left\langle c_\beta\sigma_\gamma^l, c_\alpha^\dagger\right\rangle\right\rangle_\omega. \tag{G4}$$

We proceed to consider the internal energy $U \equiv \langle H\rangle$,

$$U = \sum_\alpha \varepsilon_\alpha\langle c_\alpha^\dagger c_\alpha\rangle + \sum_{\alpha\beta\gamma,l} g^l_{\alpha\beta\gamma}\left\langle c_\alpha^\dagger c_\beta\sigma_\gamma^l\right\rangle + \sum_\gamma h_\gamma\langle\sigma_\gamma^z\rangle. \tag{G5}$$

Using the identity (that follows from the spectral representation)

$$\langle AB\rangle = i\int_{-\infty}^{\infty}\frac{d\omega}{2\pi}\frac{\langle\langle A, B\rangle\rangle_\omega^r - \langle\langle A, B\rangle\rangle_\omega^a}{e^{\beta\omega}+1}, \tag{G6}$$

and Eq. (G4) we may express the first two terms in U as

$$\sum_\alpha \varepsilon_\alpha\langle c_\alpha^\dagger c_\alpha\rangle + \sum_{\alpha\beta\gamma,l} g^l_{\alpha\beta\gamma}\left\langle c_\alpha^\dagger c_\beta\sigma_\gamma^l\right\rangle = -\int\frac{d\omega}{\pi}\sum_\alpha \mathrm{Im}\langle\langle c_\alpha, c_\alpha^\dagger\rangle\rangle_\omega^r. \tag{G7}$$

The right-hand side can be written in terms of the electronic spectral function: $\int_{\boldsymbol{k}}\mathcal{A}_{\boldsymbol{k}}(\omega) = -\frac{1}{\pi}\sum_\alpha \mathrm{Im}\langle\langle c_\alpha, c_\alpha^\dagger\rangle\rangle_\omega^r$. Inserting this form to the expression for the internal energy, we obtain the form given in Eq. (90).

APPENDIX H: SUPERCONDUCTIVITY

1. Effective action

We generalize our model to spin-1/2 fermions by altering the interaction term in Eq. (1) to

$$H_{\mathrm{int}} = \frac{1}{N}\sum_{\boldsymbol{r},s,ijl}\boldsymbol{g}_{ijl,\boldsymbol{r}}\cdot\boldsymbol{\sigma}_{l,\boldsymbol{r}}c_{i\boldsymbol{r}s}^\dagger c_{j\boldsymbol{r}s}. \tag{H1}$$

Here, $c_{i\boldsymbol{k}\alpha}^\dagger$ is the fermionic creation operator for momentum $\boldsymbol{k}$, spin $s = \uparrow, \downarrow$, and flavor index $i = 1, \cdots, N/2$ (so that the total number of electron flavors remains N), and the rest of the definitions are identical to the case in the main text.

After averaging over the coupling constants via replica trick, introducing the bilocal fields (including the new pairing field F)

$$G_{\boldsymbol{r},\boldsymbol{r}'s}(\tau, \tau') = \frac{1}{N}\sum_i \bar{c}_{i\boldsymbol{r}\alpha}(\tau)c_{i\boldsymbol{r}'s}(\tau'),$$

$$F_{\boldsymbol{r},\boldsymbol{r}'}(\tau, \tau') = \frac{1}{N}\sum_i c_{i\boldsymbol{r}\downarrow}(\tau)c_{i\boldsymbol{r}'\uparrow}(\tau'), \tag{H2}$$

$$\chi_{a,\boldsymbol{r}}(\tau, \tau') = \frac{1}{M}\sum_l \sigma_{l,\boldsymbol{r}}^a(\tau)\sigma_{l,\boldsymbol{r}}^a(\tau'),$$

and integrating over the fermions, we obtain the effective action

$$S = -N\mathrm{tr}\log\left(\hat{G}_0^{-1} - \hat{\Sigma}\right) - N\int \sum_{\boldsymbol{r},s} G_{\boldsymbol{r},\boldsymbol{r}'s}(\tau,\tau')\Sigma_{\boldsymbol{r}',\boldsymbol{r}s}(\tau',\tau) - N\int \sum_{\boldsymbol{r},\sigma}(F^{\dagger}_{\boldsymbol{r},\boldsymbol{r}'}(\tau,\tau')\Phi_{\boldsymbol{r}',\boldsymbol{r}}(\tau',\tau) + F_{\boldsymbol{r},\boldsymbol{r}'}(\tau,\tau')\Phi^{\dagger}_{\boldsymbol{r}',\boldsymbol{r}}(\tau',\tau))$$
$$- M\sum_a\sum_{\boldsymbol{r}} g_a^2\int \chi_{a,\boldsymbol{r}}(\tau,\tau')\left[\sum_s G_{\boldsymbol{r},\boldsymbol{r}s}(\tau,\tau')G_{\boldsymbol{r},\boldsymbol{r}s}(\tau',\tau) - (-1)^{\delta_{a,y}}2F^{\dagger}_{\boldsymbol{r},\boldsymbol{r}}(\tau,\tau')F_{\boldsymbol{r},\boldsymbol{r}}(\tau',\tau)\right]$$
$$+ M\int \sum_{\boldsymbol{r}s}\chi_{a,\boldsymbol{r}}(\tau,\tau')\Pi_{a,\boldsymbol{r}}(\tau',\tau) + \sum_{\boldsymbol{r}}\sum_{l=1}^{M} S_{\mathrm{TLS}}[\boldsymbol{\sigma}_{l,\boldsymbol{r}}], \tag{H3}$$

where

$$S_{\mathrm{TLS}}[\boldsymbol{\sigma}] = S_{\mathrm{Berry}}[\boldsymbol{\sigma}] - \int d\tau \boldsymbol{h}_{l,\boldsymbol{r}}\cdot\boldsymbol{\sigma}(\tau)$$
$$- \int d\tau d\tau' \sum_a \Pi_{a,\boldsymbol{r}}(\tau'-\tau)\sigma^a(\tau)\sigma^a(\tau') \tag{H4}$$

is the action of a spin-boson problem with multiple baths.

In the first term we use a 2×2 Nambu-Gor'kov formulation, sufficient for singlet pairing

$$\hat{\Sigma}_{\boldsymbol{r}\boldsymbol{r}'}(\tau,\tau') = \begin{pmatrix}\Sigma_{\boldsymbol{r}\boldsymbol{r}'\uparrow}(\tau,\tau') & \Phi_{\boldsymbol{r}\boldsymbol{r}'}(\tau,\tau')\\ \Phi^{\dagger}_{\boldsymbol{r}\boldsymbol{r}'}(\tau,\tau') & -\Sigma_{\boldsymbol{r}'\boldsymbol{r}\downarrow}(\tau',\tau)\end{pmatrix}. \tag{H5}$$

Generalizations to triplet pairing are straightforward but can only play a role for odd-frequency pairing. We use a similar expression for the propagator

$$\hat{G}_{\boldsymbol{r}\boldsymbol{r}'}(\tau,\tau') = \begin{pmatrix}G_{\boldsymbol{r}\boldsymbol{r}'\uparrow}(\tau,\tau') & F_{\boldsymbol{r}\boldsymbol{r}'}(\tau,\tau')\\ F^{\dagger}_{\boldsymbol{r}\boldsymbol{r}'}(\tau,\tau') & -G_{\boldsymbol{r}'\boldsymbol{r}\downarrow}(\tau',\tau)\end{pmatrix}. \tag{H6}$$

The bare propagator in frequency and momentum space is

$$\hat{G}_{0\boldsymbol{k}}(i\omega)^{-1} = \begin{pmatrix}i\omega-\varepsilon_{\boldsymbol{k}} & 0\\ 0 & i\omega+\varepsilon_{\boldsymbol{k}}\end{pmatrix}. \tag{H7}$$

In the limit of large M and N, with fixed ratio M/N, we can analyze the saddle point limit. We consider a saddle point that does not break time-reversal symmetry $G_{\boldsymbol{r}\boldsymbol{r}'\uparrow}(\tau,\tau') = G_{\boldsymbol{r}\boldsymbol{r}'\downarrow}(\tau,\tau')$ and drop the spin index. Performing the variation with respect to $\hat{\Sigma}$ gives

$$\hat{G}_{\boldsymbol{r},\boldsymbol{r}'}(i\omega) = \left(\hat{G}_0^{-1}(i\omega) - \hat{\Sigma}(i\omega)\right)^{-1}\big|_{\boldsymbol{r},\boldsymbol{r}'}. \tag{H8}$$

The variation with respect to G and F yield

$$\Sigma_{\boldsymbol{r},\boldsymbol{r}'}(\tau) = \delta_{\boldsymbol{r},\boldsymbol{r}'}\frac{M}{N}\sum_a g_a^2 G_{\boldsymbol{r},\boldsymbol{r}}(\tau)\chi_{a,\boldsymbol{r}}(\tau), \tag{H9}$$

$$\Phi_{\boldsymbol{r},\boldsymbol{r}'}(\tau) = -\delta_{\boldsymbol{r},\boldsymbol{r}'}\frac{M}{N}\sum_a (-1)^{\delta_{a,y}} g_a^2 F_{\boldsymbol{r},\boldsymbol{r}}(\tau)\chi_{a,\boldsymbol{r}}(\tau). \tag{H10}$$

These two equations resemble the ones that occur for electrons that couple to bosonic modes with propagator $\chi_{a,\boldsymbol{r}}(\tau)$ via a Yukawa coupling. The stationary point that follows from the variation with respect to χ is

$$\Pi_{a,\boldsymbol{r}}(\tau) = -2g_a^2\left[G_{\boldsymbol{r},\boldsymbol{r}}(\tau)G_{\boldsymbol{r},\boldsymbol{r}}(-\tau) - (-1)^{\delta_{a,y}}F^{\dagger}_{\boldsymbol{r},\boldsymbol{r}}(\tau)F_{\boldsymbol{r},\boldsymbol{r}}(-\tau)\right], \tag{H11}$$

an expression that is also analogous to the self-energy of a bosonic problem.

The TLS-correlation function $\langle\sigma^a_{l,\boldsymbol{r}}(\tau)\sigma^a_{l,\boldsymbol{r}}(\tau')\rangle$ is determined from the solution of the spin boson problem.

2. Linearized Eliashberg equations

As long as we are only interested in the onset of pairing and the superconducting phase transition is of second order we can focus on the linearized gap equation. In this case we can neglect the feedback of superconductivity on the ohmic bath. The solution of the spin-boson problem then yields the local propagator $\chi_a(\omega)$. The equation for the momentum-independent normal self-energy is

$$\Sigma(i\omega) = \frac{M}{N}T\sum_{\omega',a} g_a^2 G(i\omega')\chi_a(i\omega - i\omega')$$
$$= \frac{M}{N}T\sum_{\omega',a} g_a^2\rho_F \times \int d\varepsilon_{\boldsymbol{k}}\frac{1}{i\omega' - \varepsilon_{\boldsymbol{k}} - \Sigma(\omega')}\chi_a(i\omega - i\omega'). \tag{H12}$$

The linearized equation for the s-wave anomalous self-energy is [assuming particle-hole symmetry for simplicity, we use the fact that $i\Sigma(i\omega')$ is real]

$$\Phi(i\omega) = -\frac{M}{N}T\sum_{\omega',a} g_a^2(-1)^{\delta_{a,y}}F(i\omega')\chi_a(i\omega - i\omega')$$
$$= \frac{M}{N}T\sum_{\omega',a}\int d\varepsilon_{\boldsymbol{k}} \times \frac{\rho_F g_a^2(-1)^{\delta_{a,y}}\Phi(i\omega')\chi_a(i\omega - i\omega')}{(i\omega' - \varepsilon_{\boldsymbol{k}} - \Sigma(i\omega'))(-i\omega' - \varepsilon_{\boldsymbol{k}} + \Sigma(i\omega'))}$$
$$= \frac{M}{N}T\sum_{\omega',a}\int d\varepsilon_{\boldsymbol{k}}\frac{\rho_F g_a^2(-1)^{\delta_{a,y}}\Phi(i\omega')\chi_a(i\omega - i\omega')}{(i\omega' + i\Sigma(i\omega'))^2 + \varepsilon_{\boldsymbol{k}}^2}. \tag{H13}$$

If we perform the integration over $\varepsilon_{\boldsymbol{k}}$, we get for both self-energies the Eliashberg equations,

$$\Sigma(i\omega) = -iT\sum_{\omega'}\mathrm{sign}(i\omega')D_{\Sigma}(i\omega - i\omega'),$$
$$\Phi(i\omega) = T\sum_{\omega'}\frac{\Phi(i\omega')}{|\omega' + i\Sigma(i\omega')|}D_{\Phi}(i\omega - i\omega'), \tag{H14}$$

with

$$D_\Sigma(i\omega) = \frac{M}{N}\sum_a \rho_F g_a^2 \chi_a(i\omega),$$
$$D_\Phi(i\omega) = \frac{M}{N}\sum_a (-1)^{\delta_{a,y}} \rho_F g_a^2 \chi_a(i\omega). \tag{H15}$$

The contribution due to the coupling g_y is pair breaking and sufficiently large g_y can partially or fully destroy superconductivity.

For the solution of the linearized gap equation we introduce

$$\Delta(i\omega_n) = \frac{\omega_n \Phi(i\omega_n)}{\omega_n + i\Sigma(i\omega_n)}, \tag{H16}$$

which yields a closed equation

$$\Delta(i\omega_n) = T\sum_{n'} \mathrm{sign}(i\omega_{n'})\left(\frac{\Delta(i\omega_{n'})}{\omega_{n'}} D_\Sigma(i\omega_n - i\omega_{n'}) - \frac{\Delta(i\omega_n)}{\omega_n} D_\Phi(i\omega_n - i\omega_{n'})\right). \tag{H17}$$

One nicely finds that if $D_\Sigma(i\omega) = D_\Phi(i\omega) \equiv D(i\omega)$ (i.e., $g_y = 0$) the zeroth bosonic Matsubara frequency does not contribute to the solution of the coupled equation. Static fluctuations are irrelevant for the pairing problem, in agreement with Anderson's theorem. From now on we will assume that $g_y = 0$.

Hence, in what follows, we can just skip $n' = n$ in the sum. Then we do not have any problem with a potentially divergent $D(0)$ for $\gamma \leqslant 1$,

$$\Delta(i\omega_n) = T\sum_{n'\neq n}\left(\Delta(i\omega_{n'}) - \frac{\omega_{n'}}{\omega_n}\Delta(i\omega_n)\right)\frac{D(i\omega_n - i\omega_{n'})}{|\omega_{n'}|}. \tag{H18}$$

For even-frequency pairing we have $\Delta(i\omega_n) = \Delta(-i\omega_n)$. Hence we can write (we only consider $\omega_n > 0$)

$$\Delta(i\omega_n) = T\sum_{n'\geqslant 0}\Delta(i\omega_{n'})\frac{(1-\delta_{n,n'})D(i\omega_n - \omega_{n'}) + D(i\omega_n + i\omega_{n'})}{\omega_{n'}} - \Delta(i\omega_n)T\sum_{n'\geqslant 0}\frac{(1-\delta_{n,n'})D(i\omega_n - i\omega_{n'}) - D(i\omega_n + i\omega_{n'})}{\omega_n}. \tag{H19}$$

Next, we introduce

$$\Psi_n = \frac{\Delta(i\omega_n)}{|\omega_n|^{1/2}} \tag{H20}$$

and obtain

$$\Psi_n = T\sum_{n'\geqslant 0}\Psi_{n'}\frac{(1-\delta_{n,n'})D(i\omega_n - i\omega_{n'}) + D(i\omega_n + i\omega_{n'})}{\sqrt{\omega_n\omega_{n'}}} - \Psi_n T\sum_{n'\geqslant 0}\frac{(1-\delta_{n,n'})D(i\omega_n - i\omega_{n'}) - D(i\omega_n + i\omega_{n'})}{\omega_n}. \tag{H21}$$

We can write this as a matrix equation, where $N_{\max}$ is the maximum number of Matsubara frequencies included,

$$\Psi_n = \sum_{n'=0}^{\infty} K_{n,n'}\Psi'_n, \tag{H22}$$
$$K_{n,n'} = \delta_{n,n'}K_n^{\mathrm{diag}} + (1-\delta_{n,n'})\frac{D(i\omega_n - \omega_{n'}) + D(i\omega_n + \omega_{n'})}{\pi\sqrt{(2n+1)(2n'+1)}}, \tag{H23}$$
$$K_n^{\mathrm{diag}} = \sum_{m=0}^{\infty}\frac{(1-\delta_{n,m})D(i\omega_n - \omega_m) + (1+\delta_{n,m})D(i\omega_n + \omega_m)}{\pi(2n+1)}. \tag{H24}$$

Given this matrix equation, we first consider the behavior of T_c for a power-law form of the pairing propagator (with some high-energy cutoff Λ, so that the Matsubara sum runs up to $N_{\max} = \Lambda/T$)

$$D(i\omega_n) = A\left|\frac{\Lambda}{\omega_n}\right|^a \equiv A\left(\frac{\Lambda}{T}\right)^a d_n \tag{H25}$$

where we introduced the rescaled propagator $d_n = \frac{1}{(2\pi n)^a}$. Since $K_{n,n'}$ is linear in D, we may also define its rescaled version $K_{n,n'} = A(\frac{\Lambda}{T})^a k_{n,n'}$ where $k_{n,n'}$ is defined by replacing $D(i\omega_n)$ with d_n in the definition of $K_{n,n'}$. Defining $\kappa(a, N_{\max})$ as the largest eigenvalue of $k_{n,n'}$, the Eliashberg equation simplifies to

$$1 = A\left(\frac{\Lambda}{T_c}\right)^a \kappa(a, N_{\max}). \tag{H26}$$

The qualitative behavior of the eigenvalue can be estimated by inspecting the diagonal elements of k, namely, a simple power counting indicates whether the sum converges or not, which determines the dependence on the cutoff $N_{\max}$. In particular, for $a = 0$, $\kappa \approx \kappa_0 \log(N_{\max})$ and we find the BCS-like solution $T_c \propto \Lambda \exp(-1/A\kappa_0)$. For $a > 0$ the series converges for $n, n' \to \infty$ and $\kappa = \kappa_a$ depends only on the exponent a, giving the critical temperature $T_c = \Lambda(A\kappa_a)^{1/a}$. A numerical calculation of κ_a is shown in Fig. 8. Finally, consider

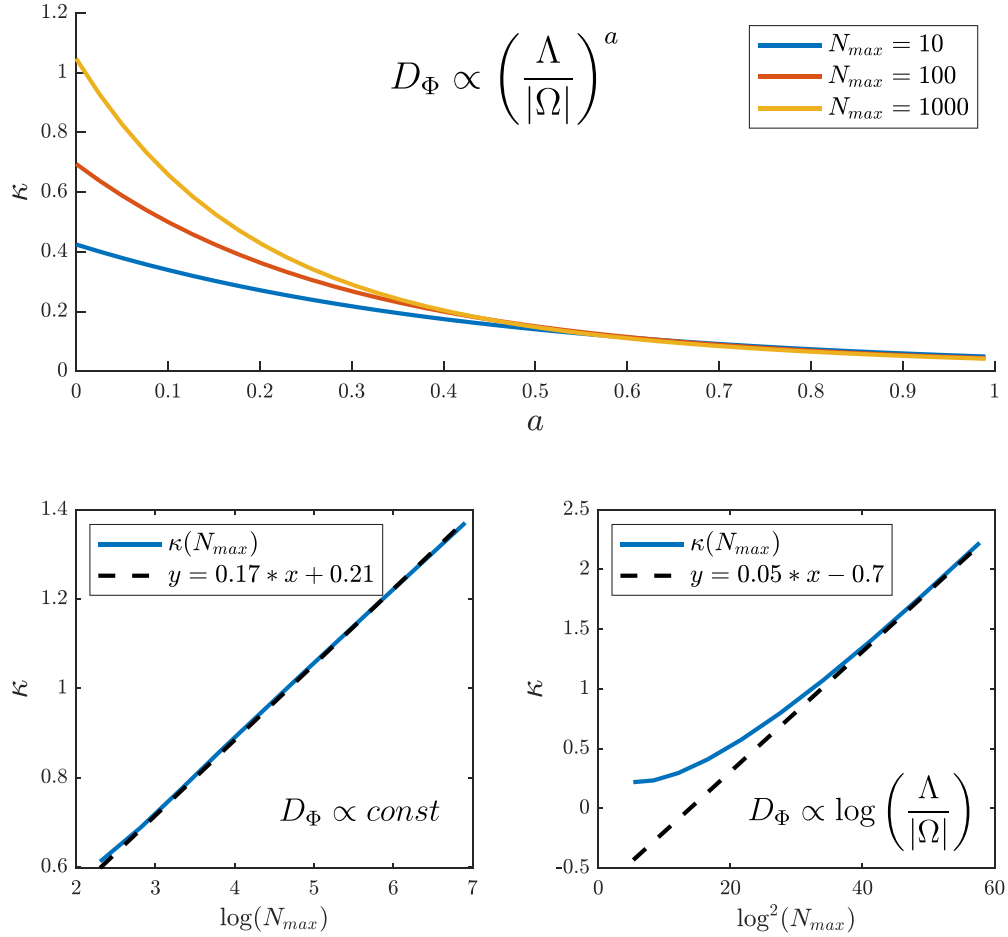

FIG. 8. Numerical calculation of the largest eigenvalue $\kappa(a, N_{\max})$ as a function of a (top) and for the special cases $a = 0$ (bottom left) and $a = 0'$ (i.e., logarithmic D_Φ) (bottom right). For any finite value of a this approaches a constant as $N_{\max} \to \infty$, while for $a = 0, 0'$ it scales as $\log(N_max x)$, $\log^2(N_m ax)$ respectively at large $N_{\max}$.

the case where $D(i\omega_n) = A\log(\Lambda/|\omega_n|)$ (corresponding to a MFL behavior of the electrons). Using $d_n = \log(N_{\max}/|n|)$ one can show numerically that $\kappa \approx \kappa_0' \log^2(N_{\max})$ such that $T_c \propto \Lambda \exp(-1/\sqrt{A\kappa_0})$. An analytic derivation of this result using the Eliashberg equation is given in [102].

3. Analytic continuation of the bosonic propagator

We start with the imaginary part of the bosonic propagator, assuming a power-law form

$$D''(\omega) = \text{sign}(\omega) A \left|\frac{\Lambda}{\omega}\right|^a. \tag{H27}$$

Analytically continuing to Matsubara frequencies (for $a < 2$), we obtain

$$D(i\Omega) = -\frac{1}{\pi}\int_{-\infty}^{\infty} \frac{d\omega}{i\Omega - \omega} D''(\omega) \tag{H28}$$

$$= \frac{2}{\pi}\int_0^{\infty} \frac{\omega d\omega}{\Omega^2 + \omega^2} D''(\omega) \tag{H29}$$

$$= \frac{2A\Lambda^a}{\pi}\int_0^{\Lambda} \frac{\omega^{1-a} d\omega}{\Omega^2 + \omega^2} \tag{H30}$$

$$= \frac{2A}{(2-a)\pi}\frac{\Lambda^2}{|\Omega|^2}\, {}_2F_1\left(1, -\frac{a}{2}, 1 - \frac{a}{2}, -\frac{\Lambda^2}{\Omega^2}\right) \tag{H31}$$

where ${}_2F_1$ is the Gaussian hypergeometric function. In order to obtain analytical results, we approximate

$$D(i\Omega) \approx \frac{2A\Lambda^a}{\pi}\left(\int_0^{\Omega} \frac{\omega^{1-a}}{\Omega^2} d\omega + \int_{\Omega}^{\Lambda} \omega^{-1-a} d\omega\right) \tag{H32}$$

$$= \frac{2A}{\pi}\left(\frac{1}{2-a}\left|\frac{\Lambda}{\Omega}\right|^a - \frac{1}{a}\left(1 - \left|\frac{\Lambda}{\Omega}\right|^a\right)\right), \tag{H33}$$

which coincides with the appropriate limits of the function ${}_2F_1$. Note that the leading behavior for $|\Omega| \ll \Lambda$ is of the form

$$D(i\Omega) \approx \frac{2A}{\pi} \times \begin{cases} \frac{1}{|a|} & a < 0 \\ \log\left(\frac{\Lambda}{|\Omega|}\right) & a = 0 \\ \frac{2}{a(2-a)}\left|\frac{\Lambda}{\Omega}\right|^a & 0 < a < 2 \end{cases}. \tag{H34}$$

We now use the above to obtain T_c in the x model.

4. Detailed analysis of the x model

We analyze the scaling of T_c for two parameter regimes: "weak coupling", for which $T_c \ll h_{c,R}$, and "strong coupling" for which $T_c \gg h_{c,R}$. We will find approximate solutions by analytically continuing the TLS susceptibility $\overline{\chi_x}$ and

identifying the most singular contribution to $D_\Phi(i\Omega)$, from which we obtain T_c using Eq. (H26).

a. Weak coupling

Here we study the susceptibility for $T, \omega \ll h_{c,R}$. From dimensional considerations, we write the averaged susceptibility as a scaling function

$$\chi_x''(\omega, T) = \frac{A_\alpha \gamma}{\omega} \left| \frac{\omega}{h_{c,R}} \right|^\gamma \min\left(1, \left(\frac{\omega}{bT}\right)^\delta\right) \tag{H35}$$

with some $\delta > 0$ and $b \sim \mathcal{O}(1)$. Analyzing the susceptibility at weak coupling and at the Toulouse point suggests that $\delta = 1$, although as we will see the exact value of δ does not qualitatively change T_c. The corresponding Matsubara frequency correlator is given by

$$\chi_x(i\Omega_n) \approx \frac{2\gamma A_\alpha}{\pi h_{c,R}} \left(\frac{1}{\gamma - 1} - \frac{2}{\gamma^2 - 1} \left| \frac{\Omega}{h_{c,R}} \right|^{\gamma - 1} - \frac{\delta}{(\gamma+1)(\gamma+1+\delta)} \frac{T^\gamma}{\Omega^2 h_{c,R}^{\gamma-1}} \right). \tag{H36}$$

The most singular contribution to D_Φ is therefore (the temperature-dependent term is not significant and can be ignored, since $\Omega \gtrsim T$)

$$D_\Phi(i\Omega) \approx 2\pi A_\alpha \lambda \times \begin{cases} \frac{\gamma}{\gamma - 1} & \gamma > 1 \\ \log\left(\frac{h_{c,R}}{|\Omega|}\right) & \gamma = 1 \\ \frac{2\gamma}{1-\gamma^2} \left| \frac{h_{c,R}}{\Omega} \right|^{1-\gamma} & \gamma < 1 \end{cases}. \tag{H37}$$

Using Eq. (H26) we find that

$$T_c / h_{c,R} \propto \begin{cases} \exp\left(-\frac{\gamma - 1}{2\pi A_\alpha \gamma \kappa_0 \lambda}\right) & \gamma > 1 + \mathcal{O}(\sqrt{\lambda}) \\ \exp\left(-\frac{1}{\sqrt{2\pi A_\alpha \kappa_0' \lambda}}\right) & \gamma = 1 \\ \left(\frac{4\pi A_\alpha \gamma \kappa_{\gamma-1}}{1-\gamma^2} \lambda\right)^{\frac{1}{1-\gamma}} & \gamma < 1 - \mathcal{O}(\sqrt{\lambda}) \end{cases}, \tag{H38}$$

where the requirement $|\gamma - 1| > \mathcal{O}(\sqrt{\lambda})$ in the BCS-like and quantum critical regimes is necessary for self-consistency. Additionally, demanding that $T_c \ll h_{c,R}$, which is assumed in taking the low-T form of the TLS susceptibility, requires $\lambda \ll 1$, i.e.,

$$1 \ll \alpha \frac{M}{N} \frac{E_F}{h_{c,R}} \propto \alpha \frac{M}{N} \left(\frac{E_F}{h_c}\right)^{\frac{1}{1-\alpha}}. \tag{H39}$$

This condition will always break down at some $\alpha < 1$. For $M/N \sim \mathcal{O}(1)$ this will happen at very small values of α, $\alpha \propto h_c/E_F$, while in the limit where TLSs are extremely sparse, $\frac{M}{N} \ll \frac{h_c}{E_F}$, this occurs at $\alpha \approx 1 - \frac{\log(\frac{E_F}{h_c})}{\log(\frac{N}{M})}$.

b. Strong coupling

We now turn to the regime $T \gg h_{c,R}$. Note that for $\alpha > 1$ this is always the case since $h_{c,R} = 0$. For frequencies $\omega \ll T$ the TLS correlation function decays exponentially with rate [37,103] [Eq (5.29)],

$$\Gamma = c \frac{h^2}{T} \left(\frac{T}{E_F}\right)^{2\alpha} \tag{H40}$$

with c some α-dependent prefactor. Note that $T \gg \Gamma$ for $T \gg h_R$. In this regime, the TLS susceptibility can be approximated as

$$\chi_x''(\omega) = \frac{1}{2\pi} \frac{\Gamma}{T} \frac{\omega}{\Gamma^2 + \omega^2}. \tag{H41}$$

(The prefactor Γ/T is due to the sum rule Eq. (C4)). For $\omega \gg T, h_R$ the analysis of Appendix D 4 can be extended for $\alpha \neq 1$ (or more precisely $|\alpha - 1| > h_c/E_F$). Overall for $\omega \gg h_{c,R}$ one finds that

$$\chi_x''(\omega, T) = 4\alpha \frac{h^2}{E_F^{2\alpha}} \frac{(\max(\omega, bT))^{2-2\alpha}}{\omega} \tag{H42}$$

with $b \sim \mathcal{O}(1)$. Analytically continuing and separating the different frequency regimes, we define

$$\begin{aligned} \chi_x(i\Omega) &= \frac{2}{\pi} \left(\int_0^\Gamma + \int_\Gamma^{bT} + \int_{bT}^\Omega + \int_\Omega^{E_F} \right) d\omega \frac{\omega \chi_x''(\omega)}{\omega^2 + \Omega^2} \\ &\equiv \chi_1 + \chi_2 + \chi_3 + \chi_4. \end{aligned} \tag{H43}$$

Thus, for $\Omega > aT \gg \Gamma$

$$\chi_1 \approx \frac{1}{3\pi^2} \frac{\Gamma^2}{T\Omega^2}, \tag{H44}$$

$$\chi_2 \approx \frac{1}{\pi^2} \frac{\Gamma}{\Omega^2} \left(1 - \frac{\Gamma}{bT}\right), \tag{H45}$$

$$\chi_3 \approx \frac{2\alpha}{\pi} \frac{h^2}{E_F^{2\alpha}} \frac{|\Omega|^{2\alpha-3}}{2\alpha - 1} \left(1 - \left(\frac{bT}{|\Omega|}\right)^{2\alpha-1}\right), \tag{H46}$$

$$\chi_4 \approx \frac{2\alpha}{\pi} \frac{h^2}{E_F^3} \frac{1}{2\alpha - 3} \left(1 - \left(\frac{|\Omega|}{E_F}\right)^{2\alpha-3}\right). \tag{H47}$$

The most singular contribution to D_Φ is given by

$$D_\Phi(i\Omega) = 2\pi\epsilon\alpha^2 b_\beta \times \begin{cases} \frac{2\alpha}{1-2\alpha} \frac{E_F^{3-2\alpha}}{T^{1-2\alpha}\Omega^2} & \alpha < 1/2 \\ \frac{E_F^2}{\Omega^2} \log\left(\frac{|\Omega|}{T}\right) & \alpha = 1/2 \\ \frac{2}{(2\alpha-1)(3-2\alpha)} \left|\frac{E_F}{\Omega}\right|^{3-2\alpha} & 1/2 < \alpha < 3/2 \\ \log\left(\frac{E_F}{|\Omega|}\right) & \alpha = 3/2 \\ \frac{1}{2\alpha-3} & \alpha > 3/2 \end{cases}, \tag{H48}$$

where $b_\beta = (\frac{1+\beta}{3+\beta})$ comes from averaging over h^2. Inserting these into Eq. (H26), we obtain

$$T_c / E_F \propto \begin{cases} \left(\frac{4\pi\alpha^2\kappa_{3-2\alpha} b_\beta}{(2\alpha-1)(3-2\alpha)} \epsilon\right)^{\frac{1}{3-2\alpha}} & \alpha < 3/2 - \mathcal{O}(\sqrt{\epsilon}) \\ \exp\left(-\frac{1}{\alpha\sqrt{2\pi b_\beta \kappa_0' \epsilon}}\right) & \alpha = 3/2 \\ \exp\left(-\frac{2\alpha-3}{2\pi\alpha^2\beta\kappa_0\epsilon}\right) & \alpha > 3/2 + \mathcal{O}(\sqrt{\epsilon}) \end{cases}. \tag{H49}$$

Note that for $\alpha \leqslant 1/2$ the prefactor in the parentheses changes, according to the corresponding expression in Eq. (H48). However, the dependence on the small parameter ϵ remains $\epsilon^{1/(3-2\alpha)}$ for all $\alpha < 3/2$.

Once again, for $\alpha < 1$ consistency requires that $T_c \gg h_{c,R}$, which translates into

$$1 \ll \alpha \frac{M}{N} \left(\frac{E_F}{h_c}\right)^{\frac{1}{1-\alpha}} \iff \lambda \gg 1, \tag{H50}$$

which is complementary to the requirement for weak coupling.

APPENDIX I: COMMENT ON CHEMICAL POTENTIAL

Here, we briefly comment that the temperature dependence of the chemical potential because of self-energy corrections is subleading throughout the phase diagram and therefore does not alter the physical picture. Here, we consider the spinless case for simplicity, the generalization to spinful electrons is straightforward. To see this, note that fixing the density is enforced via the constraint $\sum_{\boldsymbol{k}} G(\tau = 0, \boldsymbol{k}) = n$ that can be recast to the form

$$\int_{\epsilon,\omega} \nu(\epsilon)\mathcal{A}(\omega,\epsilon)n(\omega) = n \tag{I1}$$

with the spectral function $\mathcal{A}$ defined earlier and $n(\omega)$ being the Fermi-Dirac function. Define $\tilde{\nu}(\omega) \equiv \int_\epsilon \nu(\epsilon)\mathcal{A}(\omega,\epsilon)$, then $n = \int_\omega \tilde{\nu}(\omega)n(\omega)$. Assuming weak particle-hole asymmetry, $\nu(\epsilon) \equiv \nu_0 + \nu_1 \frac{\epsilon}{E_F}$, we obtain

$$\tilde{\nu}(\omega) = \nu_0 - \frac{\nu_1}{4E_F^2}(\omega - \mathrm{Re}\Sigma_R(\omega)). \tag{I2}$$

Here, we assumed, for simplicity, that the bandwidth $W \approx E_F$. Inserting $\tilde{\nu}(\omega)$ and applying the Sommerfeld expansion we see that

$$n - \mu(T)\nu_0 = -\frac{T^2}{4E_F^2}\nu_1(1 - [\partial_\omega \Sigma'(\omega, T)]_{\omega=0}) + \cdots \tag{I3}$$

and writing $\mu(T) = \mu(T=0) + \delta\mu(T)$ we see that

$$\delta\mu(T) \propto \begin{cases} \frac{T^2}{E_F} & \gamma > 1 \\ \frac{T^2 \log(h_c/T)}{E_F} & \gamma = 1 \\ \frac{T^{1+\gamma} h_c^{1-\gamma}}{E_F} & \gamma < 1 \end{cases} \tag{I4}$$

such that in all cases the correction is subleading in T/E_F.

[1] C. M. Varma, Colloquium: Linear in temperature resistivity and associated mysteries including high temperature superconductivity, Rev. Mod. Phys. **92**, 031001 (2020).

[2] C. Proust and L. Taillefer, The remarkable underlying ground states of cuprate superconductors, Annu. Rev. Condens. Matter Phys. **10**, 409 (2019).

[3] J. A. N. Bruin, H. Sakai, R. S. Perry, and A. P. Mackenzie, Similarity of scattering rates in metals showing T-linear resistivity, Science **339**, 804 (2013).

[4] A. Legros, S. Benhabib, W. Tabis, F. Laliberté, M. Dion, M. Lizaire, B. Vignolle, D. Vignolles, H. Raffy, Z. Z. Li *et al.*, Universal T-linear resistivity and Planckian dissipation in overdoped cuprates, Nat. Phys. **15**, 142 (2019).

[5] Y. Cao, D. Chowdhury, D. Rodan-Legrain, O. Rubies-Bigorda, K. Watanabe, T. Taniguchi, T. Senthil, and P. Jarillo-Herrero, Strange metal in magic-angle graphene with near Planckian dissipation, Phys. Rev. Lett. **124**, 076801 (2020).

[6] D. Chowdhury, A. Georges, O. Parcollet, and S. Sachdev, Sachdev-Ye-Kitaev models and beyond: Window into non-Fermi liquids, Rev. Mod. Phys. **94**, 035004 (2022).

[7] S. A. Hartnoll and A. P. Mackenzie, Colloquium: Planckian dissipation in metals, Rev. Mod. Phys. **94**, 041002 (2022).

[8] P. W. Phillips, N. E. Hussey, and P. Abbamonte, Stranger than metals, Science **377**, eabh4273 (2022).

[9] S. Sachdev, Quantum statistical mechanics of the Sachdev-Ye-Kitaev model and strange metals, Oxford Res. Encyclopedia Phys. (2023).

[10] H. V. Löhneysen, A. Rosch, M. Vojta, and P. Wölfle, Fermi-liquid instabilities at magnetic quantum phase transitions, Rev. Mod. Phys. **79**, 1015 (2007).

[11] C. M. Varma, Z. Nussinov, and W. van Saarloos, Singular or non-Fermi liquids, Phys. Rep. **361**, 267 (2002).

[12] S.-S. Lee, Recent developments in non-Fermi liquid theory, Annu. Rev. Condens. Matter Phys. **9**, 227 (2018).

[13] P. Gegenwart, Q. Si, and F. Steglich, Quantum criticality in heavy-fermion metals, Nat. Phys. **4**, 186 (2008).

[14] R. A. Cooper, Y. Wang, B. Vignolle, O. J. Lipscombe, S. M. Hayden, Y. Tanabe, T. Adachi, Y. Koike, M. Nohara, H. Takagi *et al.*, Anomalous criticality in the electrical resistivity of $La_{2-x}Sr_xCuO_4$, Science **323**, 603 (2009).

[15] N. E. Hussey, J. Buhot, and S. Licciardello, A tale of two metals: Contrasting criticalities in the pnictides and hole-doped cuprates, Rep. Prog. Phys. **81**, 052501 (2018).

[16] N. E. Hussey, H. Gordon-Moys, J. Kokalj, and R. H. McKenzie, Generic strange-metal behaviour of overdoped cuprates, J. Phys.: Conf. Ser. **449**, 012004 (2013).

[17] R. L. Greene, P. R. Mandal, N. R. Poniatowski, and T. Sarkar, The strange metal state of the electron-doped cuprates, Annu. Rev. Condens. Matter Phys. **11**, 213 (2020).

[18] L. Taillefer, Scattering and pairing in cuprate superconductors, Annu. Rev. Condens. Matter Phys. **1**, 51 (2010).

[19] A. Jaoui, I. Das, G. Di Battista, J. Díez-Mérida, X. Lu, K. Watanabe, T. Taniguchi, H. Ishizuka, L. Levitov, and D. K. Efetov, Quantum critical behaviour in magic-angle twisted bilayer graphene, Nat. Phys. **18**, 633 (2022).

[20] A. Ghiotto, E.-M. Shih, G. S. S. G. Pereira, D. A. Rhodes, B. Kim, J. Zang, A. J. Millis, K. Watanabe, T. Taniguchi, J. C. Hone *et al.*, Quantum criticality in twisted transition metal dichalcogenides, Nature (London) **597**, 345 (2021).

[21] C. Pfleiderer, Non-Fermi liquid puzzle of MnSi at high pressure, Physica B: Condens. Matter **328**, 100 (2003).

[22] C. Pfleiderer, D. Reznik, L. Pintschovius, H. v. Löhneysen, M. Garst, and A. Rosch, Partial order in the non-Fermi-liquid phase of MnSi, Nature (London) **427**, 227 (2004).

[23] N. Doiron-Leyraud, I. R. Walker, L. Taillefer, M. J. Steiner, S. R. Julian, and G. G. Lonzarich, Fermi-liquid breakdown in the paramagnetic phase of a pure metal, Nature (London) **425**, 595 (2003).

[24] S. Paschen and Q. Si, Quantum phases driven by strong correlations, Nat. Rev. Phys. **3**, 9 (2021).

[25] H. Zhao, J. Zhang, M. Lyu, S. Bachus, Y. Tokiwa, P. Gegenwart, S. Zhang, J. Cheng, Y.-f. Yang, G. Chen *et al.*, Quantum-critical phase from frustrated magnetism in a strongly correlated metal, Nat. Phys. **15**, 1261 (2019).

[26] N. Bashan, E. Tulipman, J. Schmalian, and E. Berg, Tunable non-Fermi liquid phase from coupling to two-level systems, Phys. Rev. Lett. **132**, 236501 (2024)

[27] F. C. Mocanu, L. Berthier, S. Ciarella, D. Khomenko, D. R. Reichman, C. Scalliet, and F. Zamponi, Microscopic observation of two-level systems in a metallic glass model, J. Chem. Phys. **158**, 014501 (2023).

[28] V. Emery and S. Kivelson, Collective charge transport in high temperature superconductors, Physica C: Superconductivity **235–240**, 189 (1994).

[29] For a recent detailed analysis of the density of tunneling defects in metallic glasses, see Ref. [27]. For cuprates, an idea similar in spirit was discussed in Ref. [28].

[30] J. Schmalian and P. G. Wolynes, Stripe glasses: Self-generated randomness in a uniformly frustrated system, Phys. Rev. Lett. **85**, 836 (2000).

[31] A. A. Patel, P. Lunts, and S. Sachdev, Localization of overdamped bosonic modes and transport in strange metals, Proc. Natl. Acad. Sci. USA **121**, e2402052121 (2024).

[32] J. L. Black, B. L. Gyorffy, and J. Jäckle, On the resistivity due to two-level systems in metallic glasses, Philos. Mag. B **40**, 331 (1979).

[33] M. A. Ruderman and C. Kittel, Indirect exchange coupling of nuclear magnetic moments by conduction electrons, Phys. Rev. **96**, 99 (1954).

[34] T. Kasuya, A theory of metallic ferro- and antiferromagnetism on Zener's model, Prog. Theor. Phys. **16**, 45 (1956).

[35] K. Yosida, Magnetic properties of Cu-Mn alloys, Phys. Rev. **106**, 893 (1957).

[36] W. A. Phillips, Tunneling states in amorphous solids, J. Low Temp. Phys. **7**, 351 (1972).

[37] A. J. Leggett, S. Chakravarty, A. T. Dorsey, M. P. A. Fisher, A. Garg, and W. Zwerger, Dynamics of the dissipative two-state system, Rev. Mod. Phys. **59**, 1 (1987).

[38] T. A. Costi and G. Zaránd, Thermodynamics of the dissipative two-state system: A Bethe-ansatz study, Phys. Rev. B **59**, 12398 (1999).

[39] U. Weiss, *Quantum Dissipative Systems*, 4th ed. (World Scientific, Singapore, 2012).

[40] P. B. Allen and R. C. Dynes, Transition temperature of strong-coupled superconductors reanalyzed, Phys. Rev. B **12**, 905 (1975).

[41] A. Auerbach, *Interacting Electrons and Quantum Magnetism* (Springer, New York, 1998).

[42] I. Esterlis and J. Schmalian, Cooper pairing of incoherent electrons: An electron-phonon version of the Sachdev-Ye-Kitaev model, Phys. Rev. B **100**, 115132 (2019).

[43] Although addressing potential replica symmetry breaking or the validity of the self-averaging of the free energy for a non-Gaussian saddle-point is challenging and beyond the scope of the current paper, it is worth noting that in a related Gaussian saddle point (of the Yukawa-SYK model) it was shown that the self-averaging property is invalidated at order N^{-2} [44].

[44] Z. D. Shi, D. V. Else, H. Goldman, and T. Senthil, Loop current fluctuations and quantum critical transport, SciPost Phys. **14**, 113 (2023).

[45] A. O. Caldeira and A. J. Leggett, Influence of dissipation on quantum tunneling in macroscopic systems, Phys. Rev. Lett. **46**, 211 (1981).

[46] A. O. Caldeira and A. J. Leggett, Quantum tunnelling in a dissipative system, Ann. Phys. (NY) **149**, 374 (1983).

[47] K. L. Hur, Entanglement entropy, decoherence, and quantum phase transitions of a dissipative two-level system, Ann. Phys. (NY) **323**, 2208 (2008).

[48] G. Camacho, P. Schmitteckert, and S. T. Carr, Exact equilibrium results in the interacting resonant level model, Phys. Rev. B **99**, 085122 (2019).

[49] V. M. Filyov and P. B. Wiegmann, A method for solving the Kondo problem, Phys. Lett. A **76**, 283 (1980).

[50] V. V. Ponomarenko, Resonant tunneling and low-energy impurity behavior in a resonant-level model, Phys. Rev. B **48**, 5265 (1993).

[51] T. A. Costi and C. Kieffer, Equilibrium dynamics of the dissipative two-state system, Phys. Rev. Lett. **76**, 1683 (1996).

[52] The difference between σ_x and σ_y, σ_z is because of the fact that after integrating out the fast modes of the bath, the operators σ_y, σ_z in the emergent low-energy theory are highly dressed polaronic versions of the bare ones, which move the high-energy bath modes along with the TLS. However, since the bath couples to the TLS in the x basis, integrating it out does not dress σ_x, and thus the "high energy" and "low energy" σ_x operators coincide. See [53] for more details.

[53] F. Guinea, Dynamics of simple dissipative systems, Phys. Rev. B **32**, 4486 (1985).

[54] P. W. Anderson, G. Yuval, and D. R. Hamann, Exact results in the Kondo problem. II. Scaling theory, qualitatively correct solution, and some new results on one-dimensional classical statistical models, Phys. Rev. B **1**, 4464 (1970).

[55] F. Guinea, V. Hakim, and A. Muramatsu, Bosonization of a two-level system with dissipation, Phys. Rev. B **32**, 4410 (1985).

[56] M. Sassetti and U. Weiss, Correlation functions for dissipative two-state systems: Effects of the initial preparation, Phys. Rev. A **41**, 5383 (1990).

[57] This result follows from dimensional analysis: If the upper integration limit can be continued to ∞, the only place where an energy scale appears is in the normalization of the distribution $1/h_{c,R}^{\gamma}$, which sets the frequency dependence since the susceptibility is dimensionless.

[58] Note that the low-frequency dependence of χ_x'' serves as a "cutoff" for $\overline{\chi_x''}$: The exponent in the averaged susceptibility does not exceed that of the individual susceptibilities, namely, $\overline{\chi_x''} \propto |\omega|$ for all $\gamma > 2$. This is equivalent to the cases where the integral in A_α diverges at the lower limit, resulting in a modification of the frequency dependence.

[59] G. Zaránd and E. Demler, Quantum phase transitions in the Bose-Fermi Kondo model, Phys. Rev. B **66**, 024427 (2002).

[60] A. H. Castro Neto, E. Novais, L. Borda, G. Zaránd, and I. Affleck, Quantum magnetic impurities in magnetically ordered systems, Phys. Rev. Lett. **91**, 096401 (2003).

[61] E. Novais, A. H. Castro Neto, L. Borda, I. Affleck, and G. Zarand, Frustration of decoherence in open quantum systems, Phys. Rev. B **72**, 014417 (2005).

[62] H. Kohler, A. Hackl, and S. Kehrein, Nonequilibrium dynamics of a system with quantum frustration, Phys. Rev. B **88**, 205122 (2013).

[63] R. Belyansky, S. Whitsitt, R. Lundgren, Y. Wang, A. Vrajitoarea, A. A. Houck, and A. V. Gorshkov, Frustration-induced anomalous transport and strong photon decay in waveguide QED, Phys. Rev. Res. **3**, L032058 (2021).

[64] N. Bashan, E. Tulipman, S. Kivelson, J. Schmalian, and E. Berg (unpublished).

[65] D. V. Khveshchenko, Quantum impurity models of noisy qubits, Phys. Rev. B **69**, 153311 (2004).

[66] D. Chowdhury, Y. Werman, E. Berg, and T. Senthil, Translationally invariant non-fermi-liquid metals with critical fermi surfaces: Solvable models, Phys. Rev. X **8**, 031024 (2018).

[67] A. A. Patel, J. McGreevy, D. P. Arovas, and S. Sachdev, Magnetotransport in a model of a disordered strange metal, Phys. Rev. X **8**, 021049 (2018).

[68] T. P. Devereaux and R. Hackl, Inelastic light scattering from correlated electrons, Rev. Mod. Phys. **79**, 175 (2007).

[69] U. Karahasanovic, F. Kretzschmar, T. Böhm, R. Hackl, I. Paul, Y. Gallais, and J. Schmalian, Manifestation of nematic degrees of freedom in the Raman response function of iron pnictides, Phys. Rev. B **92**, 075134 (2015).

[70] Note that for MFLs or NFLs, the Kramers-Kroning relations relate the low-energy regimes of the real and imaginary parts of the self-energy, such that one is completely determined by the other (independent of the UV cutoff). This is in contrast to FLs where, since $\Sigma''(\omega) \sim |\omega|^\gamma + \mathcal{O}(|\omega|^\gamma)$ (with $\gamma > 1$), the low- and high-energy sectors both contribute to the leading linear in ω behavior of $\mathrm{Re}\Sigma_{\mathrm{ret}}(\omega)$ (making Kramers Kronig relations not particularly useful if only low-energy information is accessible).

[71] E. Tulipman and E. Berg, A criterion for strange metallicity in the Lorenz ratio, npj Quantum Mater. **8**, 66 (2023).

[72] Exact results for $\alpha \ll 1$ and $\alpha = 1/2$ indicate that $\varphi = 1$.

[73] R. Görlich and U. Weiss, Specific heat of the dissipative two-state system, Phys. Rev. B **38**, 5245 (1988).

[74] T. A. Costi, Scaling and universality in the anisotropic Kondo model and the dissipative two-state system, Phys. Rev. Lett. **80**, 1038 (1998).

[75] D. Hauck, M. J. Klug, I. Esterlis, and J. Schmalian, Eliashberg equations for an electron–phonon version of the Sachdev–Ye–Kitaev model: Pair breaking in non-Fermi liquid superconductors, Ann. Phys. (NY) **417**, 168120 (2020).

[76] D. T. Son, Superconductivity by long-range color magnetic interaction in high-density quark matter, Phys. Rev. D **59**, 094019 (1999).

[77] A. Abanov and A. V. Chubukov, Interplay between superconductivity and non-Fermi liquid at a quantum critical point in a metal. I. The γ model and its phase diagram at $T = 0$: The case $0 < \gamma < 1$, Phys. Rev. B **102**, 024524 (2020).

[78] Y.-M. Wu, A. Abanov, Y. Wang, and A. V. Chubukov, Interplay between superconductivity and non-Fermi liquid at a quantum critical point in a metal. II. the γ model at a finite T for $0 < \gamma < 1$, Phys. Rev. B **102**, 024525 (2020).

[79] V. Dobrosavljević and E. Miranda, Absence of conventional quantum phase transitions in itinerant systems with disorder, Phys. Rev. Lett. **94**, 187203 (2005).

[80] A. M. Sengupta and A. Georges, Non-fermi-liquid behavior near a $T = 0$ spin-glass transition, Phys. Rev. B **52**, 10295 (1995).

[81] V. Lubchenko and P. G. Wolynes, Intrinsic quantum excitations of low temperature glasses, Phys. Rev. Lett. **87**, 195901 (2001).

[82] J. Burnett, L. Faoro, I. Wisby, V. L. Gurtovoi, A. V. Chernykh, G. M. Mikhailov, V. A. Tulin, R. Shaikhaidarov, V. Antonov, P. J. Meeson *et al.*, Evidence for interacting two-level systems from the 1/*f* noise of a superconducting resonator, Nat. Commun. **5**, 4119 (2014).

[83] D. Khomenko, C. Scalliet, L. Berthier, D. R. Reichman, and F. Zamponi, Depletion of two-level systems in ultrastable computer-generated glasses, Phys. Rev. Lett. **124**, 225901 (2020).

[84] D. Khomenko, D. R. Reichman, and F. Zamponi, Relationship between two-level systems and quasilocalized normal modes in glasses, Phys. Rev. Mater. **5**, 055602 (2021).

[85] W. Ji, T. W. J. de Geus, E. Agoritsas, and M. Wyart, Mean-field description for the architecture of low-energy excitations in glasses, Phys. Rev. E **105**, 044601 (2022).

[86] M. Thill and D. Huse, Equilibrium behaviour of quantum Ising spin glass, Physica A **214**, 321 (1995).

[87] A. J. Millis, D. K. Morr, and J. Schmalian, Local defect in metallic quantum critical systems, Phys. Rev. Lett. **87**, 167202 (2001).

[88] A. J. Millis, D. K. Morr, and J. Schmalian, Quantum Griffiths effects in metallic systems, Phys. Rev. B **66**, 174433 (2002).

[89] T. Vojta and J. Schmalian, Quantum Griffiths effects in itinerant Heisenberg magnets, Phys. Rev. B **72**, 045438 (2005).

[90] N. E. Hussey, R. A. Cooper, X. Xu, Y. Wang, I. Mouzopoulou, B. Vignolle, and C. Proust, Dichotomy in the *T*-linear resistivity in hole-doped cuprates, Philos. Trans. R. Soc. A **369**, 1626 (2011).

[91] J. M. Tranquada, P. M. Lozano, Juntao Yao, G. D. Gu, and Qiang Li, From nonmetal to strange metal at the stripe-percolation transition in $La_{2-x}Sr_xCuO_4$ Phys. Rev. B **109**, 184510 (2024).

[92] T. Park, V. A. Sidorov, F. Ronning, J.-X. Zhu, Y. Tokiwa, H. Lee, E. D. Bauer, R. Movshovich, J. L. Sarrao, and J. D. Thompson, Isotropic quantum scattering and unconventional superconductivity, Nature (London) **456**, 366 (2008).

[93] N. Doiron-Leyraud, P. Auban-Senzier, S. René de Cotret, C. Bourbonnais, D. Jérome, K. Bechgaard, and L. Taillefer, Correlation between linear resistivity and T_c in the Bechgaard salts and the pnictide superconductor $Ba(Fe_{1-x}Co_x)_2As_2$, Phys. Rev. B **80**, 214531 (2009).

[94] K. Jin, N. P. Butch, K. Kirshenbaum, J. Paglione, and R. L. Greene, Link between spin fluctuations and electron pairing in copper oxide superconductors, Nature (London) **476**, 73 (2011).

[95] M. Berben, J. Ayres, C. Duffy, R. D. H. Hinlopen, Y.-T. Hsu, M. Leroux, I. Gilmutdinov, M. Massoudzadegan, D. Vignolles, Y. Huang, T. Kondo, T. Takeuchi, J. R. Cooper, S. Friedemann, A. Carrington, C. Proust, and N. E. Hussey, Compartmentalizing the cuprate strange metal, arXiv:2203.04867.

[96] Following the procedure in Ref. [90], the derivative $d\rho/dT$ can distinguish the two behaviors provided that the $T \to 0$ resistivity is measured with sufficient accuracy.

[97] Y. Dagan, M. M. Qazilbash, C. P. Hill, V. N. Kulkarni, and R. L. Greene, Evidence for a quantum phase transition in $Pr_{2-x}Ce_xCuO_{4-\delta}$ from transport measurements, Phys. Rev. Lett. **92**, 167001 (2004).

[98] T. J. Reber, X. Zhou, N. C. Plumb, S. Parham, J. A. Waugh,

Y. Cao, Z. Sun, H. Li, Q. Wang, J. S. Wen *et al.*, Power law liquid-A unified form of low-energy nodal electronic interactions in hole doped cuprate superconductors, arXiv:1509.01611.

[99] S. Smit, E. Mauri, L. Bawden, F. Heringa, F. Gerritsen, E. van Heumen, Y. K. Huang, T. Kondo, T. Takeuchi, N. E. Hussey *et al.*, Momentum-dependent scaling exponents of nodal self-energies measured in strange metal cuprates and modelled using semi-holography, Nat. Commun. **15**, 4581 (2024).

[100] K. Harada, Y. Teramoto, T. Usui, K. Itaka, T. Fujii, T. Noji, H. Taniguchi, M. Matsukawa, H. Ishikawa, K. Kindo, D. S. Dessau, and T. Watanabe, Revised phase diagram of the high-T_c cuprate superconductor Pb-doped $Bi_2Sr_2CaCu_2O_{8+\delta}$ revealed by anisotropic transport measurements, Phys. Rev. B **105**, 085131 (2022).

[101] W. Gasser, E. Heiner, and K. Elk, *Greensche Funktionen in Festkörper- und Vielteilchenphysik* (Wiley, Hoboken, NJ, 2002).

[102] A. V. Chubukov and J. Schmalian, Superconductivity due to massless boson exchange in the strong-coupling limit, Phys. Rev. B **72**, 174520 (2005).

[103] A. J. Bray and M. A. Moore, Influence of dissipation on quantum coherence, Phys. Rev. Lett. **49**, 1545 (1982).